HIGH-RESOLUTION CHEMOSTRATIGRAPHY

IN THE "MISSISSIPPIAN LIMESTONE" OF

NORTH-CENTRAL OKLAHOMA

By

ASHLEY MARIE DUPONT

Bachelor of Science in Geology

University of Georgia

Athens, Georgia

2013

Submitted to the Faculty of the
Graduate College of the
Oklahoma State University
in partial fulfillment of
the requirements for
the Degree of
MASTER OF SCIENCE
July, 2016

HIGH-RESOLUTION CHEMOSTRATIGRAPHY

IN THE "MISSISSIPPIAN LIMESTONE" OF

NORTH-CENTRAL OKLAHOMA

Thesis Approved:

Dr. G. Michael Grammer

Thesis Adviser

Dr. Jay Gregg

Dr. Natascha Riedinger

Dr. Jim Puckette

ACKNOWLEDGEMENTS

I would first like to thank my adviser, Dr. Michael Grammer, for constantly encouraging me to be the best student I can be. I have learned so much from him in the past two years, whether in the classroom or in the field, and will forever be asking our favorite phrase “so what”. I have learned how to approach a problem from many different avenues, which has taught me how to become an integrated scientist and more importantly has given me a skillset that will allow me to be successful in my upcoming career. I’m honored to have had the opportunity of working with him for my Master’s research and am thankful to be able to call him not only my mentor, but my friend.

I would also like to thank my committee members, Dr. Puckette, Dr. Riedinger, and Dr. Gregg for pointing me in the right direction throughout my research and keeping ideas fresh in my mind. Dr. Puckette’s guidance throughout my experience here at Oklahoma State has been invaluable. I have thoroughly enjoyed getting to know him and learning about the Mississippian strata of Oklahoma through his legendary eyes. Dr. Riedinger was very helpful in keeping my elemental data in check and thoroughly scrutinized. I am very thankful to have had her helpful hand during my data review and am grateful for her willingness to meet with and help me. Dr. Gregg was very helpful in giving me my first glance into what carbonate geochemistry is all about. His guidance in the classroom has been vital to my research and I will forever be thankful for the insight he has given me.

I would also like to thank all of my friends and lab mates I have met during my time here. Stephanie LeBlanc, Buddy Price, Taylor Thompson, and Beth Vanden Berg were some of the first students I met when I visited Oklahoma State. I really enjoyed getting to know them and won’t ever forget their welcoming attitude. Yulun Wang, Ahmed El Belasy, and Ibukun Bode are also a handful of friends I would like to recognize for their guidance throughout our friendship, especially by keeping me up to date with new ideas from the scientific literature. I’d also like to recognize Lara Jaeckel, Scott Shelley, and Elizabeth Elium for keeping the lab lively and always being willing to help me, no matter how small the problem.

Lastly, and most importantly, I would like to express my love and gratitude to my family. My parents, Jon and Julie Dupont, have always been supportive of me and have kept me motivated and striving towards becoming the person I am today. My sister, Laura, has always been there for me and has kept me focused on the bright future ahead. I can’t imagine a world without the care of these three incredible individuals and will be forever grateful of their support and love. I hope I have made them proud.

Name: ASHLEY MARIE DUPONT

Date of Degree: JULY, 2016

Title of Study: HIGH-RESOLUTION CHEMOSTRATIGRAPHY IN THE "MISSISSIPPIAN LIMESTONE" OF NORTH-CENTRAL OKLAHOMA

Major Field: GEOLOGY

Abstract:

The "Mississippian Limestone" of the Mid-Continent United States is a complex and highly heterogeneous hydrocarbon play. Its heterogeneity is largely due to the mixed siliciclastic and carbonate nature of the Mid-Continent Mississippian system which yields complex reservoir lithologies and distributions that are laterally discontinuous and difficult to predict. The purpose of this study is to apply chemostratigraphy, a relatively recent method for addressing industry related correlation problems, as an additional reservoir characterization tool that provides insight into chemical attributes of Mississippian-aged sedimentation and how these chemical signatures can be used for potential chronostratigraphic applications.

High-resolution sampling (every 0.3m (1ft)) of three subsurface cores for carbon and oxygen stable isotopes has revealed predictable patterns related to facies and vertical stacking patterns as well as to globally recognized secular changes in ocean chemistry. The chemostratigraphic approach applied herein suggests more frequent 3rd order cyclicity than recently defined in other subsurface data sets in the basin which is more consistent with global ties to the individual North American stages and within the Mississippian overall. In addition, $\delta^{18}O$ values suggest a level of predictability at the 4th order scale related to shallowing upward packages and mixed meteoric input at cycle tops. Overall, stable isotope curves closely match those of well-established Mississippian global carbon cycling and have been used to suggest time boundaries in this area of the depositional system.

TABLE OF CONTENTS

Chapter Page

LIST OF TABLES

Table Page

LIST OF FIGURES

Figure Page

CHAPTER I

INTRODUCTION

1.1 "Mississippian Limestone" Play Update

The "Mississippian Limestone" has proven to be one of the more complex hydrocarbon plays in the Mid-Continent of the United States. Although historically exploited using vertical drilling methods, recent horizontal drilling techniques have been focused on targeting stacked, unconventional reservoirs in low porosity (1-2% or less) and low permeability (millidarcies) limestone units (Roundtree et al., 2010). The mixed siliciclastic and carbonate nature of the Mississippian system in the Mid-Continent (Lane and De Keyser, 1980) yields complex reservoir lithologies and distributions that are laterally discontinuous and difficult to predict. These complexities have led to nomenclature inconsistencies that complicate correlation efforts and often cause the system to be defined lithostratigraphically (Mazzullo et al., 2013; Childress and Grammer, 2015). This approach can lead to the misidentification of subsurface units and imposes a relatively simplistic view of reservoir communication within a complex depositional system.

Recent studies have demonstrated the ability to predict the Mississippian's time-transgressive and highly cyclic nature at multiple scales in the Mid-Continent region (LeBlanc, 2014; Price, 2014; Childress and Grammer, 2015; Jaeckel, 2016; Vanden Berg, 2016). The migration of repetitive facies belts due to base level rise and fall has resulted in a repeatable vertical stacking pattern comprised of shallowing-upward facies successions that suggest a hierarchy of depositional cyclicity. This hierarchy, likely related to Milankovitch cyclicity, has been found to be a major factor that controls reservoir emplacement and strongly affects communication between different depositional units vertically, laterally, and at multiple scales (Grammer et al., 2004). The resulting package may be difficult to delineate using a lithology-based approach alone, and in instances where strong chronostratigraphic ties are lacking, chemostratigraphy may be a useful method for assigning ages to depositional units and used in regional correlation. As there is a general lack of biostratigraphic data for most of the recent Mid-Continent Mississippian studies, the focus of this research is to test two geochemical methods at high-resolution sampling intervals (0.3m (1ft)) to determine their effectiveness in identifying and relating global changes during the Mississippian as well as evaluating their potential for application for regional, possibly chronostratigraphic, correlation in the subsurface.

1.2 Study Overview

The objective of this study is to develop a chemostratigraphic framework using carbon and oxygen stable isotopes and energy-dispersive x-ray fluorescence at high-resolution sampling intervals (0.3m (1ft)) in three Mississippian-aged cores in north-

central Oklahoma. The goals of this research are to establish a genetic relationship with previously defined high-resolution sequence stratigraphy in the same three cores (LeBlanc, 2014) and determine the effectiveness of chemostratigraphy as a potential chronostratigraphic and regional correlation tool. The fundamental questions addressed by this study are as follows:

1. Can carbon and oxygen stable isotopic data be used to chronostratigraphically constrain "Mississippian Limestone" core in north-central Oklahoma in the absence of biostratigraphy?
2. Do stable isotopes display predictable excursions related to the previously constrained sequence stratigraphic framework? If so, at what scale and how does this relate to higher frequency cyclicity?
3. Does carbon and oxygen stable isotopic data compare with previously established, global Mississippian-age profiles and how does this relate to secular changes in the carbon cycle?
4. Can energy-dispersive x-ray fluorescence be used as a proxy for facies interpretations by discerning relative restriction of marine waters during deposition?

Overall, this study aims to provide insight into how a chemostratigraphic approach may be useful in order to accurately correlate subsurface units within complex depositional systems, especially in areas of rapid facies changes and where biostratigraphic data is scarce. Delineating a relationship with previously defined high-

resolution sequence stratigraphy may also suggest a new hierarchy of cyclicity that may not be recognized with wireline log and facies data alone.

CHAPTER II

CHEMOSTRATIGRAPHY

2.1 Geochemistry Overview

Although sedimentary geochemistry has long been used to help explain geological phenomena, the application of characterizing depositional units based on their geochemical traits and using them for correlation within a stratigraphic framework is relatively new (Scholle and Arthur, 1980; Renard, 1986). This is largely due to recent advancements in technology and the need for understanding the distribution of complex hydrocarbon reservoirs. Although no clear definition exists in the scientific literature, chemostratigraphy may be described as the study of temporal and spatial geochemical variability of the rock record with a goal to establish genetically related, mappable rock units, defined in terms of unique geochemical composition, whether by isotopic ratios, elemental and/or elemental oxide ratios, or a combination of any or all of these (Ramkumar, 2015). For the context and goals of this study, this is a suitable definition as it explains both the scale and methods that will be tested on the subsurface dataset.

2.2 Analyses and Geochemical Proxies

Geochemical sampling within the context of chemostratigraphy falls into two categories: isotope ratios and element concentrations. Traditionally, isotope stratigraphy has utilized C, O, S, N, and Sr, while more recent methods, including B, Ca, Mo, and Fe, are being developed and explored (Sial, 2015). For the focus of this study, only the stable isotopes of carbon and oxygen are considered, as they are the most useful for carbonate geochemistry (Morse and Mackenzie, 1990; Tucker and Wright, 1990; Swart, 2015).

Traditional isotope studies have led to the establishment of geochemical profiles spanning most of the geologic record (Archean-recent) and give important insight into elemental cycling throughout earth's history (for example: Viezer et al., 1999; Buggisch et al., 2003; Saltzman, 2003; Katz et al., 2005; Maloof et al., 2005; Halverson et al., 2006; Cramer et al., 2010; Tierney, 2010). Positive and negative shifts from normal background values suggest significant alterations in the geochemical record and the use of proxies help explain why these changes occur. A geochemical proxy describes a specific element or isotope, an elemental ratio, or a combination of these that is used as an indicator of a particular geological event or process prevalent during the geologic past (Ramkumar, 2015). These processes are often related to secular changes in elemental cycling and have been used for global correlation at different scales (Bruckschen et al., 1999; Mii et al., 2001; Buggisch et al., 2008).

Elemental analyses are also divided into two primary types: major and trace element assemblages. Major elements are reported in their elemental oxide forms (Fe_2O_3, TiO_2, Al_2O_3, SiO_2, etc.) and as weight percentages while trace elements (Mo, Ni, U, Cu, etc.) are reported in their elemental form and in parts per million. Traditionally, major element assemblages aid in enhanced facies characterization whereas more recent studies focused on redox sensitive trace elements are being done in order to develop geochemical proxies related to paleoenvironments and water column conditions (Jones and Manning, 1994; Alego and Maynard, 2004; Alego et al., 2007).

Paleoredox proxies are a particular type of geochemical proxy that rely on isotopic ratios (Fe, S, and Mo) and concentrations of particular trace elements (Mo, Cu, Ni, Co, V, U, Cr, etc.) that are redox sensitive. Redox, or oxidation-reduction potential, is a measure of the free oxygen versus hydrogen sulfide in the system of interest (Lyons et al., 2009). These ratios and elemental concentrations are often compared together, sometimes in addition to total organic content (TOC), to make hypotheses regarding paleoredox conditions (oxic, suboxic, anoxic) related to different degrees of water column restriction (Raiswell et al., 1988; Lyons & Severmann, 2006; Alego et al., 2007). Water column chemistry is important for reservoir characterization and correlation as changes in circulation largely dictate faunal assemblages and facies distributions, and may control relative TOC. For the purpose of this study, geochemical proxies will be used to interpret relative depositional conditions based on certain elemental enrichments and supporting TOC data.

2.3 Stratigraphic Significance

One of the more important factors of chemostratigraphy is establishing a genetic relationship between chemically unique depositional units. Recognized by the International Stratigraphic Commission as a valuable subdiscipline of sequence stratigraphy, this implies that important ties to multiple orders of eustatic sea level cyclicity can be made and a depositional hierarchy can be defined. Unlike lithology-based sequence stratigraphy, this geochemical hierarchy helps elucidate the cause and significance of certain stratigraphic horizons with enhanced precision and in some instances can better differentiate changes in seawater composition or paleoceanographic composition in intervals where facies variability does not readily record this change. More importantly, geochemistry applied using a chemostratigraphic approach can be crucial for establishing chronostratigraphic ties and evaluating correlation potential for units in the subsurface. The high-resolution nature of the present study helps capture geochemical variability at very fine scales and imparts a level of stratigraphic significance to certain horizons not previously defined.

CHAPTER III

CARBON AND OXYGEN STABLE ISOTOPES

3.1 Stable Isotope Overview

Isotopes of an element have the same number of protons, but different numbers of neutrons which causes atoms to have similar chemical properties, but different masses. This mass difference, along with differences in physical-chemical and kinetic properties, causes variations in isotopic compositions in chemical compounds, often referred to as isotopic fractionation (Morse and Mackenzie, 1990). Isotopic fractionation is usually expressed in the form of a ratio with the heavy isotope as the numerator and the light isotope as the denominator. Isotopic ratios are generally measured relative to a standard (For carbonates: VPDB- Vienna Pee Dee Belemnite or VSMOW- Vienna Standard Mean Ocean Water) and reported using the delta notation ($\delta^{13}C$; $\delta^{18}O$) in parts per thousand (per mil, ‰; equation 1).

$$\delta^{13}C = \frac{R_x - R_{std}}{R_{std}} \qquad \text{where } R_X = {}^{13}C/{}^{12}C \text{ in sample}, \quad R_{std} = {}^{13}C/{}^{12}C \text{ in standard}$$

Equation 1. Definition of delta notation utilized in determining stable isotopic composition of samples relative to a standard.

The delta value serves as a standardized unit of measure for evaluating the geochemistry of different samples. In general, long term secular changes in $\delta^{13}C$ are due to the variations in the ratio of organic carbon (reduced reservoir) to carbon dioxide, bicarbonate, and carbonate minerals (oxidized reservoir) (Tucker and Wright, 1990; Saltzman and Thomas, 2012), while short term excursions tend to reflect changes in organic productivity and burial rates of organic carbon (Tucker and Wright, 1990). Overall, the precipitation of carbonates involves little carbon isotopic fractionation relative to dissolved inorganic carbon (DIC) in the water column, therefore, the $\delta^{13}C$ signal from inorganically or biologically precipitated carbonate in seawater is very close to that of the DIC in the oceans (Saltzman and Thomas, 2012). This allows carbonate rocks in particular to record paleoceanographic conditions and subsequent changes in elemental cycling. This has important implications for how $\delta^{13}C$ values are affected by long term secular change and short term productivity and how these values are used in chronostratigraphic correlation.

Variations in $\delta^{18}O$ are related to marine, meteoric, and burial conditions (Figure 1). This is largely due to the fractionation of oxygen isotopes due to evaporation, temperature, and rock-water interactions (Lohmann, 1988). Because the mole fraction of oxygen in a given volume of water and carbonate sample is roughly equal, oxygen native to the water volume will dominate the composition of the precipitating phase (Lohmann, 1988). This can result in the "resetting" of oxygen isotope values during post-depositional changes through the introduction of relatively light (depleted) meteoric waters or extremely light hot basinal brines. Thus, the integration of the diagenetic

history becomes an important step in discerning the true cause of any given isotopic signature (Swart, 2015). Precipitation of carbonate from marine waters and mixed marine-meteoric waters plot closest to seawater values, meteoric waters result in slightly more depleted $\delta^{18}O$ values, and burial signatures are drastically depleted (-6 to -10‰ or more) and often covariant with $\delta^{13}C$ (Figure 1). The extent of rock-water reactions can be estimated through the number of dissolution and precipitation reactions cycled through an individual volume of water, however this relies on a complex interplay of mineralogy, solubility, saturation states, and pH, all of which change as a result of the individual reactions (Lohmann, 1988). In-depth analysis of water-rock interactions is beyond the focus of this study, however the integration of the diagenetic history allows for the recognition and application of probable post-depositional alteration.

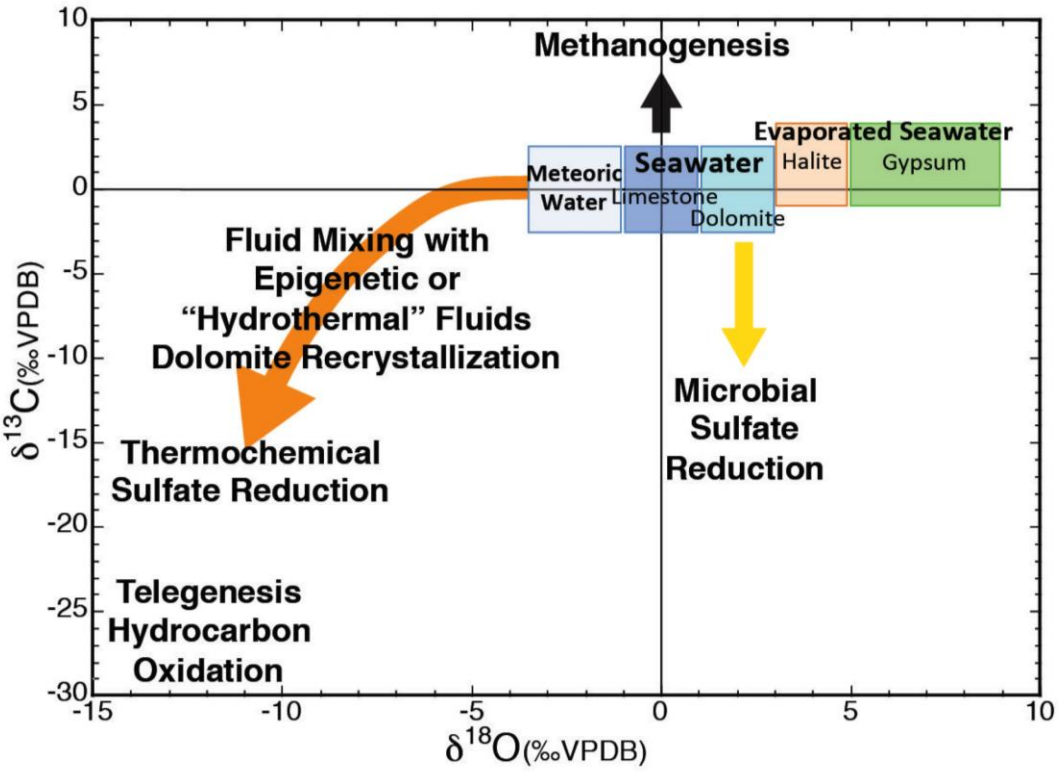

Figure 1. Cross plot of carbon and oxygen stable isotopes depicting various environments and diagenetic changes that affect isotopic signatures. In general, most variation in $\delta^{18}O$ is related to marine (near zero values), meteoric (slightly depleted values), and burial (extremely depleted values) conditions. Variations in $\delta^{13}C$ are related to methanogenesis, microbial sulfate reduction, and burial processes (Gregg and Machel, personal communication).

3.2 Global Carbon Cycling and Regional Correlation Potential

Well-established, global carbon isotopic profiles of the Mississippian from previous studies (Bruckschen et al., 1999; Mii et al., 1999;; Saltzman, 2003; Batt et al, 2007; Buggisch et al., 2008; Koch et al., 2014) are used as a correlation datasets for the Mississippian section in the cores of this study (example Figure 2). Important excursions in $\delta^{13}C$ have been recognized at different locations across the globe (Bruckschen et al., 1999; Mii et al., 2001; Buggisch et al., 2008), and despite different sampling techniques, collectively support the hypothesis that carbon signatures reflect global carbon cycling.

Key excursions (red arrows, Figure 2) serve as regional correlation points for the subsurface data set and help suggest chronostratigraphically significant horizons. Reasons for shifts in the carbon profile are strongly debated amongst different authors, but some have attributed the major positive shift (+5-8‰) in the late Kinderhookian as representing the onset of glaciation (Bruckschen et al., 1999; Mii et al, 1999; Buggisch et al., 2008), and negative late Meramecian shifts being potentially attributed to widespread meteoric diagenesis associated with the Mississippian-Pennsylvanian unconformity (Koch et al., 2014). On a global scale, causality of $\delta^{13}C$ shifts is beyond the scope of this research, however patterns recognized in many of the profiles are a key step in developing potential chronostratigraphic ties for the current Mid-Continent dataset.

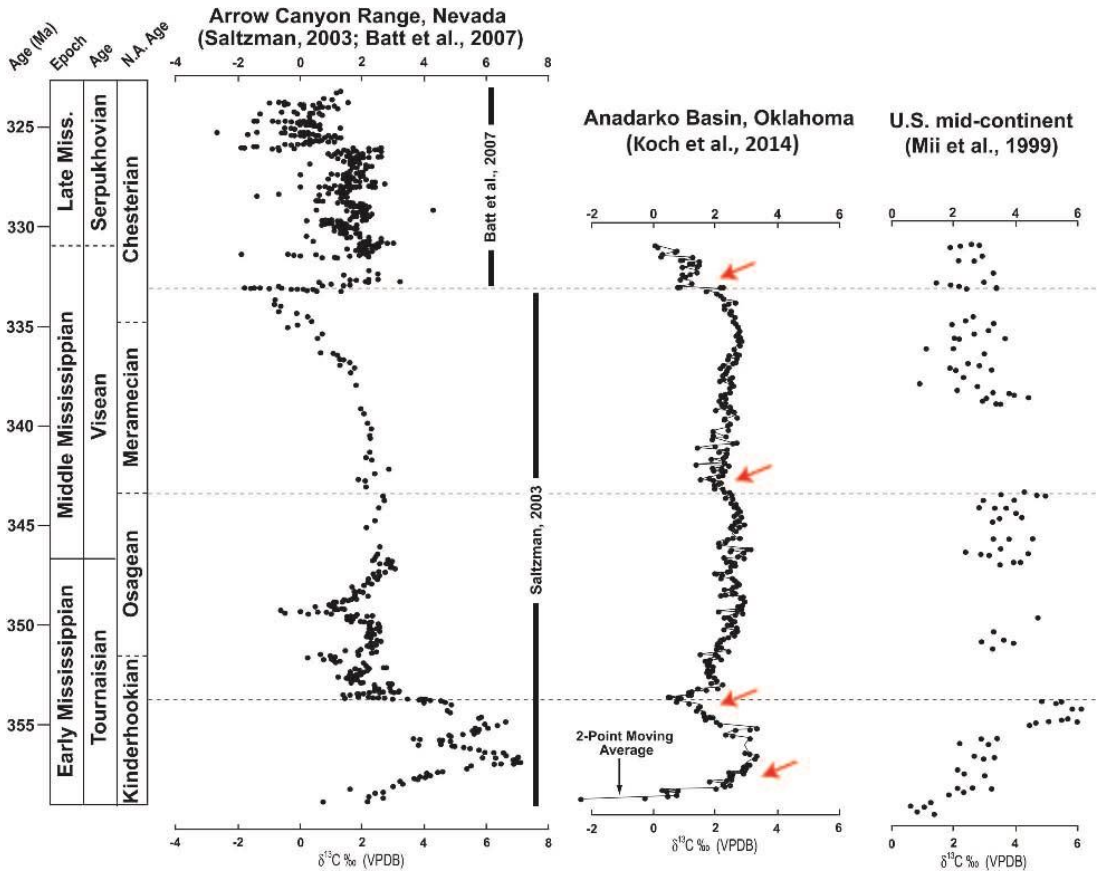

Figure 2. Comparison of carbon stable isotope curves from the global type section at Arrow Canyon, Nevada (Saltzman, 2003), Chesterian section from Idaho (Batt et al., 2007), the U.S. Mid-Continent composite section from Mii et al., 1999, and Anadarko Basin section from Koch, 2014. Red arrows depict general excursions that are used to suggest chronostratigraphic horizons for each North American stage. N.A. = North America (modified from Koch et al., 2014).

CHAPTER IV

DUPONT, A. AND GRAMMER, G.M., (TO BE SUBMITTED TO), HIGH-RESOLUTION CHEMOSTRATIGRAPHY IN THE "MISSISSIPPIAN LIMESTONE" OF NORTH-CENTRAL OKLAHOMA, IN GRAMMER ET AL., EDS., MISSISSIPPIAN RESERVOIRS OF THE MID-CONTINENT, USA- AAPG MEMOIR

4.1 Introduction

Although chemostratigraphic methods have been used in petroleum exploration since the 1980's (Scholle and Arthur, 1980), recent studies have focused on evaluating the potential for characterizing unconventional hydrocarbon reservoirs at high-resolution scales. (Rowe et al., 2012; Koch et al., 2014). Chemostratigraphy can be defined as the study of the temporal and spatial geochemical variability of the rock record with a goal to establish genetically related, mappable rock units, defined in terms of their unique geochemical composition (Ramkumar, 2015). The importance of establishing a genetic, and often an age specific, relationship between rock units is a fundamental aspect of chemostratigraphy as it allows that unit to be correlated both vertically and laterally with enhanced confidence.

Although the Mid-Continent Mississippian subsystem is known for its complex reservoir lithologies and vertical and lateral heterogeneities, recent studies (LeBlanc, 2014; Price, 2014; Childress and Grammer, 2015; Jaeckel, 2016; Vanden Berg, 2016, Childress, this volume; Vanden Berg, this volume) have demonstrated the ability to predict the types of cycles within the Mississippian units in Oklahoma and Kansas at multiple scales. A repeatable pattern comprised of shallowing-upward facies successions and a hierarchy of depositional cyclicity is recognized throughout the basin, enhancing the predictability of the depositional system from lateral facies distribution to vertical reservoir compartmentalization. Our findings suggest there are chemostratigraphic correlations in stable isotope curves of carbon and oxygen that are related to the depositional hierarchy and can be applied at the basin scale. Overall, high-resolution geochemistry suggests a revised interpretation of the initial facies-based hierarchy (LeBlanc, 2014) by utilizing a new set of cycle characteristics including high gamma ray values (<50 API units), more frequent shallowing-upward facies successions, diagenetic susceptibility, and a potential global chronostratigraphic tie.

4.1.1 Previous Studies

Carbon and oxygen stable isotope analysis is a traditional method used for chronostratigraphic correlation and paleoceanographic studies on a global scale (Bruckschen et al., 1999; Mii et al., 1999; Saltzman, 2003; Batt et al., 2007; Buggisch et al., 2008; Saltzman and Thomas, 2012) and recent studies have tested its potential for regional applications aimed at correlating stratigraphic sections in the Mid-Continent.

Koch et al. (2014) reported three important shifts in $\delta^{13}C$ that were used to suggest time boundaries for subsurface units in the Anadarko Basin deposited during the lower Tournaisian (Kinderhookian), upper Tournaisian through middle Visean (upper Kinderhookian-Meramecian), and uppermost Visean (lower Chesterian). Koch et al. (2014) reported similarities in trends between the Anadarko shelf profile and the global type section at Arrow Canyon, Nevada and concluded that $\delta^{13}C$ values overall were not facies dependent and instead reflect global changes in seawater chemistry during the Mississippian.

On a regional scale, Koch et al. (2014) considered broad energy level differences in depositional environment and proposed widespread meteoric diagenesis as the source for excursions in their shallowest depositional facies (uppermost Mississippian-lowermost Chester Group), but did not relate the geochemical signatures within the context of a high-resolution sequence stratigraphic framework. Idealized facies successions and their resulting sequence stratigraphic hierarchy are fundamental in understanding sea level-driven cyclicity within a stratigraphic section, and ties to a sequence stratigraphic framework would lead to enhanced predictability of subsurface units away from the core being utilized in the study (Grammer et al., 2004). This predictability can then be applied to different orders of cyclicity and isotopic signatures may be correlated at multiple scales. The present study's comparison of isotopic signatures to a previously defined sequence stratigraphic framework (LeBlanc, 2014) is crucial for capturing both large and small-scale geochemical variability and evaluating the potential correlation of these signatures at multiple scales.

The vertical and lateral heterogeneity of Mississippian reservoirs has led to nomenclature inconsistencies that complicate correlation efforts and often cause the system to be defined lithostratigraphically. This lithostratigraphic approach often leads to the misidentification of subsurface units and a relatively simplistic view of reservoir distribution and internal communication within a complex depositional system. Recent Mid-Continent studies have shown that the Mississippian interval represents a time-transgressive system that is characterized by repetitive facies belts that are deposited in time equivalent packages and migrate as a result of base level rise and fall (LeBlanc, 2014; Price, 2014; Childress and Grammer, 2015; Jaeckel, 2016; Vanden Berg, 2016). Multiple orders of eustatic sea level change during the Mississippian result in the lateral discontinuity of reservoir units and in instances where biostratigraphic data and strong chronostratigraphic ties are lacking, stable isotope chemostratigraphy may be a useful method for assigning ages to depositional units in the subsurface to facilitate accurate regional correlation.

4.2 Geologic Background

The three cores being evaluated in this study are interpreted to have been deposited on a distally-steepened ramp that experienced multiple orders of sea level fluctuation resulting in facies that were deposited mostly in normal marine waters with some deposited in more restricted, possibly oxygen deficient waters (LeBlanc, 2014). The Adkisson #1-33 core contains 98m (323ft) of Mississippian section and is located in Logan County, Oklahoma on the Cherokee Platform due east of the Nemaha Uplift

(Figures 3 and 4). The Winney #1-8 core contains 58m (189ft) of Mississippian section and the Elinore #1-18 core contains 44m (143ft). Both cores are located in Payne County, Oklahoma and in addition to the Adkisson #1-33 core are interpreted to represent a strike-oriented section in a relatively distal position on the distally steepened ramp (LeBlanc, 2014). All three cores contain contacts with the underlying Devonian Woodford Shale and the overlying Pennsylvanian shale, spanning the full Mississippian section represented at each location (Figure 4).

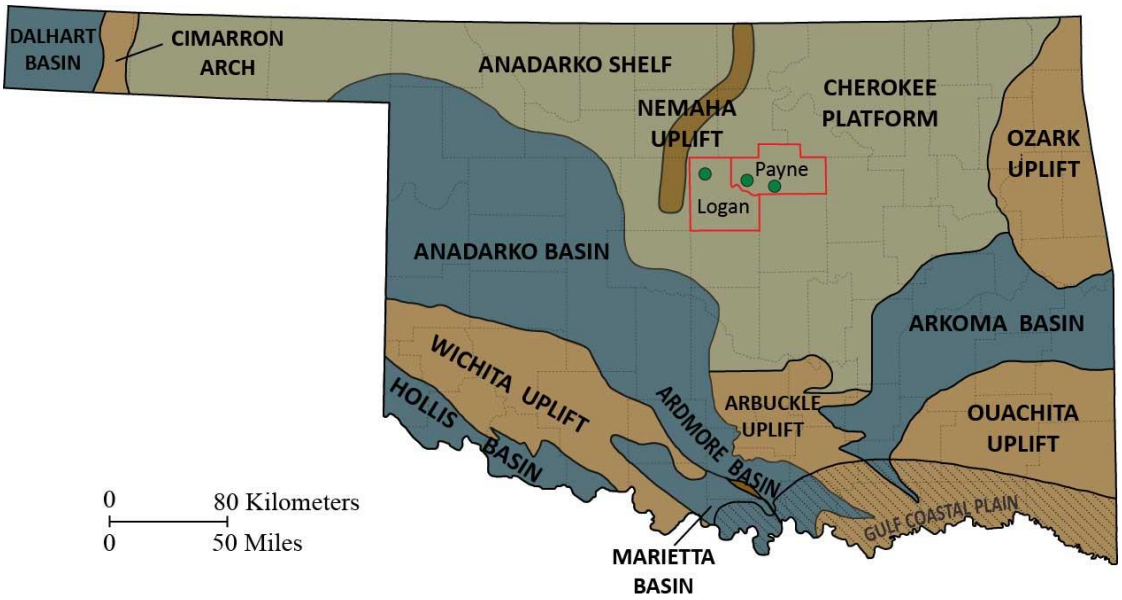

Figure 3. Map of Oklahoma showing the size and orientation of structural features relative to the study area (outlined in red). The location of the study area is on the Cherokee Platform, east of the Nemaha Uplift, with the Adkisson #1-33, Winney #1-8, and Elinore #1-18 cores denoted by green circles from west to east. The distance between the Adkisson #1-33 and the Winney #1-8 cores is approximately 27.7 km (17.2 mi) and from the Winney #-18 to the Elinore #1-18 core 24.8 km (15.5 mi). Blue regions represent depression features relative to uplifted regions (brown) (modified from Northcutt and Campbell, 1996).

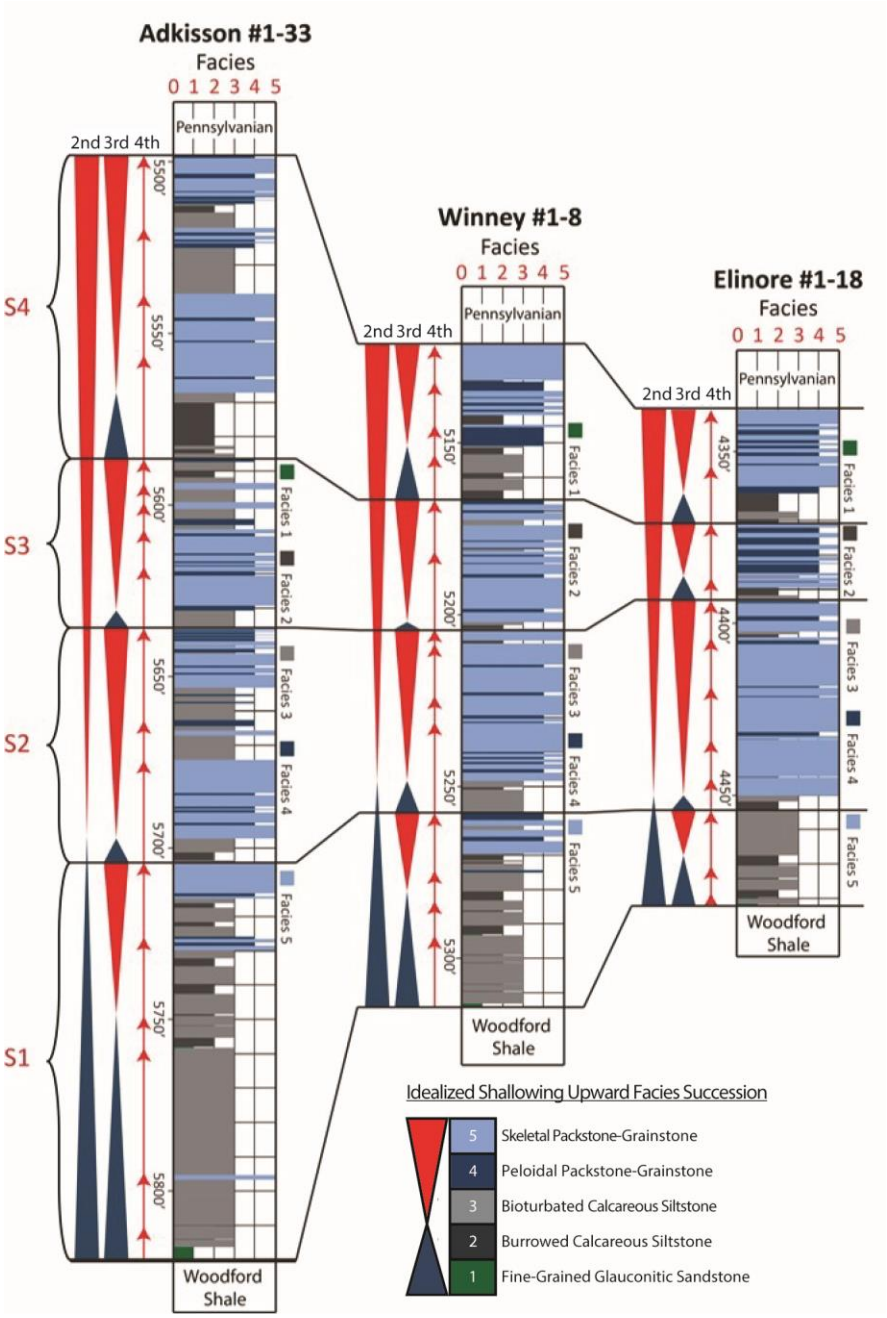

Figure 4. Revised cycle hierarchy defined by LeBlanc (personal communication) consisting of 2nd- and 3rd- order sequences and 4th-order high frequency cycles with idealized shallowing-upward facies succession shown in the bottom right. The blue triangle represents the transgressive phase and the red triangle represents the regressive phase of any given sequence. Deviations in the idealized stacking pattern may occur as a result of autocyclic processes (modified from LeBlanc, 2014).

Overall, the Mississippian represents a transitional period from greenhouse conditions dominant during the Devonian to icehouse conditions which were dominant during the Pennsylvanian and Permian (Read, 1995). In addition to climatic and oceanographic changes, a transition from greenhouse to icehouse times implies the enhanced effect of glacio-eustatic sea level change during which obliquity signal (40 k.y.) within the Milankovitch band is assumed dominant (Read, 1995). This signal, along with the combined effects of eccentricity (100 k.y. and 400 k.y.) and precessional signals (19-23 k.y.) is then superimposed on larger, 3rd order cycles (0.5- 5 m.y. duration) which have been shown to form the smallest scale of depositional sequences that are most confidently correlated within recent Mid-Continent studies (LeBlanc, 2014; Price, 2014; Childress and Grammer, 2015; Jaeckel, 2016; Vanden Berg, 2016; Childress, this volume; Vanden Berg, this volume).

Well-defined 3rd order composite sequences have been identified as global in scale and display temporal changes that reflect the greenhouse to icehouse transition (Figure 5). The Tournaisian-Visean (Kinderhookian, Osagean, and Meramecian) is characterized by relatively long 3rd order sequences (avg. 3.6 m.y., 2.3 m.y., 2.0 m.y. respectively), which may reflect low amplitude sea level change (10m) during the early Mississippian (Read, 1995). Alternatively, Late Visean-Serpukhovian strata (Chesterian) is characterized by relatively short, and more frequent 3rd order sequences (avg. 1.3 m.y.) which may reflect enhanced glacio-eustatic effects inducing rapid and high amplitude (75-100m) sea level change during the late Mississippian (Read, 1995). This has important implications for the prediction of depositional cyclicity as slight changes

in the pattern of shallowing upward facies successions, the resulting depositional hierarchy, and the potential for subaerial exposure should be expected from Early to Late Mississippian.

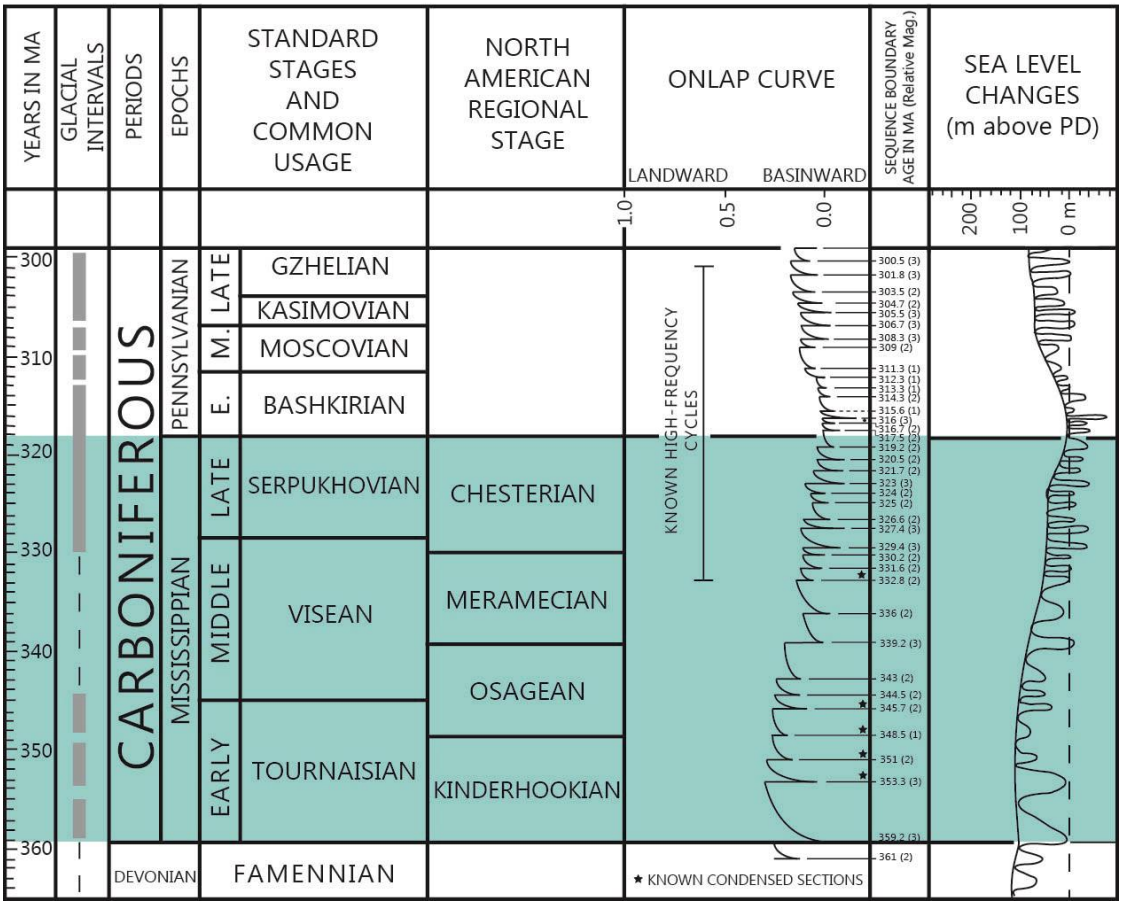

Figure 5. Diagram depicting global sea level and onlap curve for the Carboniferous Period (Mississippian Epoch highlighted in teal). Note the number of "known high-frequency cycles" (3rd Order Sequences) for each North American stage and the change in cycle duration from the Kinderhookian to the Chesterian. The relative decrease in cycle duration and enhanced cycle frequency in the Late Meramecian and Chesterian may reflect the transition from greenhouse conditions dominant during the Early Mississippian to icehouse conditions in the Late Mississippian/Pennsylvanian (modified from Haq and Schutter, 2008).

4.3 Methods

4.3.1 High Resolution Dataset

Bulk sediment samples were drilled using a microdrill from the backside of core slabs approximately every 0.3 meters (1ft) and analyzed for stable isotopes of carbon ($\delta^{13}C$) and oxygen ($\delta^{18}O$). The longer Adkisson #1-33 core was analyzed over the full Mississippian section while the Winney #1-8 and Elinore #1-18 cores were sampled over the lowermost 3rd order sequence defined by LeBlanc (2014) in order to determine its correlation potential. This sequence was chosen due to its higher percentage of muddier facies and the assumption of the Kinderhookian shift being present. A clean surface was prepared for each sample by drilling away surface residues to prevent contamination from drilling mud or other chemicals associated with the drilling and coring process.

High resolution sampling allows for the identification of small-scale heterogeneities and is similar to Koch et al. (2014) wherein bulk sediment samples were drilled approximately every 0.48 meters (1.6ft). Stable isotope analysis was conducted at the University of Miami (RSMAS) Stable Isotope Laboratory using a common acid bath interfaced to a Finnigan-MAT 251 mass spectrometer. Data is reported using the conventional per mil notation relative to Vienna Pee Dee Belemnite (VPDB). The precision for this method is +/- 0.1‰.

4.3.2 Discrete "3rd Order" Sequence Boundary Transects

In addition to high resolution analysis, high-density sampling across 3rd order sequence boundaries defined by LeBlanc (2014) was conducted. Five 5-sample transects (0.9-2.0 cm (0.35-0.8 in)) were measured across each 3rd order sequence boundary including the basal contact with the Devonian Woodford Shale and the upper contact with the Pennsylvanian shale.

4.4 Sequence Stratigraphic Framework

4.4.1 Primary Depositional Facies

Recent work suggests that Mid-Continent Mississippian facies and their vertical successions best represent deposition on a distally-steepened ramp (Price, 2014; LeBlanc, 2014; Childress and Grammer, 2015; Jaeckel, 2016; Vanden Berg, 2016; Childress, this volume; Vanden Berg, this volume). The predominant facies types present in the three cores, as defined by LeBlanc (2014), range from fine-grained, glauconitic sandstones to crinoidal-brachiopod packstones and grainstones (Figure 6) and have been interpreted to reflect a shallowing-upward succession in close proximity to fair weather wave base in a relatively distal position on the ramp. Changes in bioturbation indices and diversification of faunal assemblages support the hypothesis that facies present at the base of the succession were likely deposited in low-energy, potentially restricted conditions and facies present towards the top of the succession were deposited in normal marine conditions with improved circulation. Each facies is briefly summarized herein, for full facies characterization see LeBlanc (2014).

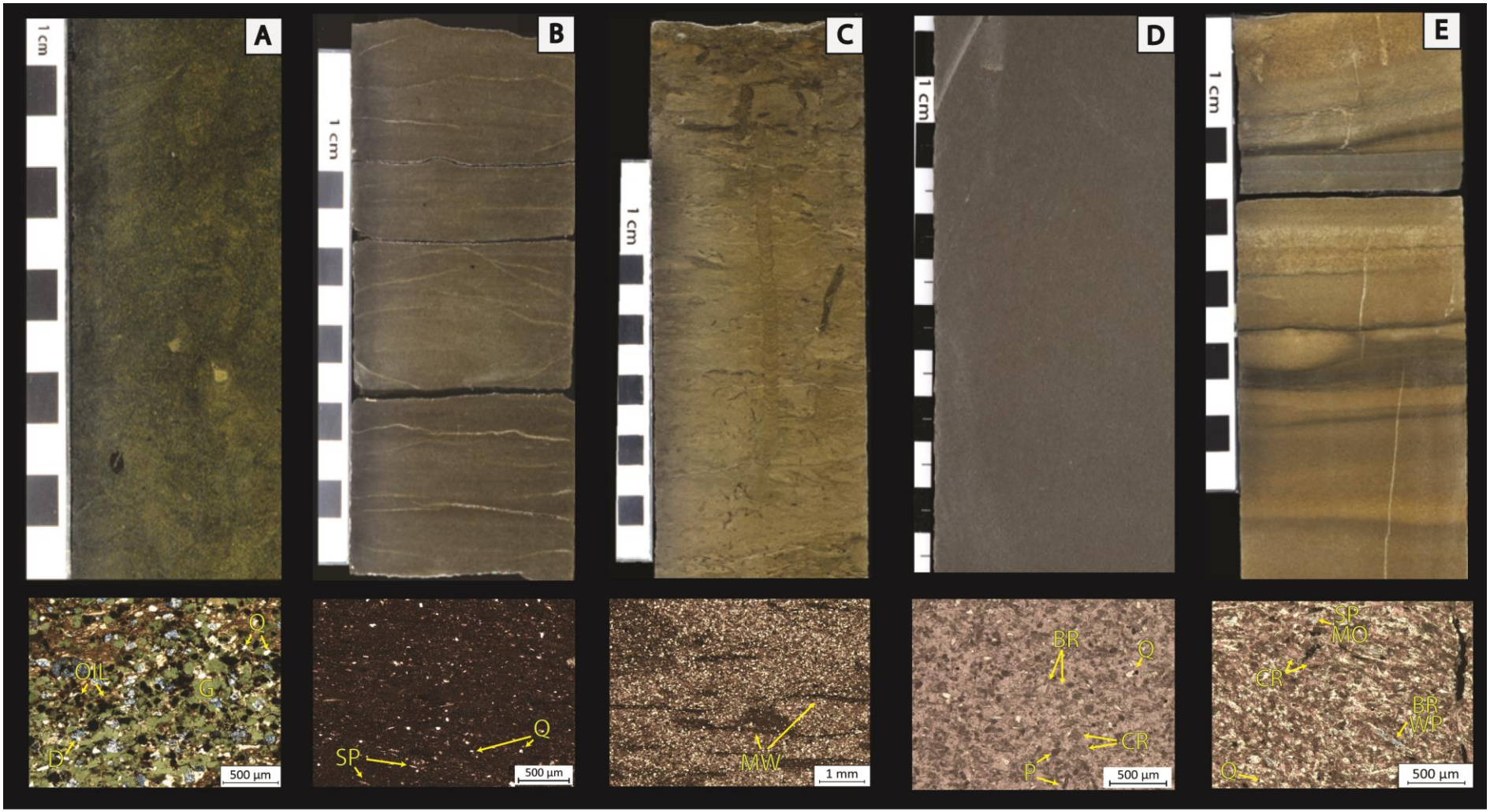

Figure 6. Core photos and photomicrographs of Facies 1-5 from LeBlanc 2014. **A)** Facies 1: Fine-grained glauconitic sandstone, distinguished by massive, dark greenish gray hand sample and abundant sand-sized glauconite grains in thin section. **B)** Facies 2: Burrowed calcareous siltstone, distinguished by brownish black to grayish black color and parting laminations in hand sample and micritic rich matrix in thin section. **C)** Facies 3: Bioturbated calcareous siltstone, distinguished by dusky yellowish brown color and bioturbated fabric in hand sample and characteristic mud wisps in thin section. **D)** Facies 4: Peloidal packstone to grainstone, distinguished by olive gray color and grain dominated texture in hand sample and abundant sand-sized peloids and skeletal debris in thin section. **E)** Facies 5: Skeletal packstone to grainstone, distinguished by truncation surfaces and variable lithology in hand sample and abundant skeletal debris and secondary porosity in thin section. **Abbreviations:** BR- brachiopod, CR- crinoid, D- dolomite, G-glauconite, MO- moldic porosity, MW- mud wisps, P- peloid, Q- quartz SP- sponge spicules, WP- interparticle porosity. Modified from LeBlanc, 2014.

Facies 1 is a fine-grained, glauconitic sandstone characterized by well-rounded to subrounded, well-sorted, silt-sized quartz grains (30-60%) and rounded to sub-rounded, moderately sorted, sand-sized glauconite grains (40-50%). Although glauconite can form in various marine environments, it is commonly interpreted to indicate deposition within an anoxic, submarine environment extending over a large area characterized by normal salinities, low energy conditions, and low sedimentation rates (Middleton et al., 2003). Facies 1 is only present in the lowermost sections of the core and is interpreted to represent deposition in a restricted, low energy environment with limited circulation and reflect the initial stages of flooding on a regional scale.

Facies 2 is a burrowed, calcareous siltstone characterized by weak calcareous laminations and localized millimeter-scale burrows. Limited abundance and low diversity of skeletal grains (siliceous sponge spicules and thin-shelled brachiopods) indicates that conditions were not suitable for a diverse, normal marine fauna (Flügel, 2010). Alternations in the degree of preservation of laminations due to millimeter-scale burrowing suggest fluctuating environmental conditions between oxygen-poor and oxygen-rich conditions (Ekdale et al., 1984). Facies 2 is interpreted to represent outer to distal ramp deposition below fair weather wave base in a low-energy, restricted environment that represents intermediate conditions between the underlying glauconitic sandstone facies and the overlying bioturbated, calcareous siltstone facies.

Facies 3 is a bioturbated, calcareous siltstone characterized by abundant fine sand-size peloids (30-40%), silt-sized quartz grains (avg. 40%), a moderate bioturbation

index (2-4 BI), and local, centimeter-scale vertical burrows. The presence of more diverse skeletal material (brachiopod and crinoid fragments), overall moderate bioturbation index, and presence of vertical burrows suggests well-circulated, normal marine conditions during deposition. Facies 3 is interpreted to represent mid- to outer-ramp sediments deposited under low to moderate energy settings.

Facies 4 is a peloidal packstone to grainstone characterized by abundant fine sand-sized peloids (50%), silt- to fine sand-sized quartz grains (35%), and skeletal debris (15%) composed of crinoid, brachiopod, and lesser amounts of bryozoan fragments. The presence of diverse and more abundant skeletal material suggests well-circulated, normal marine conditions during deposition. Facies 4 is interpreted to represent deposition within the mid-ramp or distal portion of the ramp crest environment near fair weather wave base, proximal to skeletal shoals.

Facies 5 is a skeletal packstone to grainstone characterized by disarticulated, very fine- to medium sand-size brachiopod, crinoid, bryozoan, and siliceous sponge spicule skeletal debris. Cross-bedding, occasional hummocky and swaley cross stratification, and inclined bedding planes are commonly observed in core. Intermittent muddy intervals, burrowed firmgrounds, bioturbated intervals, and shell beds are also occasionally observed. The presence of cross bedding and truncation surfaces suggests that Facies 5 may have been deposited in an active portion of a skeletal shoal, however intermittent mud-rich intervals suggest a more likely interpretation of a distal expression of a skeletal shoal complex. Hummocky cross-stratification indicates that

deposition was occasionally influenced by storm processes (Middleton et al., 2003) which has likely caused autocyclic deposits in some vertical successions. Facies 5 is distinguished from Facies 4 by its relative larger grain size and the presence of high energy bedforms and is interpreted to represent deposition within the mid-ramp or distal portion of the ramp crest environment.

By utilizing an idealized stacking pattern, LeBlanc updated her original cycle hierarchy to a revised framework (Figure 4). Due to a lack of biostratigraphic data, the hierarchy only reflects relative cyclicity without a means to temporally constrain the periodicity. This first order interpretation served as the framework for isotope sampling and provides a fundamental tie back to sequence stratigraphy allowing for a true chemostratigraphic approach to be applied.

4.5 Results and Interpretations

Note: Results display Adkisson #1-33 data only. For Winney #1-8 and Elinore #1-18 data, see discussion in Chapter VI Extended Discussion- 6.3 Inter-Core Variability

4.5.1 Bulk Data

Three hundred and sixty-four bulk sample powders yielded $\delta^{13}C$ and $\delta^{18}O$ values from -4.54 to +3.53‰ and -8.28 to -0.41‰ respectively. These values are somewhat consistent with Mississippian seawater values from Mii et al. (1999), however many $\delta^{18}O$ values and some $\delta^{13}C$ values plot outside of this range in relatively depleted fields ($\delta^{18}O$: -4.0 to -6.25‰ and $\delta^{13}C$: +1.0 to -4.5‰; Figure 7).

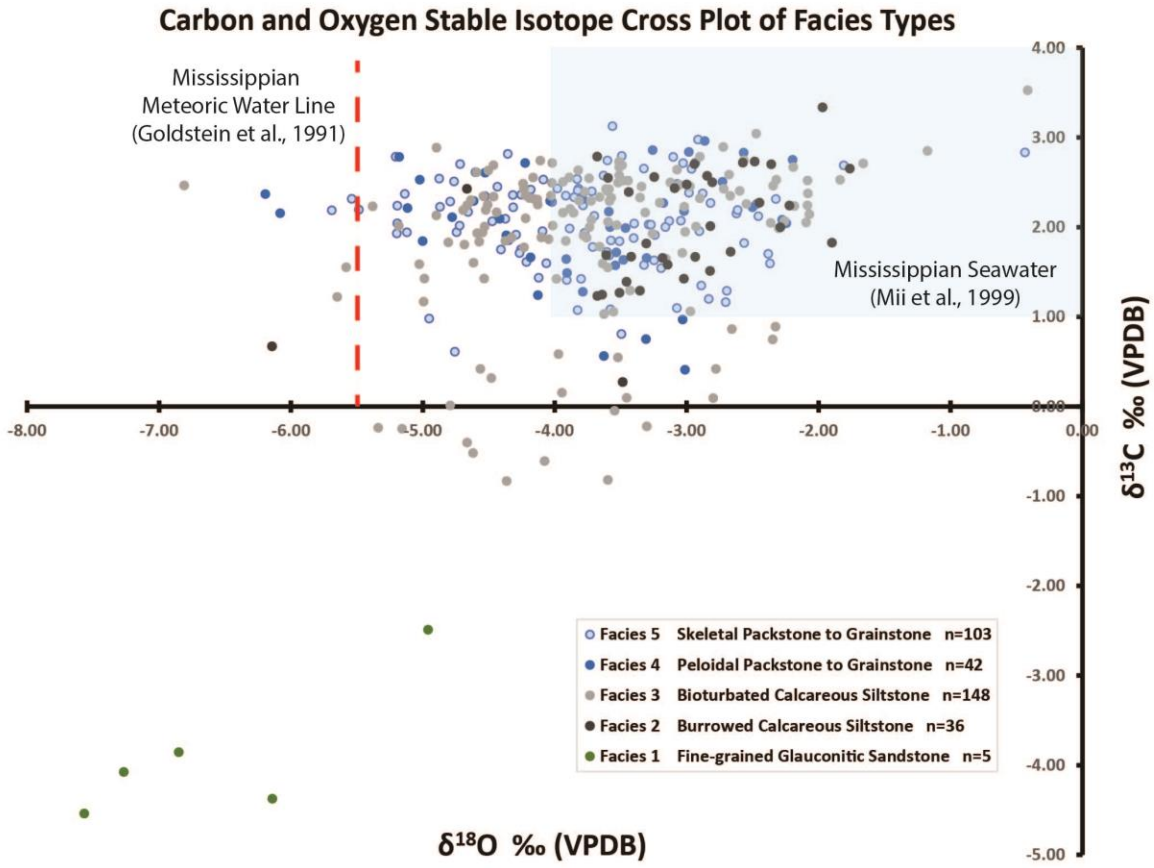

Figure 7. Carbon and oxygen stable isotope cross plot of five facies types including Mississippian seawater box from Mii et al. (1999) and Mississippian meteoric water line from Goldstein et al. (1991). 364 bulk sample powders yielded $\delta^{13}C$ and $\delta^{18}O$ values from -4.54 to +3.53‰ and -8.28 to -0.41‰ respectively. Note overall lack of variability between individual facies types and significant portion of data plotting outside of the Mississippian seawater box in relatively depleted fields.

4.5.2 Reinterpretation of "3rd Order" Sequences

Incorporating high resolution stable isotopic data with gamma ray signatures and facies relationships resulted in a new, chemostratigraphically-driven interpretation of 3rd order cyclicity for the Adkisson #1-33 (Figure 8). The criteria for choosing new 3rd order sequence boundaries are high gamma ray values (>50 API), shallowing-upwards facies

successions, and depletions <1.5 meters (5ft) below and enrichments <1.5 meters (5ft) above newly defined boundaries in $\delta^{13}C$ and $\delta^{18}O$. Thirteen 3rd order sequences have been identified using these criteria and suggest more frequent 3rd order cyclicity than previously interpreted (Figure 4). If all four North American stages are present, the reinterpreted section also suggests a loose correlation with globally recognized 3rd order sequences from Haq and Schutter (2008) (Figure 5). Of the thirteen newly identified 3rd order sequences, two are hypothesized as Kinderhookian, three as Osagean, four as Meramecian, and four as Chesterian. Deviations from this pattern (eg. abbreviated Kinderhookian, Osagean, and Chesterian strata) may be due to non-deposition or erosion associated with the Mississippian Pennsylvanian unconformity.

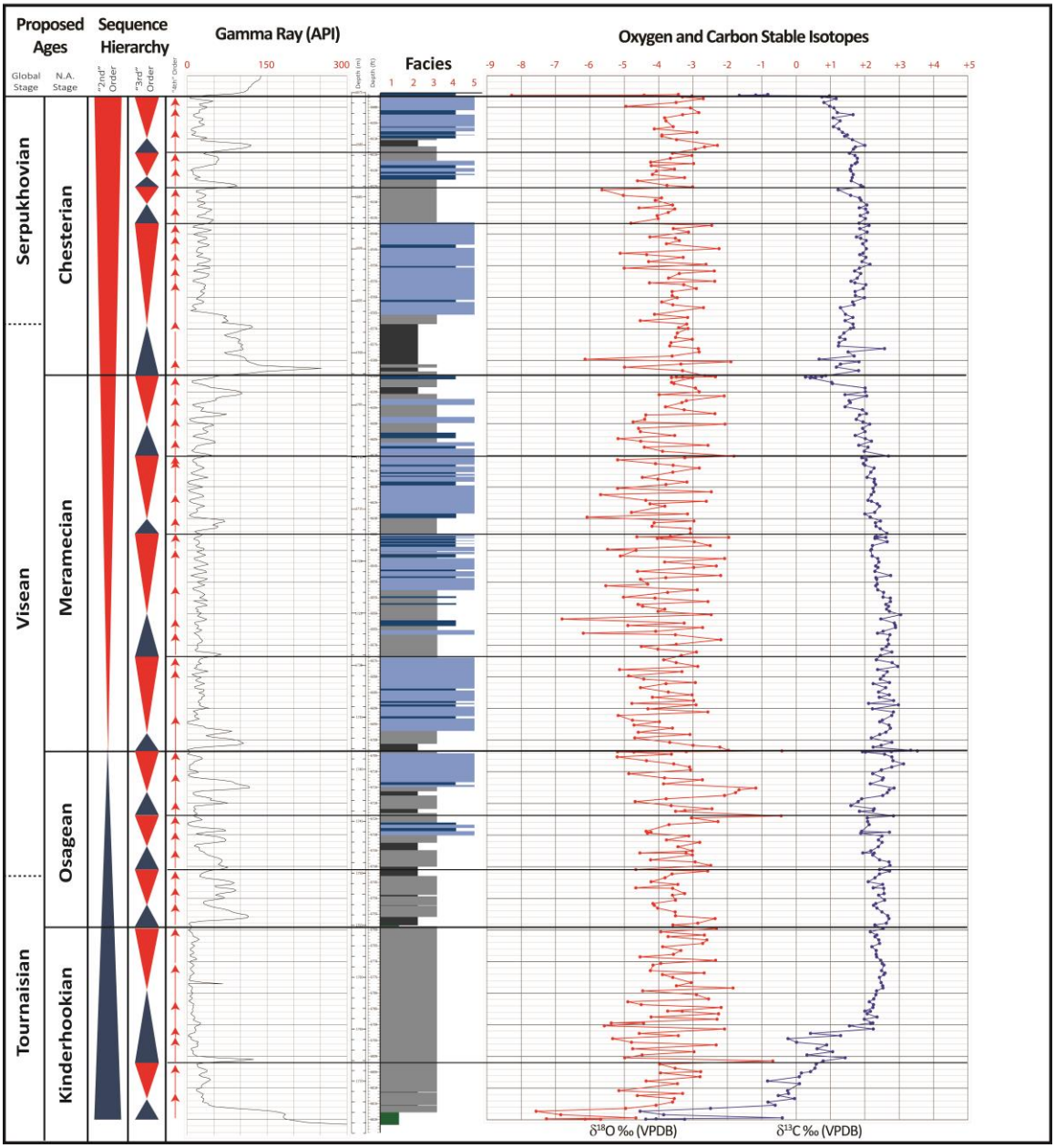

Figure 8. Chemostratigraphic interpretation of cycle hierarchy for the Adkisson #1-33. 3rd order sequence boundaries are defined using three criteria: high gamma ray signature (>50 API), shallowing upward facies succession, and carbon and oxygen stable isotopic data. North American stages are assigned through literature comparisons and observed trends in isotopic data. 4th order high frequency cycles are defined by relative depletions in $\delta^{18}O$ towards cycle tops in conjunction with higher order facies changes and cleaning upward gamma ray signature.

4.5.3 Signal Preservation and Diagenetic Considerations

Although there is a high potential for signal noise as a result of (1) the age (late Paleozoic) of these samples, (2) the bulk sediment sample type, and (3) post depositional diagenetic changes, there are observable trends in the vertical profile of the Adkisson #1-33. Overall, despite samples being derived from bulk sediment, some of the $\delta^{13}C$ and $\delta^{18}O$ values agree well with Mississippian seawater values derived from non-cathodoluminescent brachiopod shell data reported by Mii et al. (1999) (Figure 7). Mii et al. (1999) report $\delta^{13}C$ and $\delta^{18}O$ stable isotope profiles that likely reflect unaltered Mississippian seawater due to their strict preservation criteria (thin section petrography, SEM imaging, cathodoluminescence, and trace element analysis) in brachiopod shell sampling. Although some authors argue the validity of cathodoluminescence as reliable preservation criteria (Banner and Kaufman, 1994), Mii et al. (1999) report additional trace element data (Sr ratios specifically) that are in agreement with previous studies supporting the unaltered condition of the brachiopod shells.

There is a significant portion of the data, however, that plots outside of the suggested Mississippian seawater field, typically as more depleted $\delta^{13}C$ and $\delta^{18}O$ values. This effect is more pronounced in $\delta^{18}O$ values, which likely reflects the enhanced susceptibility of oxygen isotope alteration during water-rock interactions (Lohmann, 1988; Banner and Hanson, 1990) and often leads to the interpretation of an unreliable $\delta^{18}O$ curve. The data in this study, however, suggests that a pattern of depleted $\delta^{18}O$ values (~-5‰) in shallow water facies at the tops of shallowing upward successions

indicates an important chemostratigraphic relationship that may reflect mixed meteoric input near 3rd and potentially 4th order sequence boundaries. Moving average curves were constructed to minimize noise related to oxygen isotope susceptibility and also support the hypothesis of higher frequency cycles especially within larger 3rd order packages (Figure 9). Relatively depleted $\delta^{18}O$ values are similar to a meteoric water line (~-5.5‰) established from soil-formed microcomponents in subaerially exposed horizons in the Mississippian Holder Formation in New Mexico (Goldstein et al., 1991). Although there are no significant subaerial exposure horizons or pedogenic features present in the Adkisson #1-33, recent work in Kingfisher County to the immediate northwest has revealed multiple, well-developed exposure horizons characterized by dissolution pipes and chert breccia in a single core (Flinton, 2015). This suggests that Mississippian strata in the present study area could have been affected by some level of meteoric input and the difference (~0.5‰) in the $\delta^{18}O$ data from the Adkisson #1-33 may reflect a mixed value rather than a pure meteoric signal.

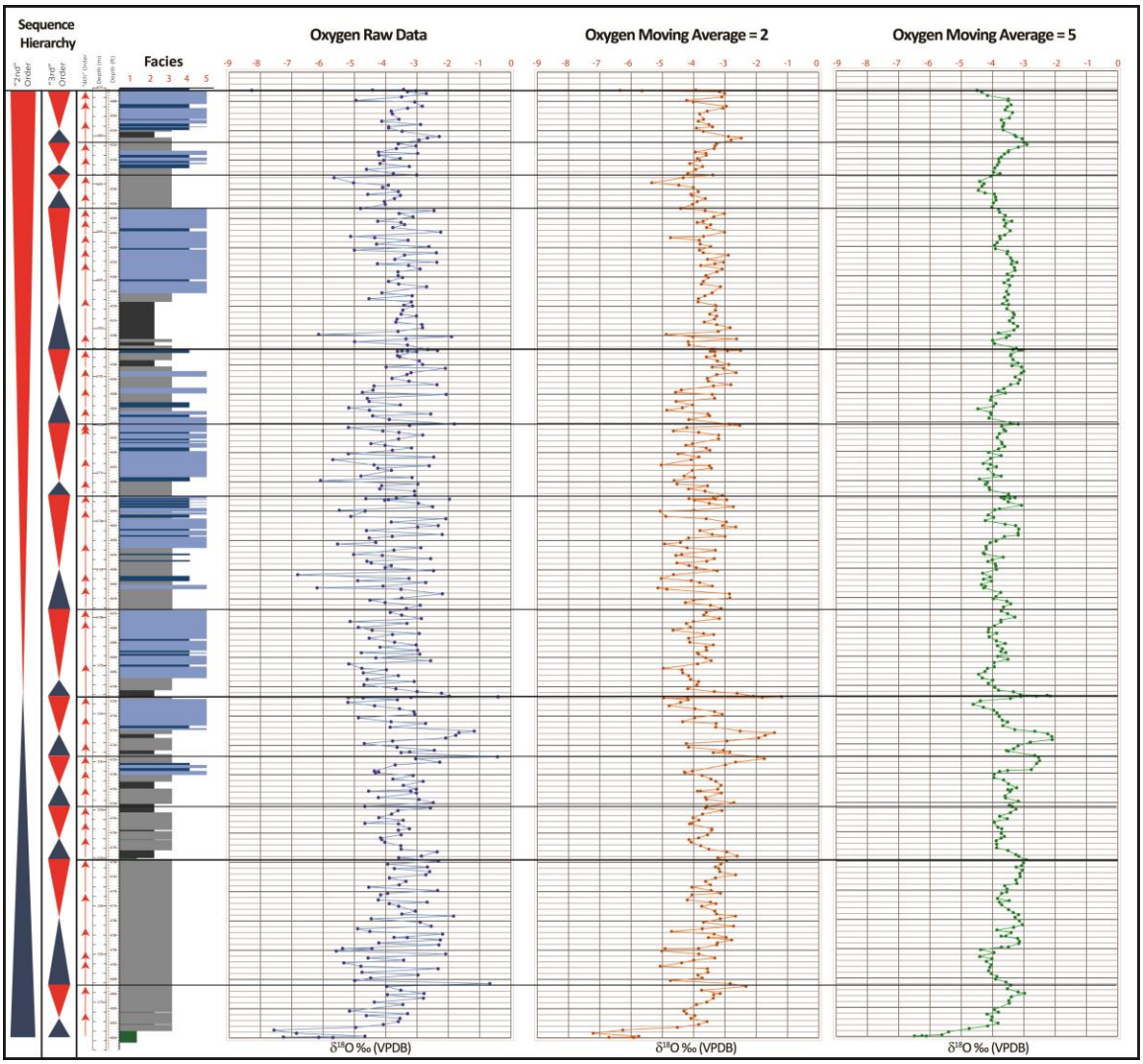

Figure 9. Revised chemostratigraphically-driven hierarchy for the Adkisson #1-33 with raw oxygen data and moving average curves. Note that moving average profiles reduce noise and suggest high-frequency cycles capped by depleted $\delta^{18}O$ values within larger 3rd order packages.

These findings are consistent with the diagenetic history established for the Adkisson #1-33, in which two types of early calcite cement were identified using thin section petrography and cathodoluminescence (T. Ewald, personal communication). Bladed, partially isopachous cement was reported most prevalent in Facies 4 and Facies 5 and interpreted to reflect rapid precipitation in a marine environment. Syntaxial blocky cement, reported most prevalent in Facies 5, was interpreted to represent

precipitation in reducing, marine phreatic environment (T. Ewald, personal communication). The higher position of facies within the stacking pattern and enhanced probability of being affected by mixed marine-meteoric waters likely caused a relatively depleted final $\delta^{18}O$ value to be recorded in some of these samples. This depletion is due to the fractionation between ^{16}O and ^{18}O wherein meteoric waters contain a higher percentage of ^{16}O relative to ^{18}O and results in a lighter, depleted $\delta^{18}O$ value (Lohmann, 1988). The enhanced diagenetic susceptibility of skeletal rich facies may also play a role in recording relatively depleted ^{18}O values as syntaxial blocky cement most commonly occurs as overgrowths on crinoid and brachiopod fragments (T. Ewald, personal communication). Alternatively, micrite-rich facies near the base of 3rd order sequences are less commonly affected by isopachous and fringing cements (T. Ewald, personal communication). Basal facies tend to plot within the seawater field established by Mii et al. (1999) and suggest the recording of a relatively unaltered seawater signal.

4.5.4 $\delta^{13}C$ Global Signal Potential

In addition to the patterns observed at the 3rd order scale, tentative ages have been assigned to the Mid-Continent profiles of this study using a compilation of literature datasets hypothesized to reflect global carbon cycling (Grossman, 1993; Bruckschen et al., 1999; Mii et al., 1999; Saltzman, 2003; Batt et al., 2007; Buggisch et al., 2008; Koch et al., 2014). Although it was not possible to direct the current samples to selective cements or shells that have not undergone diagenesis, the patterns and trends of isotopic composition within the bulk samples are comparable to published

curves of the individual Mississippian stages and show similar variations in isotopic composition that are often attributed to local paleogeographic factors in other Mississippian sections (Grossman, 1993; Bruckschen et al., 1999; Mii et al., 2001; Grossman et al., 2008). Figures 8 and 10 depict each of the proposed North American stages that are characterized by specific $\delta^{13}C$ trends that resemble assumed global patterns.

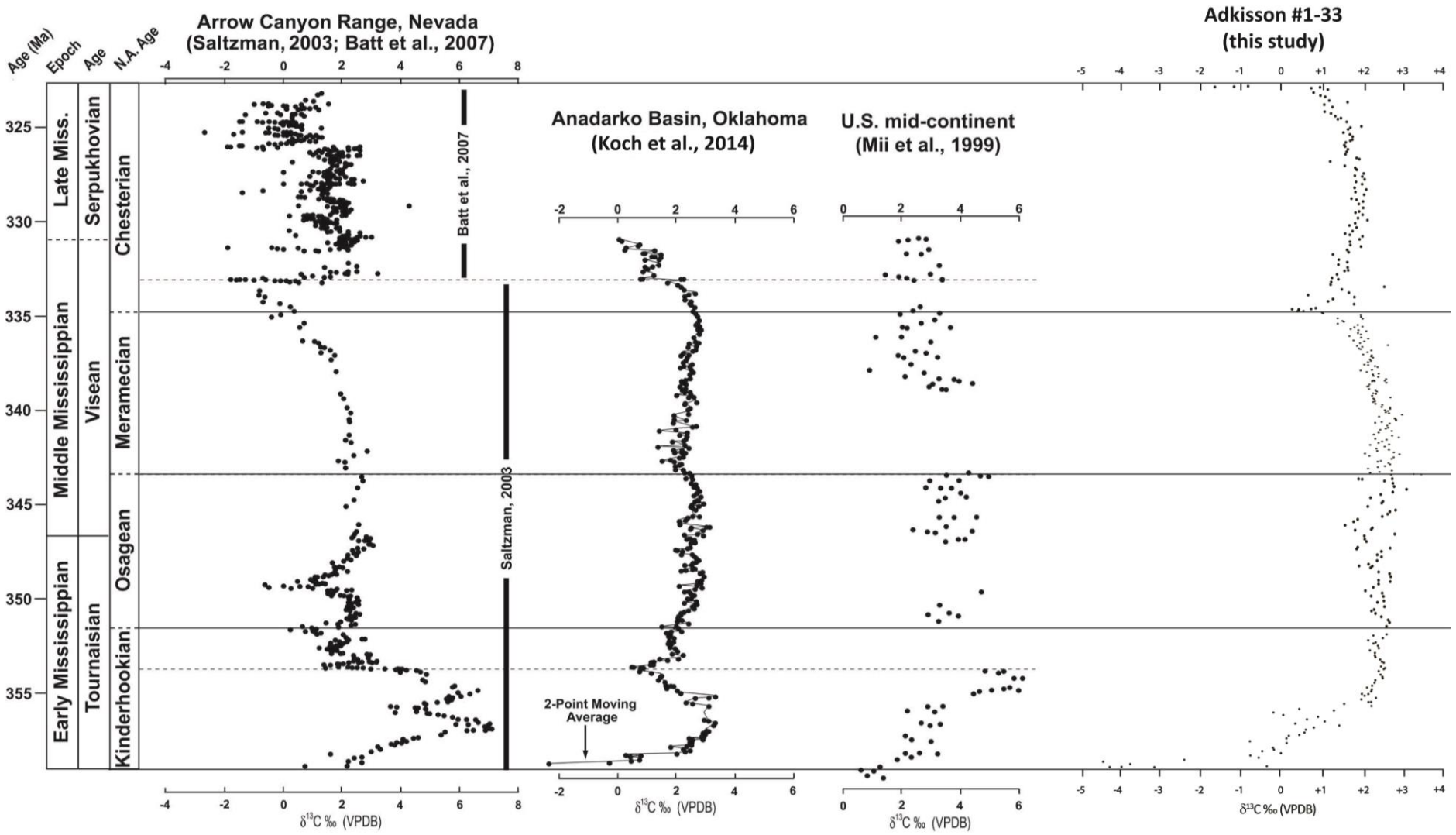

Figure 10. Carbon stable isotope profiles depicting Mississippian global carbon signatures for each North American Stage. Note similarities in early Kinderhookian positive shifts in all four curves, stabilization during Osagean and Meramecian strata, and negative shifts in Late Meramecian-Early Chesterian strata. Modified from Koch et al. (2014).

4.5.4.1 Kinderhookian

The proposed Kinderhookian stage records a positive $\delta^{13}C$ excursion from -4.54‰ near the base to +2.53‰ near the top (difference +7.07‰). This is the most significant excursion of the dataset and resembles the well-known positive shift in the Early to Middle Tournaisian (Bruckschen et al., 1999; Mii et al., 1999; Saltzman, 2003; Buggisch et al., 2008; Koch et al., 2014). This excursion, often covariant with $\delta^{18}O$, is hypothesized to represent a significant alteration in carbon cycling, the causality of which is strongly debated among different authors. Although the Mid-Continent excursion in this study begins with the most depleted $\delta^{13}C$ of published values (-4.54‰) and only achieves a slightly positive maximum value (+2.53‰), the magnitude of the shift (~+6-7‰) is consistent with previous studies. Koch et al. (2014) report a similar excursion from -2.3‰ to +3.3‰.

A marked $\delta^{13}C$ depletion from ~+1.5 to -0.25‰ (difference -1.75‰) occurs near the middle of the proposed stage and is consistent with a Middle to Late Kinderhookian negative excursion present in global profiles (Mii et al., 1999; Saltzman, 2003; Koch et al., 2014). Recent outcrop-based carbon and oxygen stable isotope work in the Tri-state region of northeastern Oklahoma, southwestern Missouri, and northwestern Arkansas suggests this negative excursion may be related to the deposition of the Late Kinderhookian Northview Formation (Sessions et al., this volume). The excursion has been dated through the use of high-resolution biostratigraphy (Sessions et al., this volume; Boardman et al., 2013) and similarities in the isotope curves suggests the

presence of Middle to Late Kinderhookian strata in the Adkisson #1-33. The subsequent enrichment seen in the Mid-Continent data of the present study is also somewhat consistent with the slow enrichment of the Late Kinderhookian Pierson Formation near +2.0‰ $\delta^{13}C$ of Sessions et al. (this volume). The similarity in observed trends, including the major positive excursion early in the stage, the negative excursion in the middle to late stage, and the stabilization near +2-3‰ later in the stage, suggests a correlation with established global profiles and recent Mississippian Mid-Continent work in the Tri-state region (Saltzman, 2003; Mii et al., 1999; Koch et al., 2014; Sessions et al., this volume).

The thickness of the proposed Kinderhookian unit (18.3m (~60ft)) is consistent with the depositional model of diachronous, prograding carbonate wedges proposed for the northeastern Oklahoma, southwestern Missouri, and northwestern Arkansas Tri-state region for Lower to Middle Mississippian strata (Boardman et al., 2013). Outcrop-based sequence stratigraphy in this proximal position suggests the Kinderhookian thickness ranges from 3m (9.8ft) to 5.5m (18ft) (Childress and Grammer, 2015, Childress, this volume, Sessions et al., this volume), however the relative distal positioning of the Adkisson #1-33 likely recorded a thicker section of Kinderhookian strata as prograding clinoforms continued to the southwest into the basin. In addition to variable sedimentation rates and preservation related to the more distal positioning, syndepositional faulting associated with the Nemaha Uplift may also have created additional accommodation space that allowed sediment to be funneled into local depositional lows (LeBlanc, 2014) resulting in the deposition of a relatively thick

Kinderhookian section. In their work to the immediate northwest in Garfield County, Koch et al. (2014) also report a thick Kinderhookian interval (36.6m (~120ft)) based on global patterns recognized in $\delta^{13}C$.

4.5.4.2 *Kinderhookian Osagean Boundary*

The boundary between the proposed Kinderhookian and Osagean stages is characterized by a high gamma ray signature (>100 API units) and the occurrence of Facies 1 (glauconitic sandstone). Isotopic data does not show significant enrichments or depletions associated with this boundary, however lack of geochemical evidence is common across this horizon, particularly in other Mid-Continent studies (Mii et al., 1999; Koch et al., 2014). Therefore, the assignment of this boundary relies primarily on gamma ray and facies data, both of which support a significant alteration in deposition from relatively well oxygenated Facies 3 (characterized by very low gamma ray values, <5 API units) to relatively restricted, oxygen poor Facies 1 (characterized by high gamma ray values, >100 API units).

Using the criteria established by Amorosi (2012), the glaucony present at this horizon is characteristic of a simple omission surface. Preliminary energy-dispersive x-ray fluorescence data suggests the glaucony is relatively immature, characterized by a low percentage (2-3%) of K_2O and is reflected in the sample's light green "nascent" hue. Although the glaucony is not representative of a mega condensed, globally correlative surface, this may represent a relatively proximal expression of the same surface. In this case, the relatively thin (~6cm) deposit would not have experienced the same

magnitude or duration of restriction and would have relatively immature glaucony compared to exclusively basinal deposits. Induced coupled plasma mass spectrometry and oriented XRD mounts are needed to confirm K_2O weight percentages and clay mineralogy with confidence. Additionally, Facies 1 is not present after its occurrence at this horizon, which may further support a significant deepening episode.

4.5.4.3 *Osagean*

The proposed Osagean stage is characterized by a relatively stable $\delta^{13}C$ profile between +2.0 and +3.0‰ with high amplitude changes (up to 1‰ shifts in 3.05m (10ft)) occurring in the uppermost 7.6m (25 feet) (Figure 8). This relatively stable profile is similar to that of Koch et al. (2014) wherein Late Tournaisian and Early Visean strata maintain an average 1‰ range in $\delta^{13}C$ values for the entire stage. Conversely, Buggisch et al. (2008) and Saltzman (2003) report stability only during the late Osagean and more frequent excursions (up to 2‰ $\delta^{13}C$) near the basal Kinderhookian boundary. The variability in the uppermost portion of both $\delta^{13}C$ and $\delta^{18}O$ profiles may be related to more frequent depositional cyclicity driven by sea level change and enhanced facies variability due to the diagenetic susceptibility of shallower water facies. Although $\delta^{13}C$ values are less susceptible to diagenetic alteration compared to $\delta^{18}O$ (Banner and Kaufman, 1994), repeated exposure to relatively depleted, mixed marine-meteoric water may have caused a slight (0.5-1‰) lowering of $\delta^{13}C$. This is consistent with the systematic depletion of both $\delta^{13}C$ and $\delta^{18}O$ in the 1.5 meters (5ft) below the Osagean Meramecian stage boundary, which may be evidence of repeated exposure to depleted

waters. Carbon isotopes also tend to be covariant with $\delta^{18}O$ over this interval, which may suggest the influence of higher frequency, potentially 4th order, cyclicity (discussed in later section). The $\delta^{18}O$ curve also shows a relative depletion from base to top, which may reflect more mixed marine-meteoric input towards the top of the section overall. These isotopic trends, in conjunction with a cleaning-upward gamma ray signature, are consistent with the overall shallowing-upward facies succession towards the end of the stage and the diagenetic history for shallow water facies.

4.5.4.4 *Osagean Meramecian Boundary*

The boundary between the proposed Osagean and Meramecian stages is characterized by the above-mentioned depletion immediately below and a marked enrichment immediately above in both $\delta^{13}C$ and $\delta^{18}O$ values (Figure 11). Although there is a general lack of geochemical evidence for this boundary in the literature, the enrichment may signify an important flooding surface. Katz et al. (2007) report $\delta^{13}C$ curves of Lower Mississippian strata across 3rd order sequences that exhibit the highest values of enrichment at maximum flooding surfaces in relatively distal positions within the depositional system. The proposed boundary is characterized by the most enriched values of the dataset (+3.53‰ $\delta^{13}C$ and -0.41‰ $\delta^{18}O$), records +1.6‰ and +4.79‰ shifts in $\delta^{13}C$ and $\delta^{18}O$ respectively, and based on facies present, occurs in a relatively distal position on the distally-steepened ramp. Based on the newly defined chemostratigraphic framework, this enrichment may represent a horizon on the composite sequence scale, larger than the 3rd order scale excursions reported in Katz et

al. (2007), but smaller than the single, 2nd order sequence of the entire Mississippian. Smaller positive enrichments (+0.5 to +1‰) in $\delta^{13}C$, similar in scale to Katz et al. (2007), also occur in the transgressive portion of the newly defined 3rd order sequences in the Osagean strata leading up to this boundary. These may represent several deepening upward episodes evidenced by high gamma ray signatures (50-100 API units) and the repeated occurrence of Facies 2. Overall, this additional evidence suggests the expression of relatively restricted, potentially deeper water horizons with the most significant deepening episode occurring at the proposed stage boundary. This is consistent with regional findings of Curtis and Champlin (1959) wherein an early Meramecian marine transgression was suggested to have caused the submergence of most of Oklahoma and resulted in deposition of relatively restricted facies.

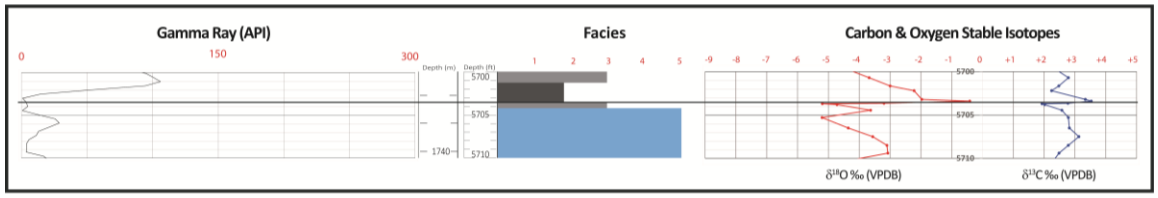

Figure 11. Proposed Osagean Meramecian boundary characterized by a systematic depletion in isotope values in the 1.5 meters (5ft) below and a rapid enrichment in the 0.3 meters (1ft) above the boundary. This transition may be the geochemical expression of repeated exposure to relatively depleted, mixed marine-meteoric waters below sequence boundary and the following marine transgressive surface characterized by enriched isotope values (+3.53‰ and -0.41‰ in $\delta^{13}C$ and $\delta^{18}O$ respectively).

4.5.4.5 *Meramecian*

The proposed Meramecian stage is characterized by a relatively stable $\delta^{13}C$ profile between +2.0 and +3.0‰ in the lowermost 9.14m (30ft), a steady depletion from +3.04 to +0.27‰ (difference -2.77‰) in the uppermost 23 meters (75ft), and a marked

depletion from +2.05‰ to +0.44‰ (difference -2.49‰) occurring in the last 1.5 meters (5ft) (Figure 8). A similar depletion is recorded in Upper Meramecian and Lower Chesterian strata with the most depleted $\delta^{13}C$ values occurring near the Meramecian-Chesterian boundary (Mii et al., 1999; Saltzman, 2003; Batt et al., 2007; Koch et al., 2014). It has been suggested that the Meramecian-Chesterian $\delta^{13}C$ decline may be due partly to the growth of the organic carbon reservoir and partly to intensified eastern Panthalassan upwelling in response to the closure of the seaway between Laurussia and Gondwana (Popp et al., 1986; Mii et al., 1999). Alternatively, a minor regression proposed by Curtis and Champlin (1959) in the Late Meramecian may be the result of potential facies driven effects related to diagenetic susceptibility of shallow water facies causing an overall depletion in $\delta^{13}C$ values. This pattern is somewhat consistent with the current dataset as the proposed Meramecian stage is characterized by the highest percentage of shallow water facies and has the most consistently depleted $\delta^{18}O$ values of any other stage. However, the Late Meramecian of the present study is characterized by a relatively higher percentage of deeper water facies and relatively enriched $\delta^{18}O$ values compared to the early and middle portions of the stage. This suggests influences other than repeated exposure to mixed meteoric waters, at least at the very top of the section near the Chesterian boundary. Global influence may have had more of an impact on isotopic signature at this portion of the stage which is consistent with seawater signal preservation in deeper water facies.

4.5.4.6 *Meramecian Chesterian Boundary*

The proposed Meramecian-Chesterian boundary is characterized by a marked depletion in $\delta^{13}C$ (-1.74‰ over 1.2m (4ft)) just below and an enrichment in $\delta^{13}C$ (+1.55‰ over 0.9m (3ft)) just above (Figure 8). A lack of a distinct shallowing upward facies package and relatively enriched $\delta^{18}O$ values beneath the boundary suggest a deviation from the pattern of potential mixed marine-meteoric input at 3rd order sequence boundaries seen downsection. Clean gamma ray signature (~15 API units), occurrence of Facies 4, and significantly depleted $\delta^{13}C$ values at the top of the Meramecian suggest a carbonate-dominated deposit that may have been altered due to repeated mixed meteoric input, however enriched $\delta^{18}O$ values do not agree with this hypothesis. It may be possible that the relatively enriched $\delta^{18}O$ values, which are consistent with Mississippian seawater field established by Mii et al. (1999), and slightly depleted $\delta^{13}C$ values collectively represent microbial sulfate reduction despite their occurrence in a relatively shallow facies. This may be associated with the suggested deepening in the early Chesterian (Curtis and Champlin, 1959) evidenced by the large deposit of relatively restricted Facies 2 and high gamma ray signature (>50 API units). Slightly depleted $\delta^{13}C$ values may also reflect times of enhanced oxidation of organic matter (Swart, 2015), which may be more consistent with glacio-eustatic changes of the Late Mississippian. The discrepancy in the two curves may also be the result of the dominance of a global $\delta^{13}C$ signal during the Late Meramecian, which may not be recorded in $\delta^{18}O$ values.

The enrichment in $\delta^{13}C$ values above the boundary is of similar magnitude (+1.5‰) reported in Late Visean-Early Serpukhovian strata, which is hypothesized to represent a climatic link between enhanced organic carbon burial and potential onset of glaciation during the Serpukhovian (Buggisch et al., 2008). Additionally, basinal subsidence is suggested to have been much greater during the Chesterian relative to earlier Mississippian stages (Curtis and Champlin, 1959), which may have enhanced the distribution of relatively restricted facies and caused increases in the burial rate of organic carbon. This is consistent with the large (3.65m (~12ft)) deposit of Facies 2 that occurs at the base of the proposed Chesterian section, which is also characterized by the highest gamma ray values (100-250 API units) of the entire dataset. The rapid depletion in $\delta^{18}O$ values just above the boundary may be related to mixed marine-meteoric signatures in deep water facies associated with rapid and high amplitude sea level fall. Large drops in sea level, which were likely more frequent during Late Mississippian, may have caused deep water facies to be uncharacteristically exposed to mixed marine meteoric waters. Alternatively, the rapid depletion may be evidence of hydrothermal input, however the magnitude of the shift would likely be in the -10‰ range as opposed to only -6 to -7‰. Recent fluid inclusion work (Mohammadi and Gregg, this volume) suggests the likelihood of at least some alteration by basinal fluids in Mid-Continent Mississippian sections, which may also cause relatively depleted isotope values. Additional analysis of this boundary is needed to delineate the high frequency changes and discrepancy between the two isotope curves.

4.5.4.7 *Chesterian*

The proposed Chesterian stage is characterized by an early-stage, gradual enrichment in $\delta^{13}C$ from +0.27 to +2.15‰ (difference +1.88‰), a mid-stage stabilization at approximately +2.0‰ (~0.4‰ range), and a late-stage, gradual depletion from +1.89 to +0.97‰ (difference -0.92‰) (Figure 8). This high-resolution pattern is somewhat unique compared to global datasets, however the general trend of relatively depleted (~+1‰) $\delta^{13}C$ values is similar to patterns recognized in the Mid-Continent (Mii et al., 1999; Koch et al., 2014). The gradual depletion in $\delta^{13}C$ in the uppermost 10 meters (33ft) may be related to an increase in higher order cyclicity, however relatively enriched $\delta^{18}O$ values again do not support the hypothesis of increased exposure to depleted, mixed marine-meteoric waters. Alternatively, the more frequent preservation of Mississippian seawater values suggests less diagenetic alteration in shallow water facies as both $\delta^{13}C$ and $\delta^{18}O$ values tend to plot within the Mississippian seawater field of Mii et al. (1999). The lack of mixed marine-meteoric signature in Facies 5 may support a Chesterian section frequently affected by storm related events. In this case, the repeated deposition of Facies 5 in a relatively distal position with a lack of mixed influence would produce a relatively stable $\delta^{18}O$ profile consistent with Mississippian seawater values that have not been diagenetically altered. This is consistent with increased basinal subsidence suggested for Chesterian strata, thus this portion of the section may actually record a relatively deep deposit of large autocyclic packages between fair weather and storm wave base.

The most depleted $\delta^{18}O$ value of the entire dataset occurs just below the Chesterian-Pennsylvanian boundary (-8.28‰) and records a negative shift of -5.25‰ over only ~0.15 m (0.5ft). $\delta^{13}C$ values are also significantly depleted (-1.65‰) and record a shift of -2.62‰ over the same footage. Extensive fluid inclusion work in Mississippian Mid-Continent rocks in south-central Kansas suggests late hydrothermal alteration of the upper Mississippian associated with the retardation of hot basinal brine migration at the low porosity, low permeability Pennsylvanian shale contact (Goldstein, this volume). Although this is characteristic of only one sample, the two samples above the boundary are also relatively depleted ($\delta^{13}C$: -1.17, -0.82‰ and $\delta^{18}O$: -4.43, -3.43‰), especially in $\delta^{13}C$ relative to the majority of the dataset.

4.5.6 $\delta^{18}O$ High Frequency Cycles and "4th Order" Potential

Traditionally, $\delta^{18}O$ data from bulk sediment without comparison to a suite of targeted sample types (cement, unaltered shells, micrite) has not been considered for characterizing stable isotope values of Mississippian strata. Although there is considerable variability in the $\delta^{18}O$ data of this study, with values that range from -0.41‰ to -8.28‰ and can change rapidly (up to 5.25‰) over short transects (0.3m (<1ft)), there is a discernable pattern of high frequency cycles that are characterized by relatively enriched bases (~-2.0‰) and relatively depleted tops (~-5.0 to -6.0‰) (Figure 9). Forty-four of these cycles, characterized by depleted $\delta^{18}O$ values near the top, have been identified and are hypothesized to reflect high frequency, potentially 4th order, shallowing-upward cycles that have been affected by mixed marine-meteoric input at

cycle tops. Shallowing-upward cycles tend to be capped by shallow water facies, and plot in relatively depleted fields relative to the Mississippian seawater box (Figure 12). The suggestion of repeated exposure to relatively depleted waters is consistent with subregional findings of Flinton (2015) wherein multiple subaerial exposure horizons were identified in a single core. Although there are no exposure horizons recognized in the Adkisson #1-33, the potential for exposure to mixed meteoric waters is probable within this area of the depositional system and likely occurs at multiple scales related to the stratigraphic hierarchy.

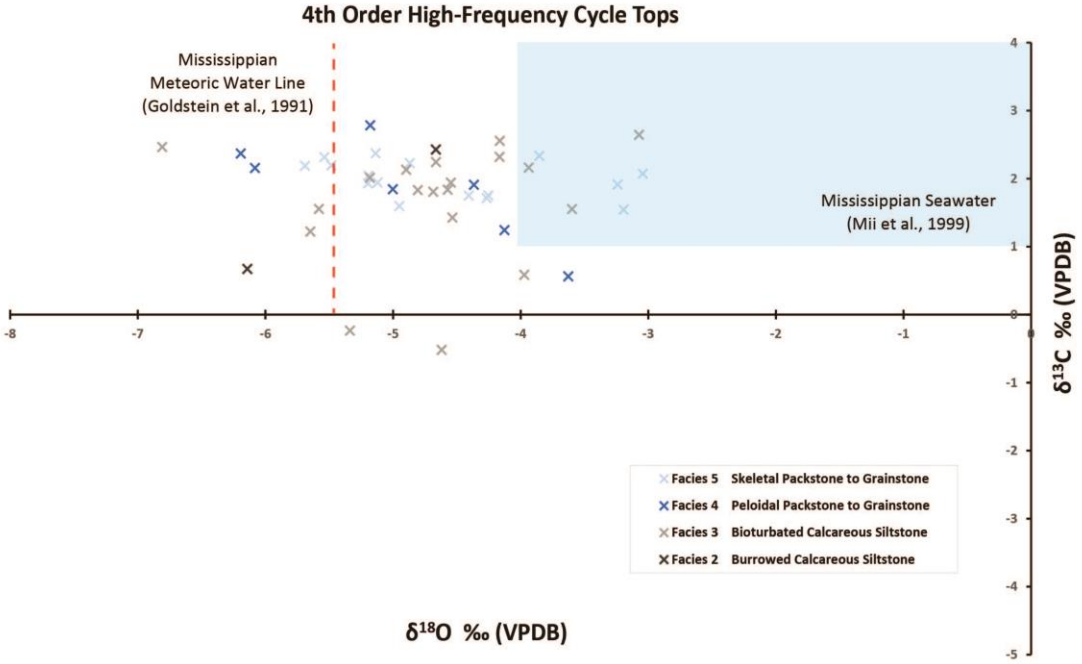

Figure 12. Cross plot of 4th order high-frequency cycle tops with facies denoted by colored x's. Cycles tend to be capped with shallow water facies and plot in relatively depleted fields relative to Mississippian seawater suggesting mixed marine-meteoric input at these horizons.

High frequency cycles may or may not be characterized by a cleaning-upward gamma ray signature, which suggests a resolution limitation of gamma ray curves at this

scale. Although some cycles are picked more confidently than others, patterns seen in $\delta^{18}O$ values may be extremely useful in defining higher order cyclicity that may not be predicted using facies and gamma ray data alone, especially in distal areas of the depositional system where subaerial exposure surfaces are lacking. This has important consequences when considering the potential for cemented, flow baffling horizons that can compartmentalize reservoir units that may not be identified based on stacking patterns alone.

4.6 Conclusions

Overall, the relative distal position of the study area has important consequences for isotopic signatures reported herein. It is difficult for samples only experiencing marine diagenesis (and potentially some mixed meteoric) to become significantly altered from original $\delta^{13}C$ values, thus facies deposited below average sea level fall for the particular period are preferred for chronostratigraphy because they avoid most diagenetic effects (Swart, 2015). This suggests the $\delta^{13}C$ curve in this study may indeed retain a global signal despite being derived from mixed input, bulk sediment. Although there are shallow water facies present, there are no significant exposure horizons in the Adkisson #1-33, thus the study area may represent a relatively ideal location for developing a chronostratigraphic tie. Assuming a full Mississippian section, the Adkisson #1-33 also lacks significant exposure despite the switch from probable low amplitude (10m) sea level change during early Mississippian to high amplitude (75-100m) changes during late Mississippian (Read, 1995), unlike cores in

neighboring Kingfisher County where several exposure horizons are developed in a single core. This may support syndepositional faulting associated with the Nemaha Uplift wherein the downthrown block (Logan County) created more accommodation space and funneled sediment into a local depocenter while the upthrown block (Kingfisher County) experienced simultaneous episodes of subaerial exposure (Flinton, 2015). Evidence for this type of subregional variability in diagenetic history, indicated here by carbon and oxygen isotopic values, may be crucial for understanding reservoir compartmentalization and porosity evolution related to meteoric and mixed marine-meteoric input over relatively short distances.

The integration of high-resolution carbon and oxygen stable isotope profiles with gamma ray curves, high-resolution sequence stratigraphy, and diagenetic history has revealed key patterns that can be used to delineate potential global signatures and Milankovitch band cyclicity and with a chemostratigraphic approach. A refined interpretation of the Adkisson #1-33 suggests more frequent 3rd order cyclicity than previously defined which is more consistent with global ties to the individual North American stages and within the Mississippian overall. Incorporation of biostratigraphic data (Hunt, in progress) will help further constrain the accuracy of these isotopic trends and further aid in correlation efforts.

Although there are a significant number of data points that plot outside of the Mississippian seawater field established by Mii et al. (1999), the incorporation of the diagenetic history suggests new 4th order boundaries related to mixed marine-meteoric

input at cycle tops. Overall, this high frequency pattern recognized in $\delta^{18}O$ values may provide important insight where facies data cannot especially in distal areas of the depositional system where subaerial exposure surfaces are lacking. A fundamental component in understanding reservoir distribution is appreciating the level at which subsurface units can be compartmentalized, especially in a mixed lithology system. The integrated chemostratigraphic approach applied in this study provides key insight in enhancing the predictability of subsurface units in terms of reservoir heterogeneity and how relates to geochemical trends and high-resolution sequence stratigraphy.

CHAPTER V

ENERGY DISPERSIVE X-RAY FLUORESCENCE

5.1 Analyses and Unconventional Applications

X-ray fluorescence spectrometry (XRF) is a method commonly used to determine major and trace elements in a wide variety of geological samples. XRF is one of the few analytical techniques in which these elemental determinations can be made on solid samples. This is one of the major benefits of XRF as it avoids the dissolution stage that is a prerequisite for most other atomic spectroscopy methods of similar sensitivity (Potts and Webb, 1992). Energy-dispersive x-ray fluorescence (ED-XRF) systems are well known for their ability to perform extremely rapid qualitative and semi-quantitative analysis of both major and trace elements (Potts and Webb, 1992). The energy dispersive distinction is based on the type of spectrometer within the device that simultaneously detects the polychromatic spectrum of fluorescent x-rays (Potts and Webb, 1992). Advancements in instrumentation have allowed for more rapid and precise analyses and unconventional reservoir characterization has been a major focus for recent hydrocarbon exploration efforts (Rowe et al., 2012; Ramkumar, 2015).

After data collection, elements are often compared in the form of ratios, on ternary diagrams, or by applying statistical analysis to help generate geochemical proxies regarding deposition (Alego et al., 2007; Rowe et al., 2012; Rowe et al., 2015). In addition to trace metal analysis, recent studies utilizing high-resolution XRF have begun to explore how elemental assemblages and mineral proxies can be used to predict rock brittleness (Chatellier et al., 2015).

5.2 Data and Methods

The same high-resolution sampling methods (approximately 0.3m (1ft)) used for stable isotope analysis were also utilized for ED-XRF analysis. Sample sites of carbon and oxygen isotopes match that of ED-XRF sites as close as physically possible as the carbon and oxygen samples were sourced from the back of the slab and ED-XRF samples from the face. ED-XRF data also includes high-resolution sampling of the lowermost 3rd order sequence defined by LeBlanc (2014) for the two cores (Winney #1-8; Elinore #1-18) located in Payne County (Figure 3).

Systems checks and calibrations with the USGS Cody Shale standard (SCo-1; crustal.usgs.gov) were performed every ten samples in order to monitor the quality of the analysis. Correction factors were used at a similar frequency to correct measurements that fell outside of one standard deviation. In instances where correction factors >1.6 were necessary for correction, this data was eliminated from further analysis. Given that ED-XRF data tends to be used for semi-quantitative analysis, there is potential for cross-checking samples with inductively coupled plasma analysis and mass

spectrometry (ICP-MS). ICP-MS techniques, although destructive and take longer to complete, can detect trace elements more accurately and to a more precise measurement than some ED-XRF devices (Hosseininejad et al., 2013). X-ray diffraction (XRD) data may be used to help guide mineralogical proxies, especially in areas where XRF data is unavailable.

5.3 Results and Interpretations

A total of 487 measurements were conducted on the three cores being evaluated. Unavailability of helium purge analysis, which is suggested for the measurement of light elements (Mg, Al, Si, P), likely affected the accuracy of these elements. Mg, Al, and P measurements required significant correction factors ranging from 0.25 to 3.96, which eliminated them from being confidently correlated. Almost all trace element data was below the limit of detection, which may be due to the resolution of the instrument or dilution by carbonate sediments. Data reported focuses on three major elements: Fe, Ti, and K which show relative enrichments at key horizons and correlate well with gamma ray and TOC measurements (Figure 13). Normalizing Fe measurements over Ti and K show that iron enrichment coincides with depositional evidence of more restricted Facies 1 and 2 with glauconite-bearing Facies 1 being the most enriched (Figure 14). Data from the Winney #1-8 (Figure 15) and Elinore #1-18 (Figure 16) do not display patterns recognized in the Adkisson #1-33 which is likely due to abbreviated datasets resulting from instrument malfunction. Low resolution datasets are most useful in these areas.

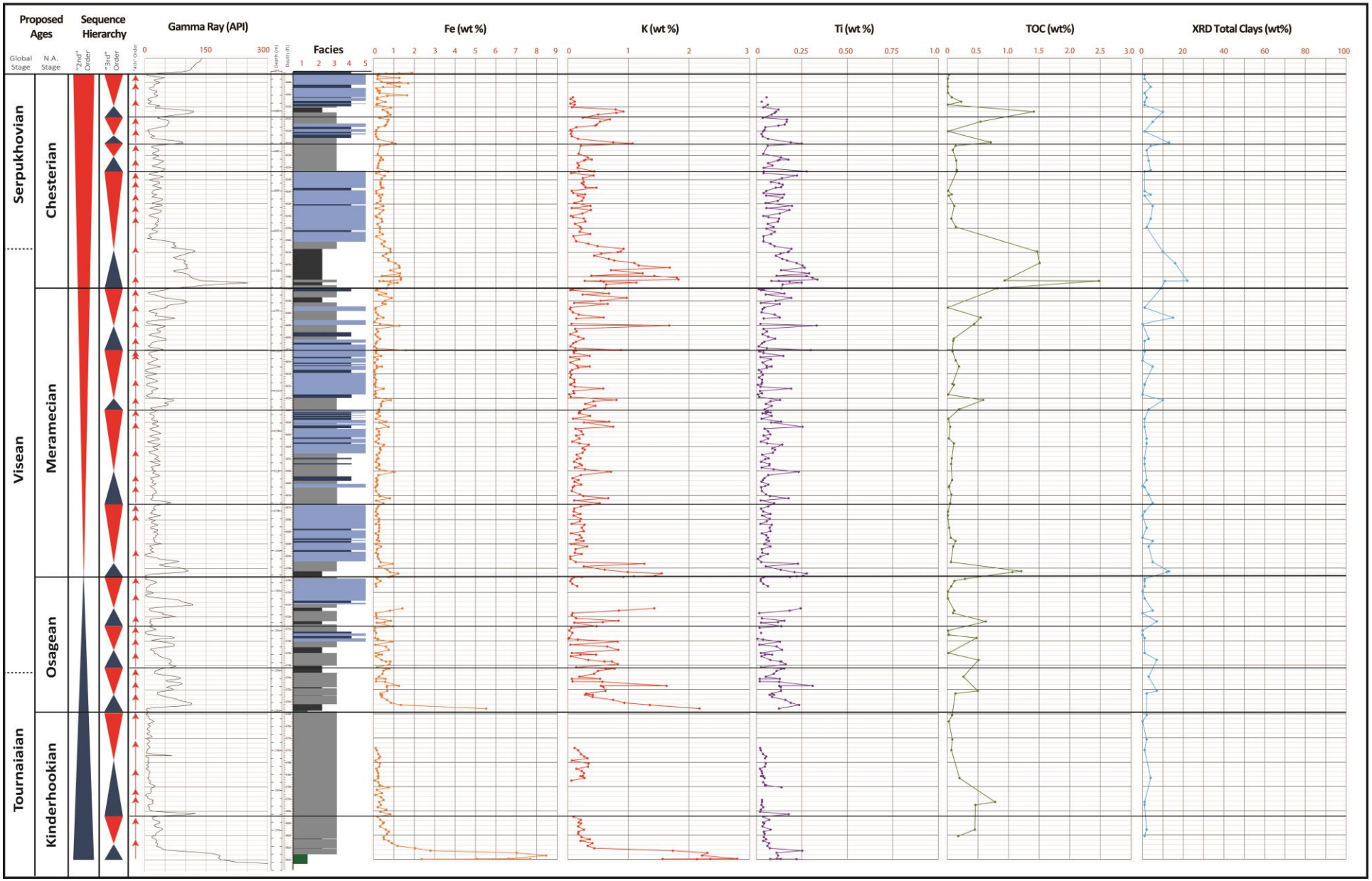

Figure 13. ED-XRF profiles of Fe, K, and Ti reported in weight percentages with gamma ray profile, low-resolution TOC and XRD total clays curves, and newly interpreted chemostratigraphic framework for the Adkisson #1-33. Elemental enrichments of Fe, Ti, and K as well as TOC are associated with Facies 1 and 2 suggesting a relationship with restricted facies and Mississippian stage boundaries. In the absence of a fully integrated dataset, elemental profiles could be used as a predictive tool for relatively enriched TOC zones.

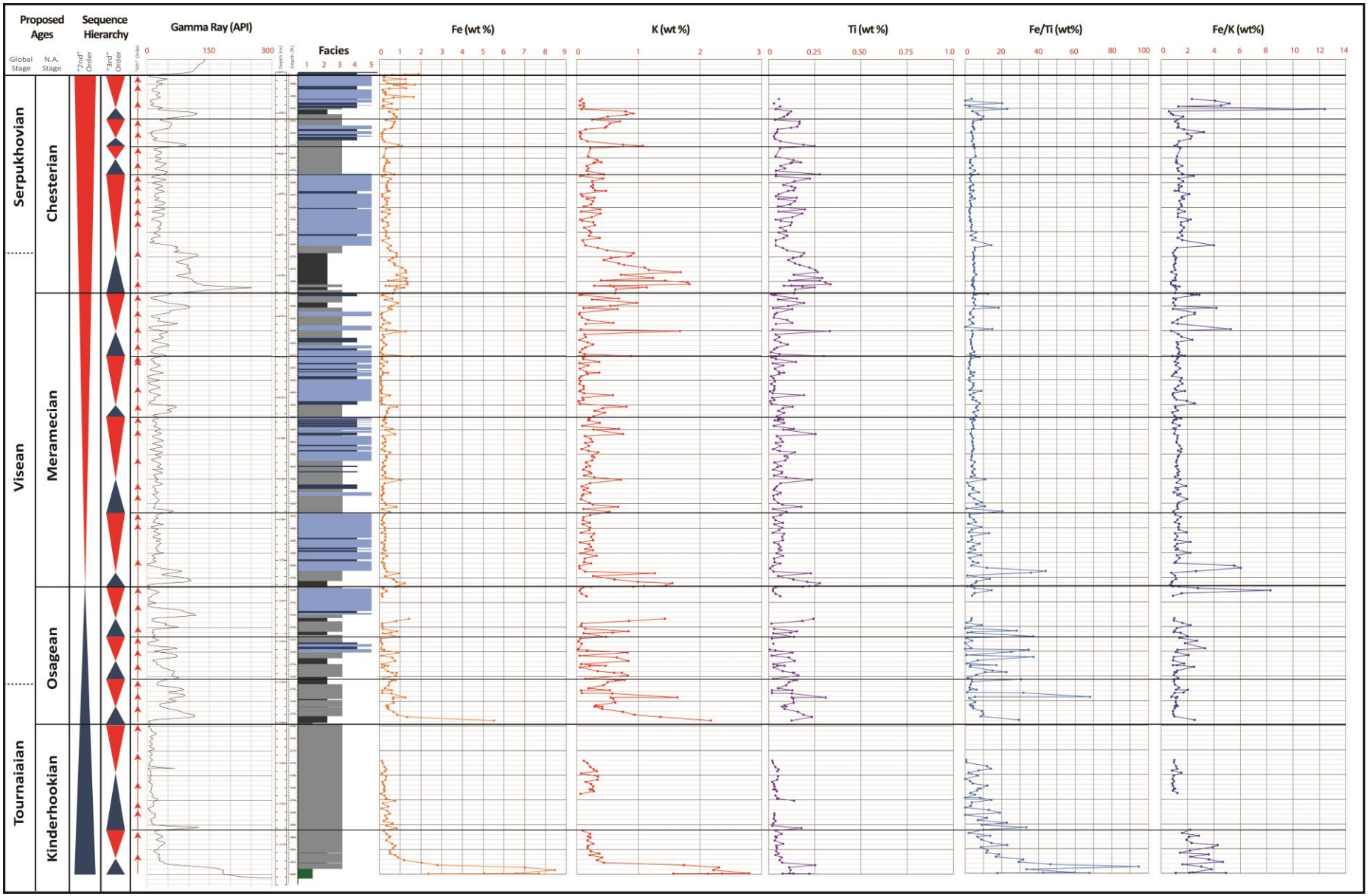

Figure 14. ED-XRF profiles of Fe, K, and Ti reported in weight percentages with gamma ray profile and normalized Fe curves for the Adkisson #1-33. Fe enrichments are more prevalent near the base of the core and tend to correlate with more restricted Facies 1 and Facies 2 with the significant enrichments of Facies 1 likely associated with the presence of glauconite.

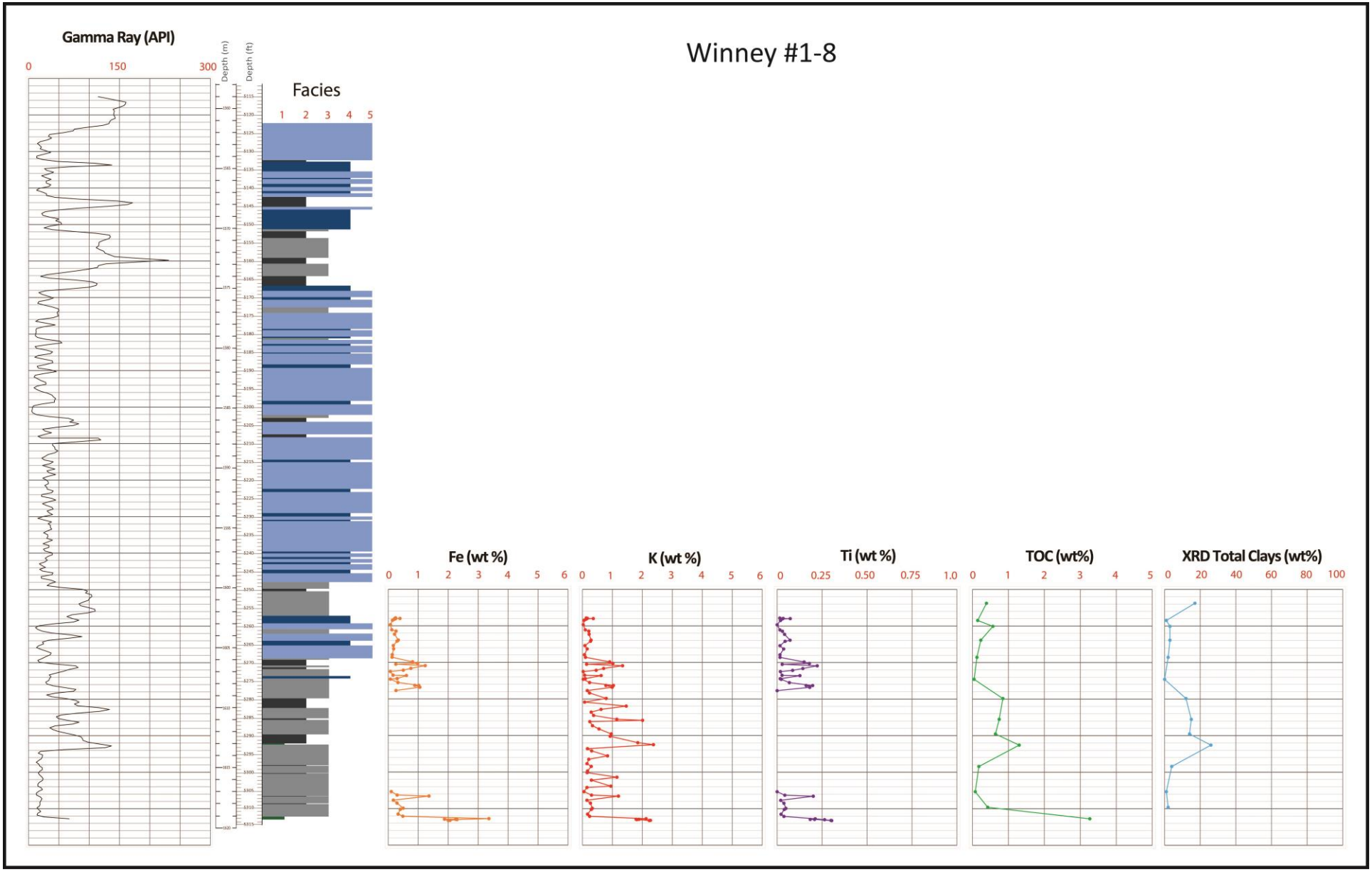

Figure 15. ED-XRF profiles of Fe, K, and Ti reported in weight percentages with gamma ray profile, low-resolution TOC and XRD total clays curves for the Winney #1-8. Abbreviated datasets are a result from machine malfunction, however enrichments at the base of the core in Facies 1 and Facies 2 suggest a relationship with low energy, potentially more restrictive, less oxygenated bottom water.

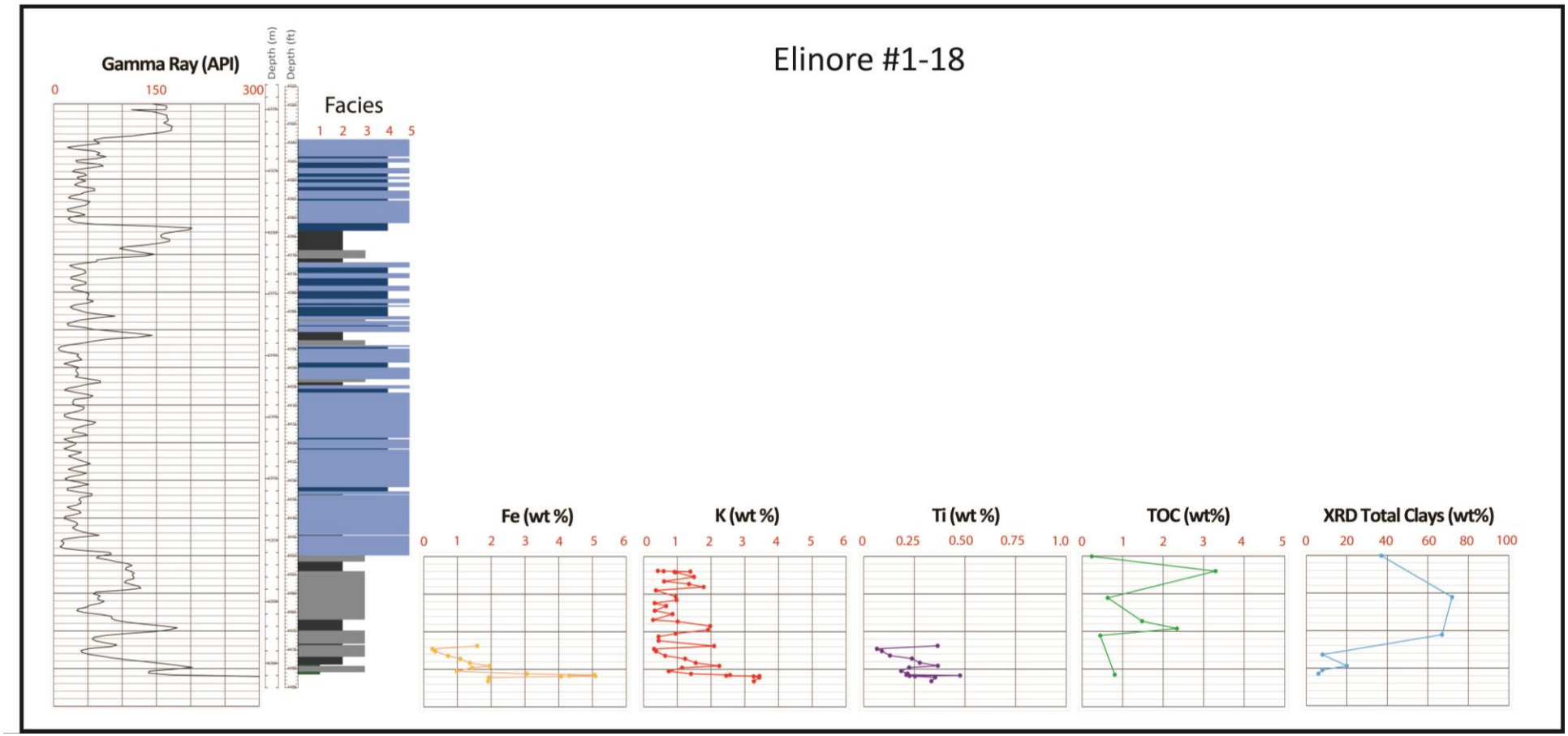

Figure 16. ED-XRF profiles of Fe, K, and Ti reported in weight percentages with gamma ray profile, low-resolution TOC and XRD total clays curves for the Elinore #1-18. Abbreviated datasets are a result from machine malfunction, however enrichments in TOC and high total clay content suggest potential Ti enrichments.

5.3.1 Facies Relationships and Stage Boundaries

Although only a few elements could be measured with some degree of confidence, there is a distinct relationship between relative elemental enrichment, facies type, and potential stage boundaries (Figure 13). Facies 1 and Facies 2 contain the highest percentage of Fe, K, and Ti (Table 1) which likely supports the interpretation of deposition in relatively calm and potentially restricted marine waters. Although no trace element proxies (U, V, Mo, Zn etc.) (Alego and Maynard, 2004; Alego et al., 2007) were detected at useful concentrations, Fe enrichments in association with relatively higher values of TOC could indicate a less oxygenated water column conditions with a higher amount of reactive detrital iron minerals and organic matter (Berner, 1984). Additional analysis utilizing iron speciation and degree of pyritization are needed before Fe can be used to indicate bottom water chemistry (Raiswell, 1988; Lyons and Severmann, 2006). Normalization of Fe data with Ti suggests that the highest enrichments near the base of the core is related to deposition of glauconite rich Facies 1 (Figure 14), and lesser, but noticeable enrichment is associated with Facies 2. In the absence of a reliable Al measurement, Ti and K enrichments match well with high clay intervals (illite/mica), evidenced by low-resolution (i.e. not oriented clay mounts) XRD analysis (Figure 13), which also suggests, along with depositional evidence, the presence of low energy depositional conditions.

Relative elemental enrichments and relatively high TOC zones are covariant with high gamma ray values which has important implications for correlation potential.

Collectively, the most marked increases in gamma ray and TOC curves correspond to the stage boundaries defined by the recently established chemostratigraphic framework. This suggests that in the absence of a fully integrated dataset, certain curves may be used as a predictive tool for elemental concentrations, relative organic carbon richness, or for correlating key horizons. XRF data in particular may be most useful as a first order approach for creating high-resolution profiles that can be used to guide sampling in organic rich areas or other zones of interest.

Facies	Avg. Fe (wt%)	n=	Avg. K (wt%)	n=	Avg. Ti (wt%)	n=	Avg. Leco TOC (%)	n=
5	0.32	114	0.18	99	0.067	100	0.125	24
4	0.21	42	0.13	38	0.053	33	0.06	22
3	0.42	133	0.34	120	0.079	128	0.331	33
2	0.84	43	0.9	43	0.174	43	1.27	6
1	5.99	5	2.28	5	0.146	5	N/A	N/A

Table 1. Table of average elemental concentrations measured by ED-XRF for each of the 5 facies defined by LeBlanc, 2014. Facies 1 and 2 have the highest relative percentages of Fe, K, Ti, and TOC. This supports the hypothesis that deposition likely occurred in relatively calm and potentially restricted marine waters.

CHAPTER VI

EXTENDED DISCUSSION

6.1 Stable Isotope Limitations

As bulk sediment sampling does not intentionally target specific unaltered sample sites (cements or unaltered shell material), there are several limitations associated with this type of stable isotope analysis. The $\delta^{13}C$ signature measured from bulk carbonate sediment is a complex interplay of sedimentological, physical-chemical, and biological processes (Wendler, 2013). There are several factors that affect the $\delta^{13}C$ of a sample including $\delta^{13}C_{DIC}$ of the ambient water, pH, mineralogy, rate of precipitation, residence time, carbonate grain type, vital effects, and diagenetic alterations both syndepositionally and with burial (Wendler, 2013; Swart, 2015). Therefore, it is important to understand the enhanced potential for a mixed effect due to any or all of the above. Although $\delta^{18}O$ signatures depend on fewer initial factors, namely the $\delta^{18}O$ of the fluid, temperature, mineralogy, pH, and kinetic effects, they are much more susceptible to resetting during water-rock interactions than carbon isotopes (Lohmann, 1988; Swart, 2015). Therefore, more confidence is placed in the $\delta^{13}C$ curve for chronostratigraphic correlations and $\delta^{18}O$ profiles are highly scrutinized.

6.2 ED-XRF Limitations

Although advances in ED-XRF methodology have demonstrated the potential for rapid and reliable quantitative measurements on clean, flat drill core (Rowe et al., 2012), lack of matrix-specific calibration and additional quantitative analyses prevent results from this study from being anything more than qualitative. A carbonate standard closer in composition to the samples that were analyzed would have been more applicable for the present dataset and helium purged analysis would have provided increased confidence in light element measurements. Additionally, XRF analysis measures elements in concentrations, not mineralogical states (Potts and Webb, 1992). Therefore, it is likely that several elements are hosted in various mineral forms and geochemical proxies based on these concentrations must be defined with extreme care. Although, XRD data was not available at the same resolution as the XRF analysis, it helped guide proxy use in certain intervals.

6.3 Inter-Core Variability

In addition to the extended ED-XRF dataset, carbon and oxygen stable isotopes were also sampled for the lowermost 3rd order sequence defined by LeBlanc, 2014 (Figure 17). The pronounced Kinderhookian shift at the base of the additional cores occurs in different magnitudes relative to the pattern seen in the Adkisson #1-33. A majority of the positive shift is absent in the Winney #1-8, which is likely due to the difficulty in achieving stable isotope values for the lowermost 5 samples. The slow enrichment from near zero to 2‰ is similar to patterns seen in the presumed mid-Kinderhookian in the Adkisson #1-33, and the occurrence of Facies 1 and similarities in

the gamma ray curve suggest the Kinderhookian-Osagean boundary at this horizon. Although the stage above this boundary is characterized by a lower average $\delta^{13}C$ value (~1-2‰) relative to the Adkisson #1-33, gamma ray patterns and vertical facies successions suggest the strata may be Osagean in age.

The Elinore #1-18 records a positive excursion from ~-5.5 to 1‰, similar to the ~+6‰ excursion in the Adkisson #1-33. This suggests that despite a distinct change in gamma ray signature, that most of the strata covered represents the Kinderhookian section of the core. This could represent facies changes into calmer, more restricted waters, a change of which could be expected over the large distance between the cores (Winney #1-8 to Elinore #1-18; 25km (15.5mi). In general, less variability is expected between strike-oriented cores due to the migration patterns of facies belts, however there is still a level of heterogeneity that can be expected over short distances within a depositional system. Overall, the difference in the total thickness of the Mississippian section between the three cores may be due to Late or post Mississippian timed erosion or non-deposition associated with syndepositional faulting (LeBlanc, 2014).

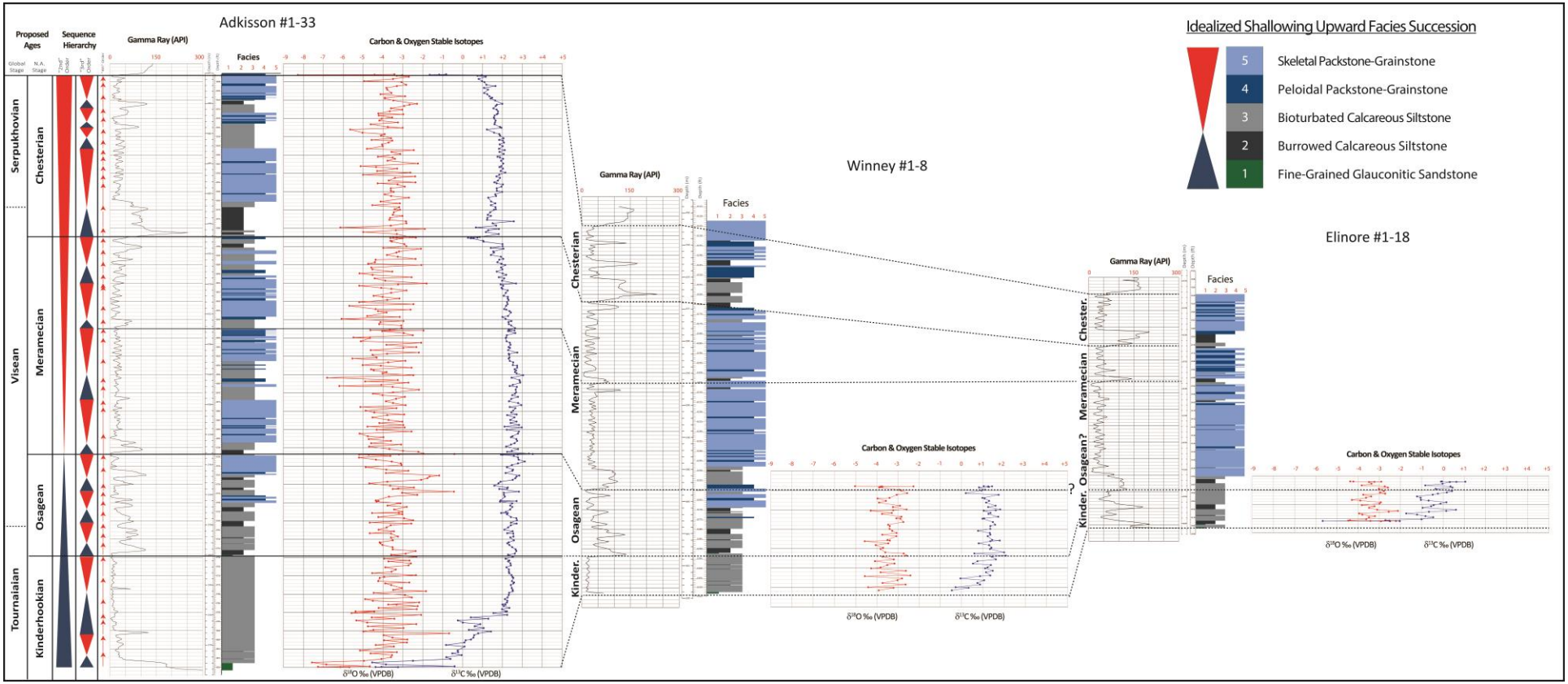

Figure 17. Total gamma ray (API units), facies, and carbon and oxygen stable isotope profiles of the Adkisson #1-33 and the lowermost 3rd order sequence of the Winney #1-8 and Elinore #1-18 defined by LeBlanc (2014). A pronounced Kinderhookian shift is absent in the Winney #1-8, which may be due to the lack of sample readings in the five lowermost samples. A slow positive trend $\delta^{13}C$ in association with a distinct gamma ray kick and appearance of Facies 1 suggests the boundary between Kinderhookian and Osagean strata. Relative stabilization of $\delta^{13}C$ above this boundary may suggest the occurrence of Osagean strata, which is also supported by a similar gamma ray signature found in the Adkisson #1-33 over this interval. Stable isotope data from the Elinore #1-18 shows a pronounced shift in $\delta^{13}C$, however the gamma ray profile has changed character. This may suggest facies changes which would be expected over such a large distance between each core even alone strike. Dashed lines indicate potential correlation horizons based on gamma ray, facies, and stable isotope data. The abbreviated sections in the Winney #1-8 and Elinore #1-18 may be due to non-deposition or erosion.

CHAPTER VII

SUMMARY AND CONCLUSIONS

This study utilized an integrated approach in order to define a chemostratigraphic framework for cored Mississippian strata in north-central Oklahoma. This was achieved through incorporating high-resolution carbon and oxygen stable isotopic data and energy-dispersive x-ray fluorescence with high-resolution sequence stratigraphy. Additional datasets including wireline log, x-ray diffraction, total organic content, and diagenetic data were incorporated into the framework in order to better understand controls on carbon and oxygen isotope signatures and how they relates to vertical stacking patterns at multiple scales. Key conclusions from this study are as follows:

1. High-resolution chemostratigraphy suggests a new interpretation of more frequent 3rd order cyclicity than previously recognized from facies and wireline logs.
2. This cyclicity correlates with published, global $\delta^{13}C$ datasets which suggest the delineation of the Mississippian profile into the four North American Stages.
3. This delineation forms the basis for creating a chronostratigraphic tie in the absence of biostratigraphy that may be useful for correlation at the basin scale.

4. Differences in carbon and oxygen stable isotopic curves between cores suggest a level of uncertainty when using gamma ray curves alone for correlation.
5. $\delta^{18}O$ stable isotopic data suggests changes in isotopic ratios are related to higher frequency, potentially 4th order cyclicity, due to mixed meteoric input near the tops of shallowing upward successions and enhanced diagenetic susceptibility of shallow water facies.
6. This data provides new insight regarding the degree of compartmentalization related to mixed meteoric cemented horizons at the 4th order scale.
7. ED-XRF data suggests relative enrichments in Fe, Ti, and K may be related to deposition in relatively restricted marine waters. Integration of low resolution TOC and XRD data help support this hypothesis.
8. High-resolution ED-XRF data may be most useful in creating a first order geochemical framework to be used to determine the position of targeted sampling for TOC rich zones with more precise analyses.

REFERENCES

Amorosi, A., 2012, The occurrence of glaucony in the stratigraphic record: distribution patterns and sequence-stratigraphic significance: International Association of Sedimentologists Special Publications, v.45, p. 37-54.

Alego, T.J., and Maynard, J.B., 2004, Trace element behavior and redox facies in core shales of Upper Pennsylvanian Kansas-type cyclothems: Chemical Geology, v. 206, p. 289-318.

Alego, T. J., Lyons, T.W., Blakey, R.C., and Over, D.J., 2007, Hydrographic conditions of the Devono-Carboniferous North American Seaway inferred from sedimentary Mo-TOC relationships: Paleogeography, Paleoclimatology, Paleoecology, v. 256, p. 204-230.

Banner, J.L., and Hanson, G. N., 1990, Calculation of simultaneous isotopic and trace element variations during water-rock interaction with applications to carbonate diagenesis: Geochimica et Cosmochimica Acta, v.54, p.3123-3137.

Banner, J.L., and Kaufman, J., 1994, The isotopic record of ocean chemistry and diagenesis preserved in non-luminescent brachiopods from Mississippian carbonate rocks, Illinois and Missouri: GSA Bulletin, v.106, p. 1074-1082.

Batt, L.S., Montanez, I.P., Isaacson, P., Pope, M.C., Butts, S.H., and Abplanalp, J., 2007, Multi-carbonate component reconstruction of mid-carboniferous (Chesterian) seawater δ13C: Paleogeography, Paleoclimatology, Paleoecology, v. 256, p. 298-318.

Berner, R.A., 1984, Sedimentary pyrite formation:an update: Geochimica et Cosmochimica Acta, v.48, p. 605-615.

Boardman, D.R., Thompson, T.L., Godwin, C., Mazzullo, S.J., Wilhite, B.W., and Morris, B.T., 2013, High-resolution conodont zonation for Kinderhookian (Middle Tournaisian) and Osagean (Upper Tournaisian-Lower Visean) strata of the western edge of the Ozark Plateau, North America: Shale Shaker (September-October 2013) p.98-151.

Bruckschen, P., Oesmann, S., and Veizer, J., 1999, Isotope stratigraphy of the European Carboniferous: Proxy signals for ocean chemistry, climate and tectonics: Chemical Geology, v. 161, p. 127–163.

Buggisch, W., Keller, M., and Lehnert, O., 2003, Carbon isotope record of Late Cambrian to Early Ordovician carbonates of the Argentine Precordillera: Paleogeography, Paleoclimatology, Paleoecology, v.195, p. 357-373.

Buggisch, W., Joachimski, M.M., Sevastopulo, G., and Morrow, J.R., 2008, Mississippian $\delta^{13}C_{carb}$ and conodont apatite $\delta^{18}O$ records—Their relation to the Late Paleozoic Glaciation: Palaeogeography, Palaeoclimatology, Palaeoecology, v.268, p.273-292, doi:10.1016/j.palaeo.2008.03.043.

Chatellier, J., Moslow, T., and Haverslew, B., 2015, Lessons from high-resolution continuous XRF on stratigraphy and geomechanics of shale: AAPG Search and Discovery Article #41656.

Childress, M., and Grammer, G.M., 2015, High resolution sequence stratigraphic architecture of a Mid-Continent Mississippian outcrop in Southwest Missouri: Shale Shaker (August 2015) p. 206-234.

Childress, M. and Grammer, G. M., (for submission to), Characteristics of Debris Flows and Outrunner Blocks – Evidence for Mississippian-age Deposition on a Distally Steepened Ramp, in Grammer et al., eds., Mississippian Reservoirs of the Mid-Continent, USA, AAPG Memoir.

Cramer, B.D., Loydell, D.K., Samtleben, C., Munnecke, A., Kaljo, D., Mannik, P., Martma, T., Jeppsson, L., Kleffner, M.A., Barrick, J.E., Johnson, C.A., Emsbo, P., Joachimski, M.M., and Saltzman, M.R., 2010, Testing the limits of Paleozoic chronostratigraphic correlation via high-resolution (<500 kyr) integrated conodont, graptolite, and carbon isotope ($\delta^{13}C_{carb}$) biochemostratigraphy across the Llandovery-Wenlock (Silurian) boundary: Is a unified Phanerozoic timescale achievable? Geological Society of America Bulletin, v. 122, p.1700-1716.

Curtis, D.M., and Champlin, S.C., 1959, Depositional environments of Mississippian limestones of Oklahoma: Tulsa Geological Society Digest, v.27, p.90-103.

Ekdale, A.A., Bromley, R.G., and Pemberton, S.G., 1984, Ichnology – Trace fossils in sedimentology and stratigraphy, SEPM Short Course No. 15, 317 p.

Flinton, K., 2015, The effects of high-frequency cyclicity on reservoir characteristics of the “Mississippian Limestone”, Anadarko Basin, Kingfisher County, Oklahoma, Master’s thesis, Oklahoma State University, Stillwater, Oklahoma, p. 186.

Flügel, E., 2010, Microfacies of carbonate rocks: Anaylsis, interpretation, and application, 2nd Ed., Springer-Verlag, Berlin, Heidelberg, New York, 1007 p.

Grammer, G.M., Harris, P.M., and Eberli, G.P., 2004, Integration of outcrop and modern analogs in reservoir modeling: Overview with examples form the Bahamas, in

G.M. Grammer, P.M. Harris, and G.P Eberli, eds., Integration of outcrop modern analogs in reservoir modeling: AAPG Memoir 80, p. 1-22.

Goldstein, R H., Anderson, J.E., and Bowman, M.W., 1991, Diagenetic responses to sea-level change: Integration of field, stable isotope, paleosol, paleokarst, fluid inclusion, and cement stratigraphy research to determine history and magnitude of sea-level fluctuation: Sedimentary Modeling, p.139-162.

Goldstein, R.H., (for submission to), Major impacts of multiple stages of hydrothermal fluid flow on Mississippian carbonate reservoirs of the Mid-Continent, in Grammer et al., eds., Mississippian Reservoirs of the Mid-Continent, USA, AAPG Memoir.

Grossman, E.L., Mii, H., and Yancey, T.E., 1993, Stable isotopes in Late Pennsylvanian brachiopods from the United States: Implications for Carboniferous paleooceanography: GSA Bulletin, v.105, p. 1284-1296.

Grossman, E.L., Yancey, T.E., Jones, T.E., Bruckschen, P., Chuvashov, B., Mazzullo, S.J., and Mii, H., 2008, Glaciation, aridification, and carbon sequestration in the Permo-Carboniferous: The isotopic record from low latitudes: Palaeogeography, Palaeoclimatology, Palaeoecology, v.268, p. 222-233.

Halverson, G.P., Hoffman, P., Schrag, D., Maloof, A., and Rice, H.N., 2006, Toward a Neoproterozoic composite carbon-isotope record, GSA Bulletin, v. 117, p. 1181-1207.

Haq, B. U., and Schutter, S. R., 2008, A chronology of Paleozoic sea-level changes, Science, v. 322, p. 64-68.

Hosseininejad, S., Pedersen, P.K., Spencer, R.J., and Nicholas, M. P. B., 2013, Use of XRF elemental data to quantify mineralogy and reservoir properties of an Upper Cretaceous oil and gas shale reservoir, Eastern Saskatchewan and South western Manitoba: URTeC article #1618654, Unconventional Resources Technology Conference (URTeC) Denver, Colorado, August 12-14.

Jaeckel, L., 2016, High-resolution sequence stratigraphy and reservoir characterization of Mid-Continent Mississippian carbonates in North-Central Oklahoma and South-Central Kansas, Master's thesis, Oklahoma State University, Stillwater, Oklahoma, 413 p.

Jones, B., and Manning, D.A.C., 1994, Comparison of geochemical indices used for the interpretation of palaeoredox conditions in ancient mudstones: Chemical Geology, v. 111, p. 111-129.

Katz, M.E., Wright, J.D., Miller, K.G., Pak, D.K., Shackleton, N.J., Thomas, E., 2005, Biological overprint of the geological carbon cycle: Marine Geology, v.217, p. 323-338.

Katz, D.A., Buoniconti, M.R., Montanez, I.P., Swart, P.K., Eberli, G.P., and Smith, L.B., 2007, Timing and local perturbations to the carbon pool in the lower Mississippian Madison Limestone, Montana and Wyoming: Palaeogeography, Palaeoclimatology, Palaeoecology (2007), 23 p. doi:10.1016/j.palaeo.2007.02.048.

Koch, J.T., Frank, T.D., and Bulling, T.P., 2014, Stable-isotope chemostratigraphy as a tool to correlate complex Mississippian marine carbonate facies of the Anadarko shelf, Oklahoma and Kansas: AAPG Bulletin, v.98, no. 6, p. 1071-1090.

Lane, H.R., and De Keyser, T.L., 1980, Paleogeography of the Late Early Mississippian (Tournaisian 3) in the Central and Southwestern United States, Paleozoic Paleogeography of West-Central United States: Rocky Mountain Paleogeography Symposium 1, p. 149-162.

LeBlanc, S., 2014, High resolution sequence stratigraphy and reservoir characterization of the "Mississippian Limestone" in North-Central Oklahoma, Master's thesis, Oklahoma State University, Stillwater, Oklahoma, 455 p.

Lohmann, K. C., 1988, Geochemical patterns of meteoric diagenetic systems and their application to studies of paleokarst, in N. P. James and P. W. Choquette, eds., Paleokarst: New York, Springer-Verlag, p. 58–79.

Lyons, T.W., Anbar, A.D., Severmann, S., Scott, C., and Gill, B.C., 2009, Tracking euxinia in the ancient ocean: a multiproxy perspective and Proterozoic case study: Annual Review Earth Planet Science, v. 37, p. 507-534, doi: 10.1146/annurev.earth.36.031207.124233.

Lyons, T.W., and Severmann, S., 2006, A critical look at iron paleoredox proxies: new insights from modern euxinic marine basins: Geochemica et Cosmochemica Acta, v.70, p. 5698-5722, doi:10.1016/j.gca.2006.08.021.

Maloof, A.C., Schrag, D.P., Crowley, J.L., and Bowring, S.A., 2005, An expanded record of Early Cambrian carbon cycling from the Anti-Atlas Margin, Morocco: Canadian Journal of Earth Sciences, v. 42, p. 2195-2216.

Mazzullo, S.J., Boardman, D.R., Wilhite, B.W., Godwin, G., and Morris, B.T., 2013, Revisions of outcrop lithostratigraphic nomenclature in the lower to middle Mississippian subsystem (Kinderhookian to basal Meramecian series) along the shelf-edge in southwest Missouri, northwest Arkansas, and northeast Oklahoma: Shale Shaker, v.63, no.6, p.414-454.

Middleton, G.V., Church, M.J., Coniglio, M., Hardie, L.A., and Longstaffe, F.J., 2003, Encyclopedia of sediments and sedimentary rocks: Amsterdam, Kluwer Academic Publishers, 821 p.

Mii, H., Grossman, E.L., and Yancey, T.E., 1999, Carboniferous isotope stratigraphies of North America: implications for Carboniferous paleoceanography and Mississippian glaciation: GSA Bulletin, v.111, no.7, p.960-973.

Mii, H., Grossman, E.L., Yancey, T.E., Chuvashov, B., and Egorov, A., 2001, Isotopic records of brachiopod shells from the Russian Platform—evidence for the onset of mid-Carboniferous glaciation: Chemical Geology, v. 175, p. 133-147.

Mohammadi, S., and Gregg, J.M., (for submission to), Late diagenesis of Mississippian carbonates in north-central Oklahoma, in Grammer et al., eds., Mississippian Reservoirs of the Mid-Continent, USA, AAPG Memoir.

Morse, J.W., and Mackenzie, F.T., 1990, Geochemistry of Sedimentary Carbonates: Developments in Sedimentology 48, Elsevier, Netherlands, 707 p.

Northcutt, R. A., and Campbell, J. A., 1996, Geologic Provinces of Oklahoma, Transactions of the 1995 AAPG Mid-Continent Section Meeting, p. 128-134.

Price, B., 2014, High resolution sequence stratigraphic architecture and reservoir characterization of the Mississippian Burlington/Keokuk Formation Northwestern Arkansas, Master's thesis, Oklahoma State University, Stillwater, Oklahoma, 154 p.

Popp, B.N., Anderson, T.F., and Sandberg, P.A., 1986, Brachiopods as indicators of original isotopic compositions in some Paleozoic limestones: GSA Bulletin, v.97, p.1262-1269.

Potts, P.J., and Webb, P.C., 1992, X-ray fluorescence spectrometry, in Hall, G.E.M., eds., Geoanalysis: Journal of Geochemical Exploration, v. 44, p.251-296.

Read, J.F., 1995, Overview of carbonate platform sequences, cycle stratigraphy and reservoirs in greenhouse and icehouse worlds, in Read, J.F., Kerans, C., Weber, L.J., Sarg, J.F., and Wright F.M., eds., Milankovitch sea level changes, cycles, and reservoirs on carbonate platforms in greenhouse and icehouse worlds: SEPM Short Course 35, 102 p.

Raiswell, R., Buckley, F., Berner, R.A., and Anderson, T.F., 1988, Degree of pyritization of iron as a paleoenvironmental indicator of bottom-water oxygenation: Journal of Sedimentary Petrology, v. 58, p. 812-819.

Ramkumar, M., 2015, Toward standardization of terminologies and recognition of chemostratigraphy as a formal stratigraphic method, in M. Ramkumar, ed., Chemostratigraphy: Concepts, Techniques, and Applications: Amsterdam, Elsevier, p. 17-36.

Renard, M., 1986, Pelagic carbonate chemostratigraphy (Sr, Mg, ^{18}O, ^{13}C): Marine Micropaleontology, v. 10, p. 117-164.

Roundtree, R., Wright, J., and Miskimins, J., 2010, Unconventional resource recovery improvement using conventional reservoir engineering strategies: AAPG Search and Discovery Article #80088, AAPG International Conference and Exhibition Rio de Janeiro, Brazil, November 15-18.

Rowe, H., Hughes, N., and Robinson, K., 2012, The quantification and application of handheld energy-dispersive x-ray fluorescence (ED-XRF) in mudrock chemostratigraphy and geochemistry: Chemical Geology, v. 324-325, p. 122-131, doi:10.1016/j.chemgeo.2011.12.023.

Rowe, H., Loucks, R., and Kerans, C., 2015, Core chemostratigraphy and elemental geochemistry along a dip-section, Pearsall Formation, Lower Cretaceous, Central to South TX: UTReC article #2154897, Unconventional Resources Technology Conference (URTeC) San Antonio, Texas, July 20-22.

Saltzman, M.R., 2003, Late Paleozoic ice age: Oceanic gateway or pCO_2?: Geology, v. 31, no.2, p.151-154.

Saltzman, M.R. and Thomas, E., 2012, Carbon isotope stratigraphy, in Gradstein, F., Ogg. J., Schmitz, M.D., and Ogg, G., eds., The Geologic Time Scale 2012: Elsevier, p. 207- 232, doi: 10.1016/B978-0-444-59425-9.00011-1.

Scholle, P.A., and Arthur, M.A., 1980, Carbon isotope fluctuations in Cretaceous pelagic limestones: Potential stratigraphic and petroleum exploration tool: AAPG Bulletin, v.64, no.1, p.67-87.

Sessions, J.P., Opfer, C.L., and Scott, R.W., (for submission to), Isotope chemostratigraphy and sequence stratigraphy of the Lower Mississippian St. Joe Group in Northeastern Oklahoma to Southwestern Missouri, in Grammer et al., eds, Mississippian Reservoirs of the Mid-Continent, USA, AAPG Memoir.

Sial, A.N., Gaucher, C., Ferreira, V.P., Pereira, N.S., Cezario, W.S., Chiglino, L., and Lima, H.M., 2015, Isotope and elemental chemostratigraphy, in M. Ramkumar, ed., Chemostratigraphy: Concepts, Techniques, and Applications: Amsterdam, Elsevier, p. 37-70.

Swart, P.K., 2015, The geochemistry of carbonate diagenesis: The past, present and future: Sedimentology, v. 62, p.1233-1304. doi: 10.1111/sed.12205.

Tierney, K., 2010, Permian carbonate and strontium isotope stratigraphy in Nevada and China: Implications for a greenhouse-icehouse transition: Unpublished PhD, Ohio State University.

Tucker, M.E., and Wright, V.P., 1990, Carbonate Sedimentology: Blackwell Scientific Publications, Oxford, 498 p.

U.S. Geological Survey Geochemical Reference Materials and Certificates, Cody Shale, SCo-1, http://crustal.usgs.gov/geochemical_reference_standards/codyshale.html; date accessed Jan 2016.

Vanden Berg, B., 2016, An integrated analysis of carbonate mudrocks and mixed carbonate-siliciclastic reservoirs to define the effects of micro- to nano-meter scale pore architecture on the ability to predict porosity or permeability, Ph.D. dissertation, Oklahoma State University, Stillwater, Oklahoma.

Vanden Berg, B., LeBlanc, S., and Grammer, G.M., (for submission to), Using high resolution sequence stratigraphy and characterization of the micro- to nanopore architecture to predict high porosity and permeability intervals in carbonate mudrocks: examples from the Mid-Continent "Mississippian Limestone", in Grammer et al., eds., Mississippian Reservoirs of the Mid-Continent, USA, AAPG Memoir.

Viezer, J., Ala, D., Azmy, K., Bruckschen, P., Buhl, D., Bruhn, F., Carden, G.A.F., Diener, A., Ebneth, S., Godderis, Y., Jasper, T., Korte, C., Pawellek, F., Podlaha, O.G., and Strauss, H., 1999, $^{87}Sr/^{86}Sr$, $\delta^{13}C$ and $\delta^{18}O$ evolution of Phanerozoic seawater: Chemical Geology, v. 161, p. 59-88.

Wendler, I., 2013, A critical evaluation of carbon isotope stratigraphy and biostratigraphic implications for Late Cretaceous global correlation: Earth-Science Reviews, v. 126, p. 116-146, doi:10.1016/j.earscirev.2013.08.003.

APPENDIX A

WHOLE CORE PHOTOGRAPHS WITH SAMPLE LOCATIONS

Core photographs are shown in white light and are labeled using the abbreviations from LeBlanc (2014) shown below. All cores are photographed in boxes that are 2 feet in length and are oriented with the shallowest depths at the top left of the image and the deepest depths at the bottom right. All scales are in feet with smaller dashes corresponding to tenths of a foot. To the left of each 2ft interval are facies types defined by LeBlanc (2014) depicted by a colored line corresponding to colors used in the idealized facies stacking pattern. The bottom and top of the "Mississippian Limestone" are marked using solid yellow lines. 3rd order sequence boundaries defined by LeBlanc (2014) are marked by a solid red line and 4th order high frequency cycles are marked by a dashed red line. Carbon and oxygen stable isotope and XRF locations are marked with white arrows. Red arrows mark stable isotope and XRF locations with additional thin sections, XRD, and TOC measurements from LeBlanc (2014). Additional XRF locations without stable isotope measurements or additional thin section, XRD, or TOC measurements are marked with purple arrows.

Core and Thin Section Image Labels							
Feature Key						Porosity Key	
BF	bone fragment	GB	grain bed	PY	pyrite	FR	fracture
BR	brachiopod	GST	gastropod	Q	quartz	IP	interparticle
BU	burrow	HCS	hummocky cross stratification	S	stylolite	IX	intercrystalline
BY	bryozoan	IC	intraclast	SK	undifferentiated skeletal fragments	MO	moldic
C	coral	L	lamination	SP	spicule	VU	vug
CH	chert	M	mud/mudstone	TS	truncation surface	WP	intraparticle
CON	conodont	ME	micritic envlope	XB	cross-bedding	WX	intracrystalline
CR	crinoid	MW	mud whisp				
D	dolomite	O	ostracode				
FG	firm ground	OIL	oil/dead oil				
FR	fracture	P	peloid				
G	glauconite	PH	phosphate				

Core #1

Adkisson #1-33 SWD

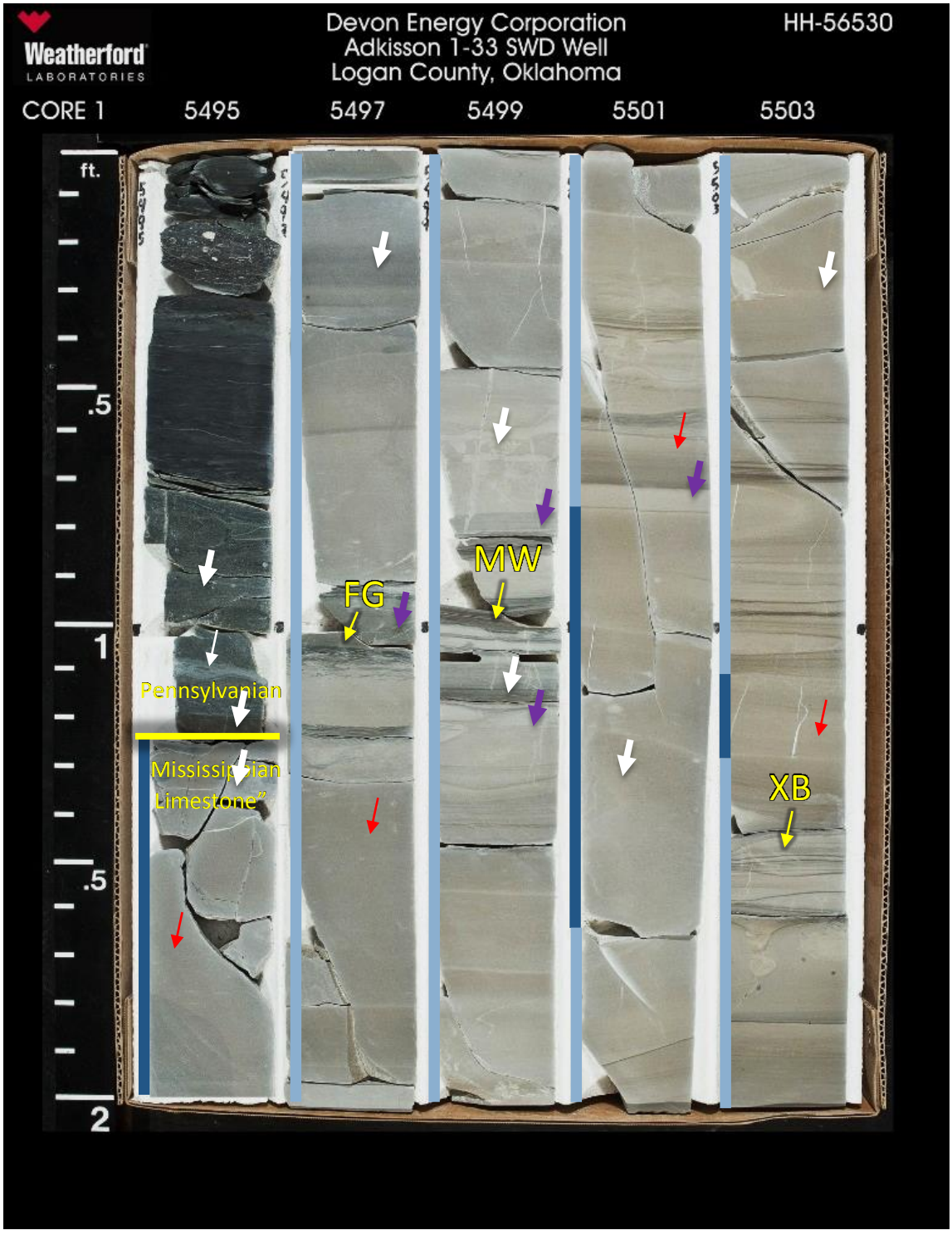
Weatherford
LABORATORIES
Devon Energy Corporation
Adkisson 1-33 SWD Well
Logan County, Oklahoma
HH-56530
CORE 1
5495
5497
5499
5501
5503
ft.
.5
1
.5
2
FG
MW
XB
Pennsylvanian
Mississippian
Limestone"

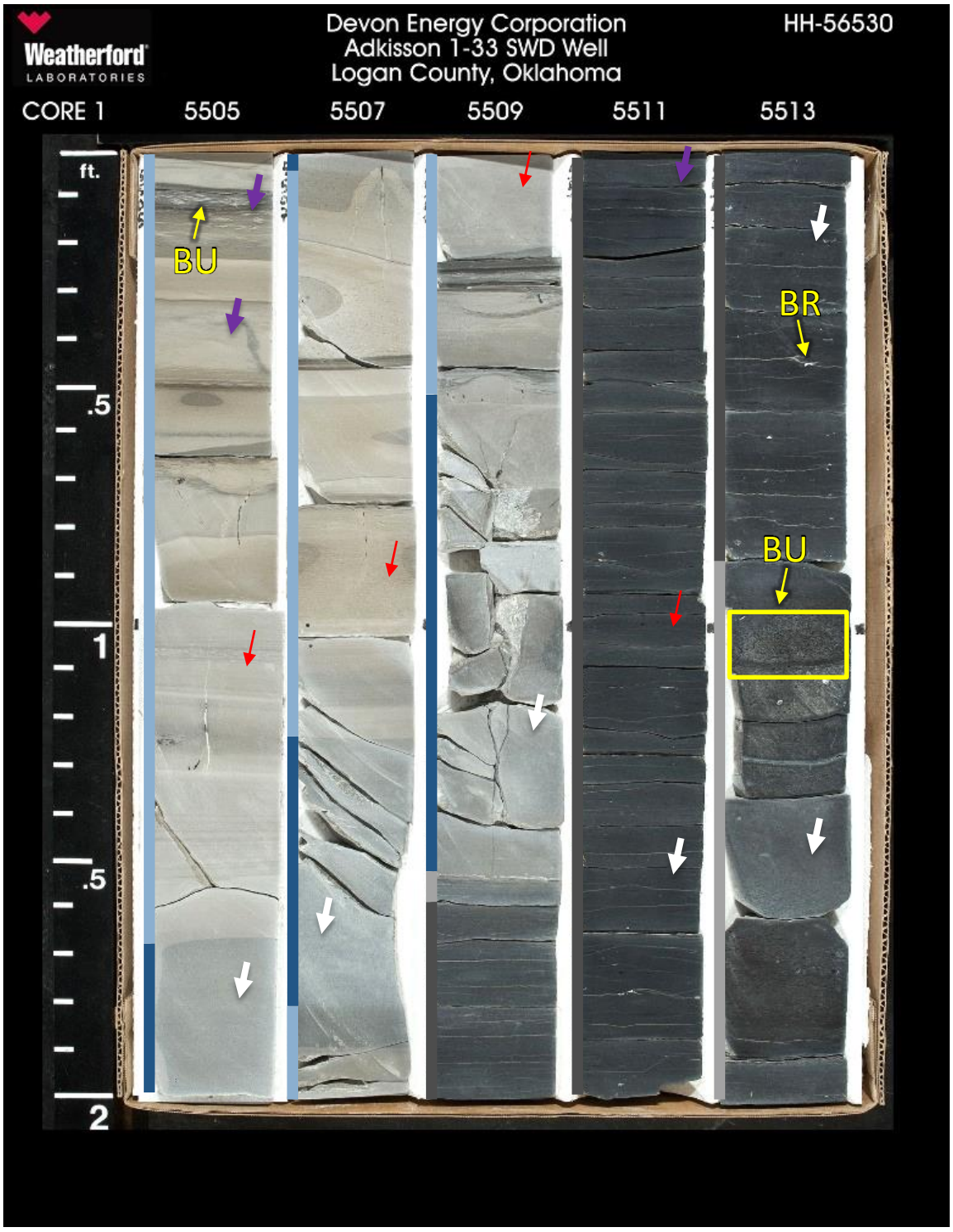
Weatherford
LABORATORIES
Devon Energy Corporation
Adkisson 1-33 SWD Well
Logan County, Oklahoma
HH-56530
CORE 1
5505
5507
5509
5511
5513
ft.
.5
1
.5
2
BU
BR
BU

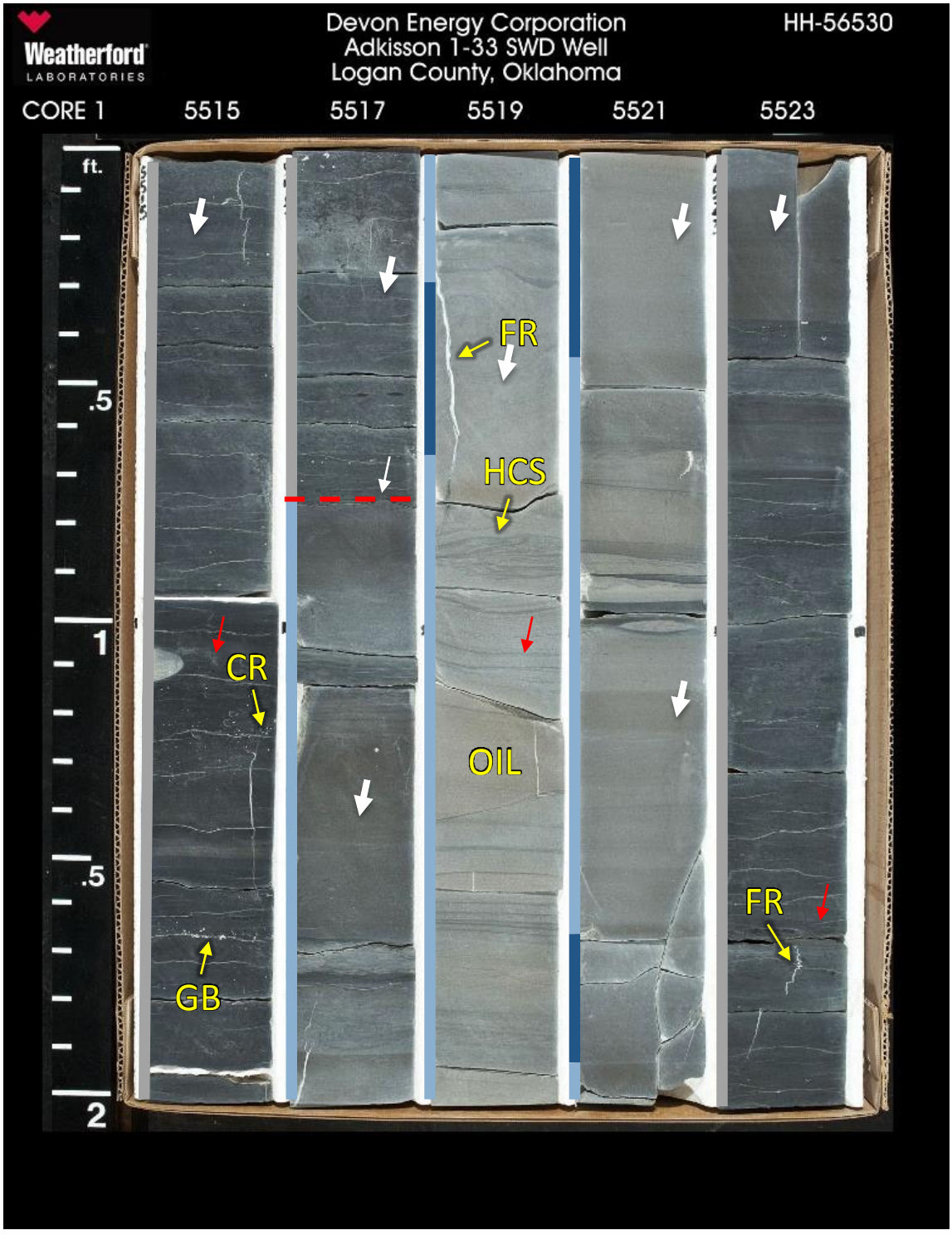
Weatherford
LABORATORIES
Devon Energy Corporation
Adkisson 1-33 SWD Well
Logan County, Oklahoma
HH-56530
CORE 1
5515
5517
5519
5521
5523
ft.
.5
1
.5
2
FR
HCS
CR
OIL
GB
FR

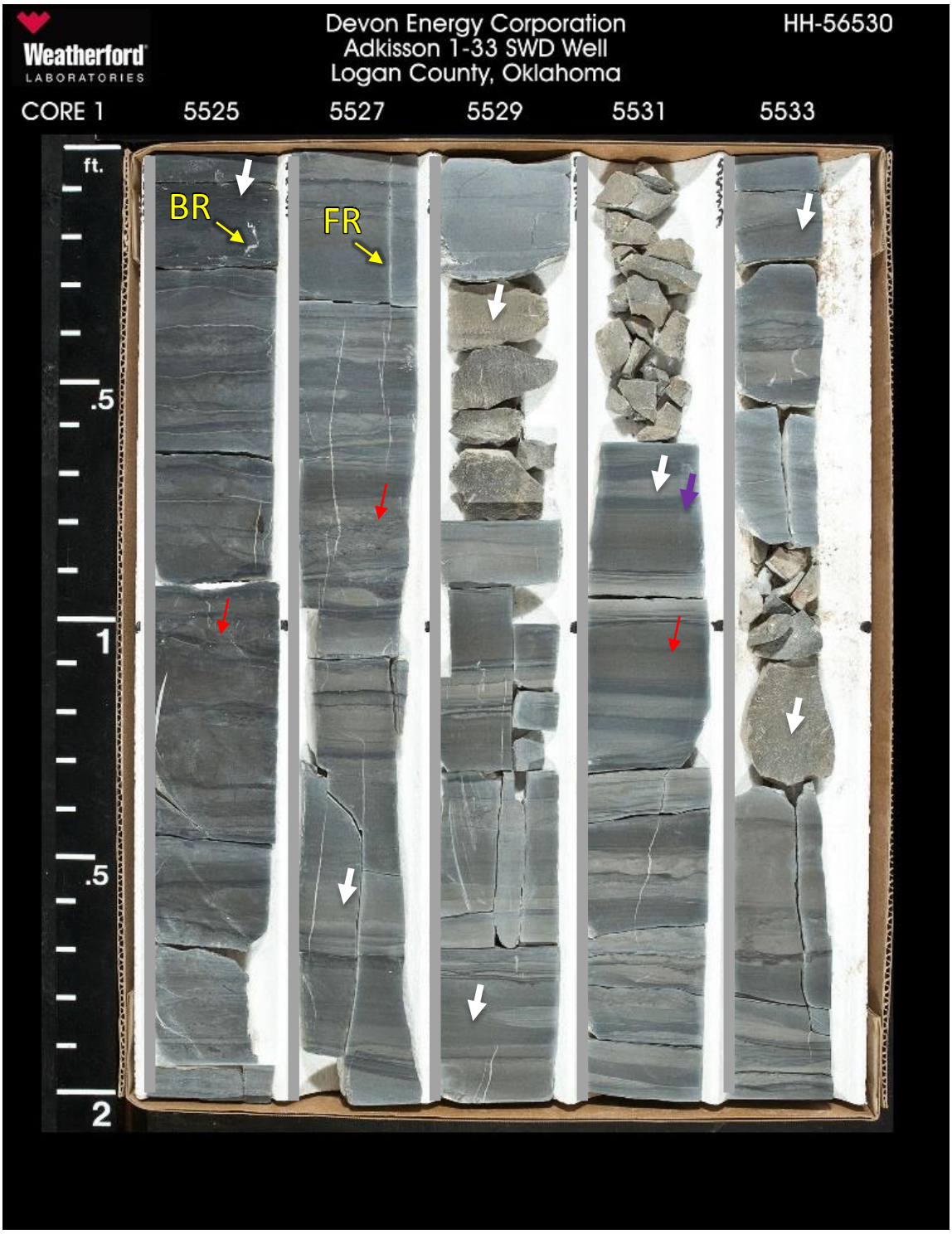
Weatherford
LABORATORIES
Devon Energy Corporation
Adkisson 1-33 SWD Well
Logan County, Oklahoma
HH-56530
CORE 1
5525
5527
5529
5531
5533
ft.
BR
FR
.5
1
.5
2

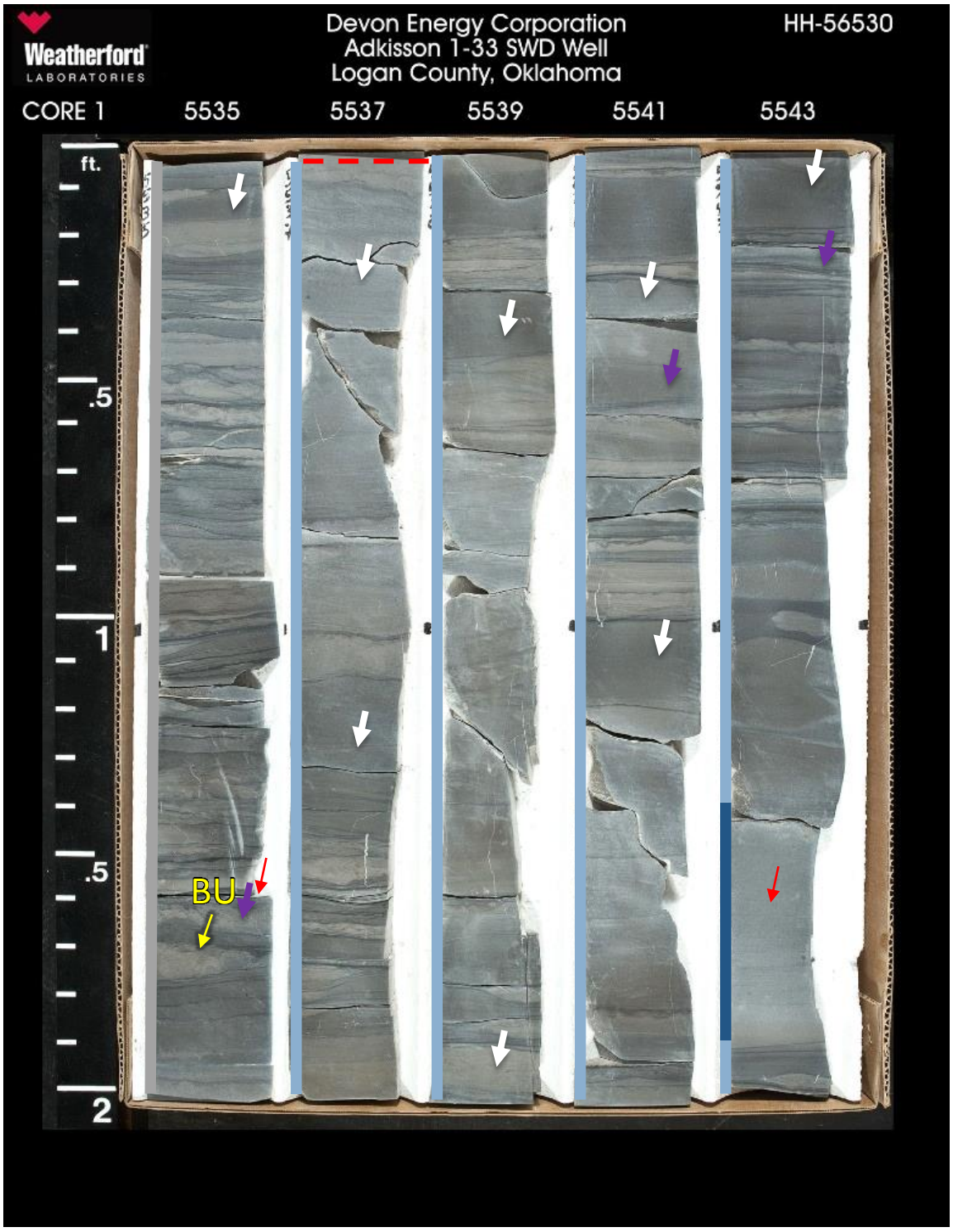
Weatherford
LABORATORIES
Devon Energy Corporation
Adkisson 1-33 SWD Well
Logan County, Oklahoma
HH-56530
CORE 1
5535
5537
5539
5541
5543
ft.
.5
1
.5
2
BU

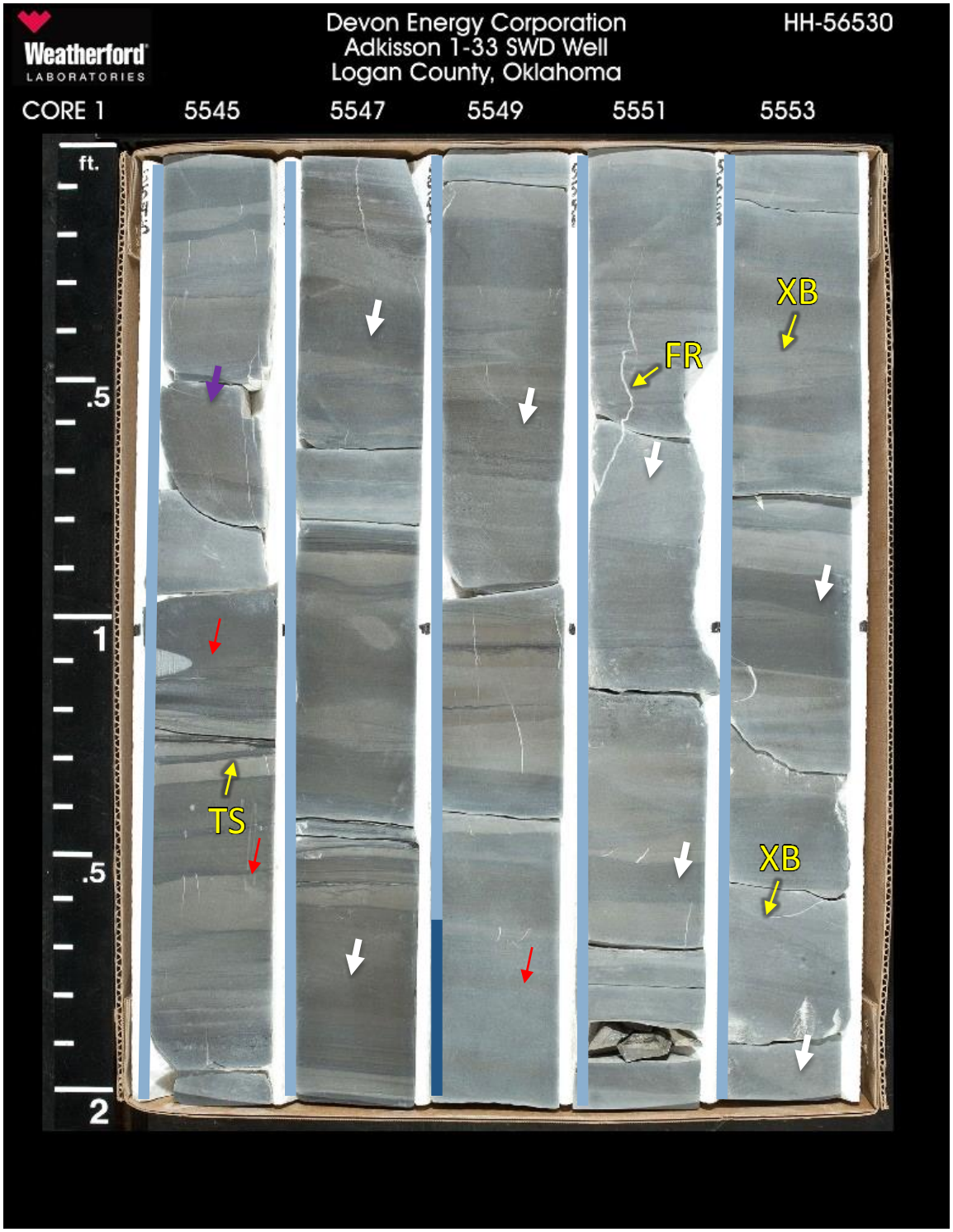
Weatherford
LABORATORIES
Devon Energy Corporation
Adkisson 1-33 SWD Well
Logan County, Oklahoma
HH-56530
CORE 1
5545
5547
5549
5551
5553
ft.
.5
1
.5
2
XB
FR
TS
XB

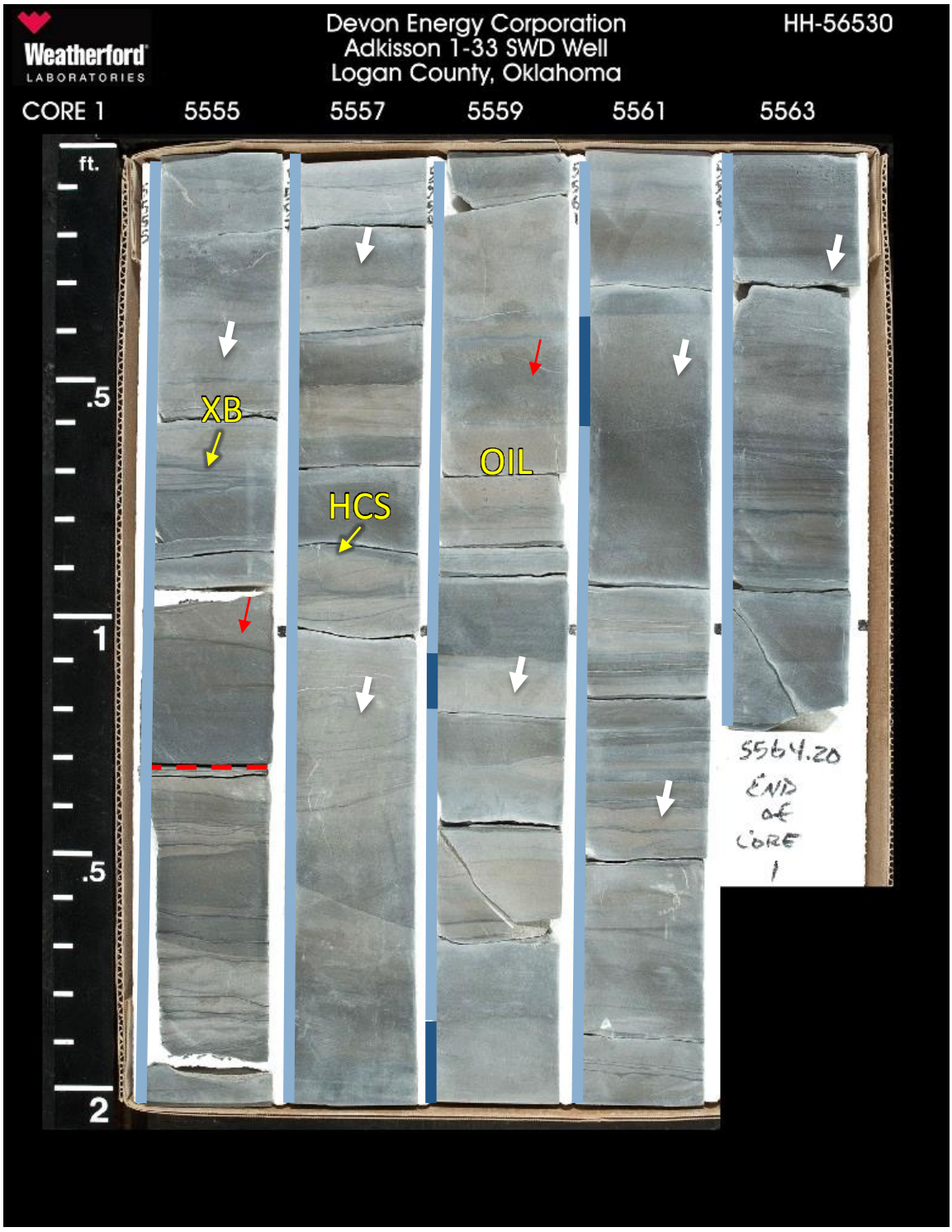
Weatherford
LABORATORIES
Devon Energy Corporation
Adkisson 1-33 SWD Well
Logan County, Oklahoma
HH-56530
CORE 1
5555
5557
5559
5561
5563
ft.
.5
1
.5
2
XB
HCS
OIL
5564.20
END
OF
CORE
1

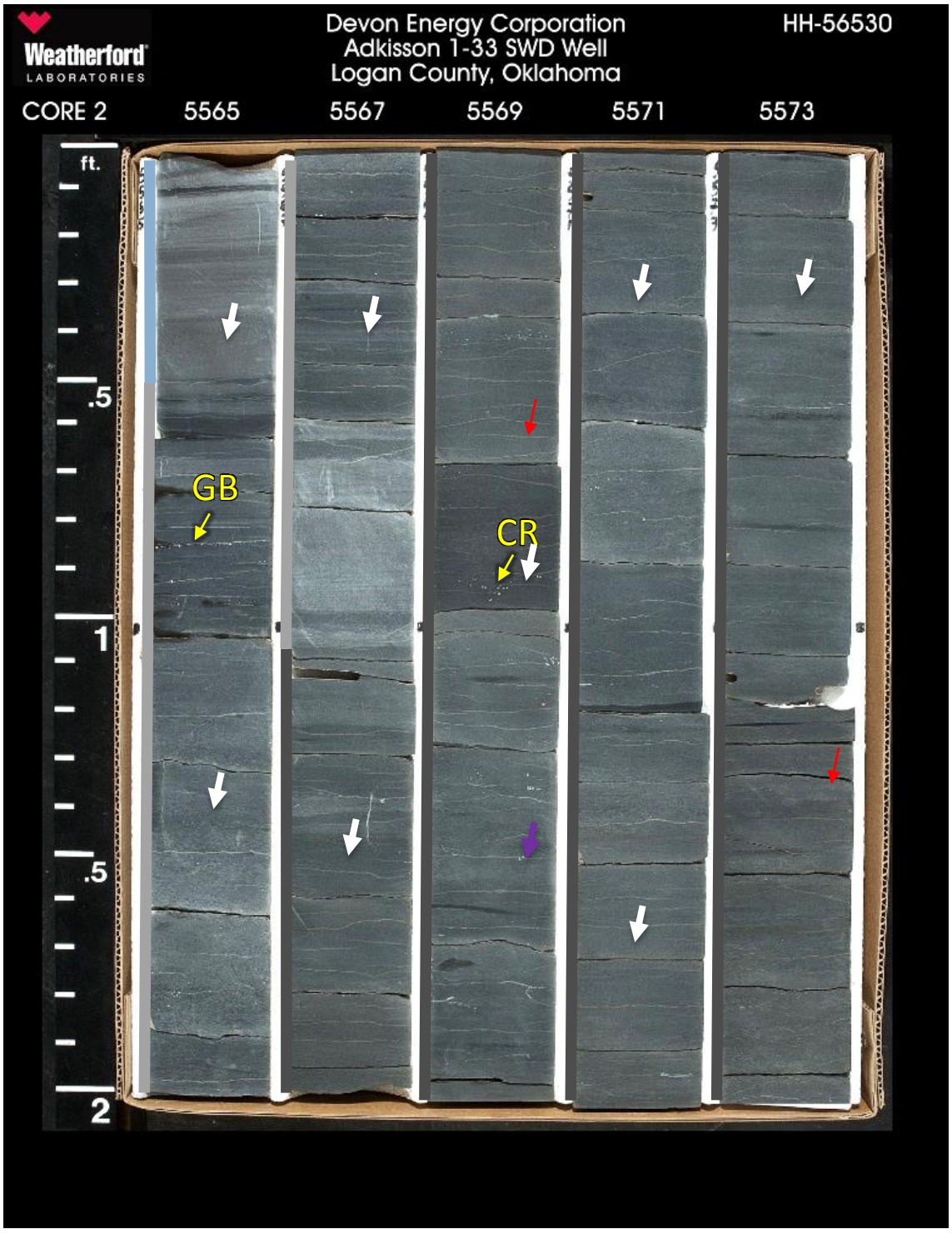
Weatherford
LABORATORIES
Devon Energy Corporation
Adkisson 1-33 SWD Well
Logan County, Oklahoma
HH-56530
CORE 2
5565
5567
5569
5571
5573
ft.
.5
1
.5
2
GB
CR

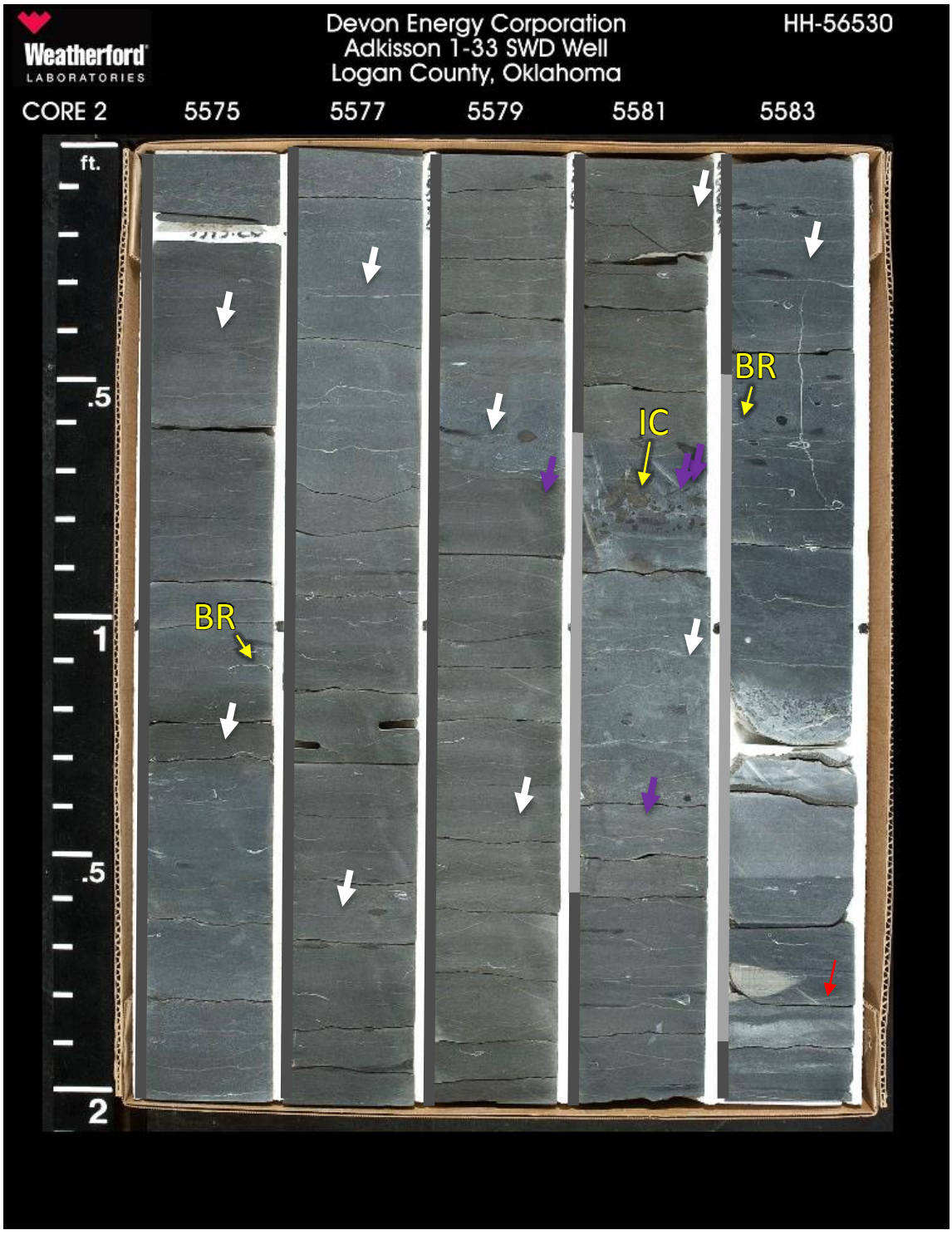
Weatherford
LABORATORIES
Devon Energy Corporation
Adkisson 1-33 SWD Well
Logan County, Oklahoma
HH-56530
CORE 2
5575
5577
5579
5581
5583
ft.
.5
1
.5
2
BR
IC
BR

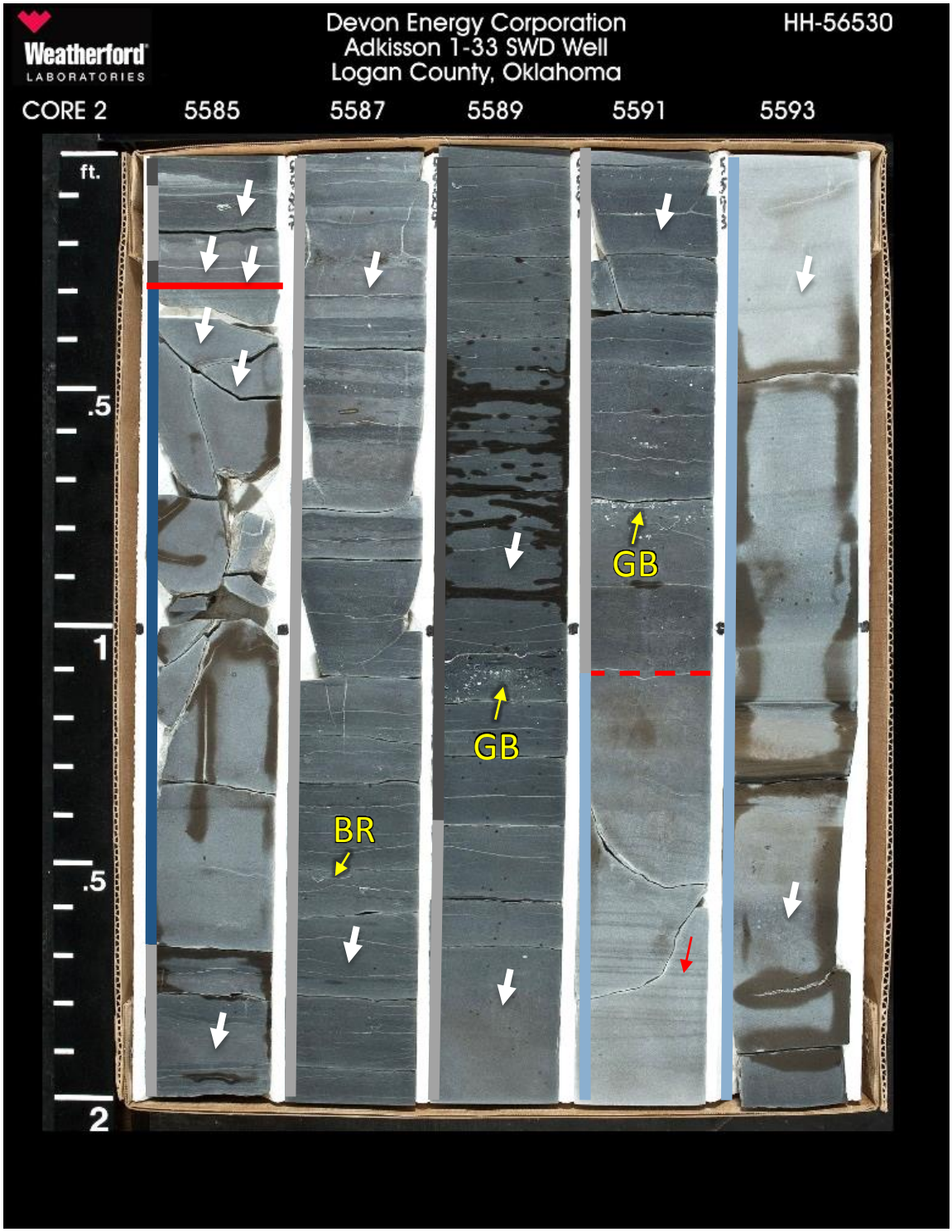
Weatherford
LABORATORIES
Devon Energy Corporation
Adkisson 1-33 SWD Well
Logan County, Oklahoma
HH-56530
CORE 2
5585
5587
5589
5591
5593
ft.
.5
1
.5
2
GB
GB
BR

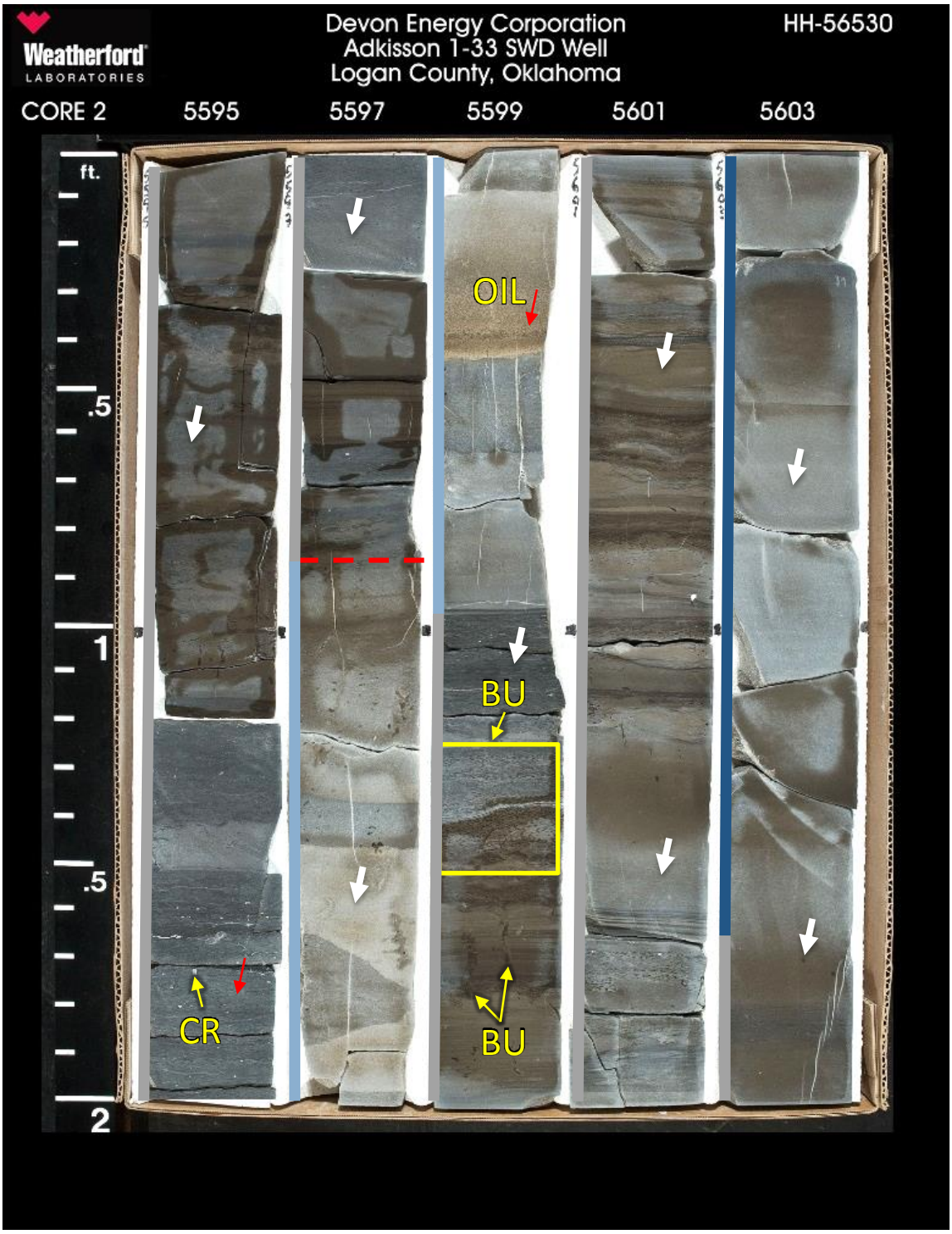
Weatherford
LABORATORIES
Devon Energy Corporation
Adkisson 1-33 SWD Well
Logan County, Oklahoma
HH-56530
CORE 2
5595
5597
5599
5601
5603
ft.
.5
1
.5
2
OIL
BU
CR
BU

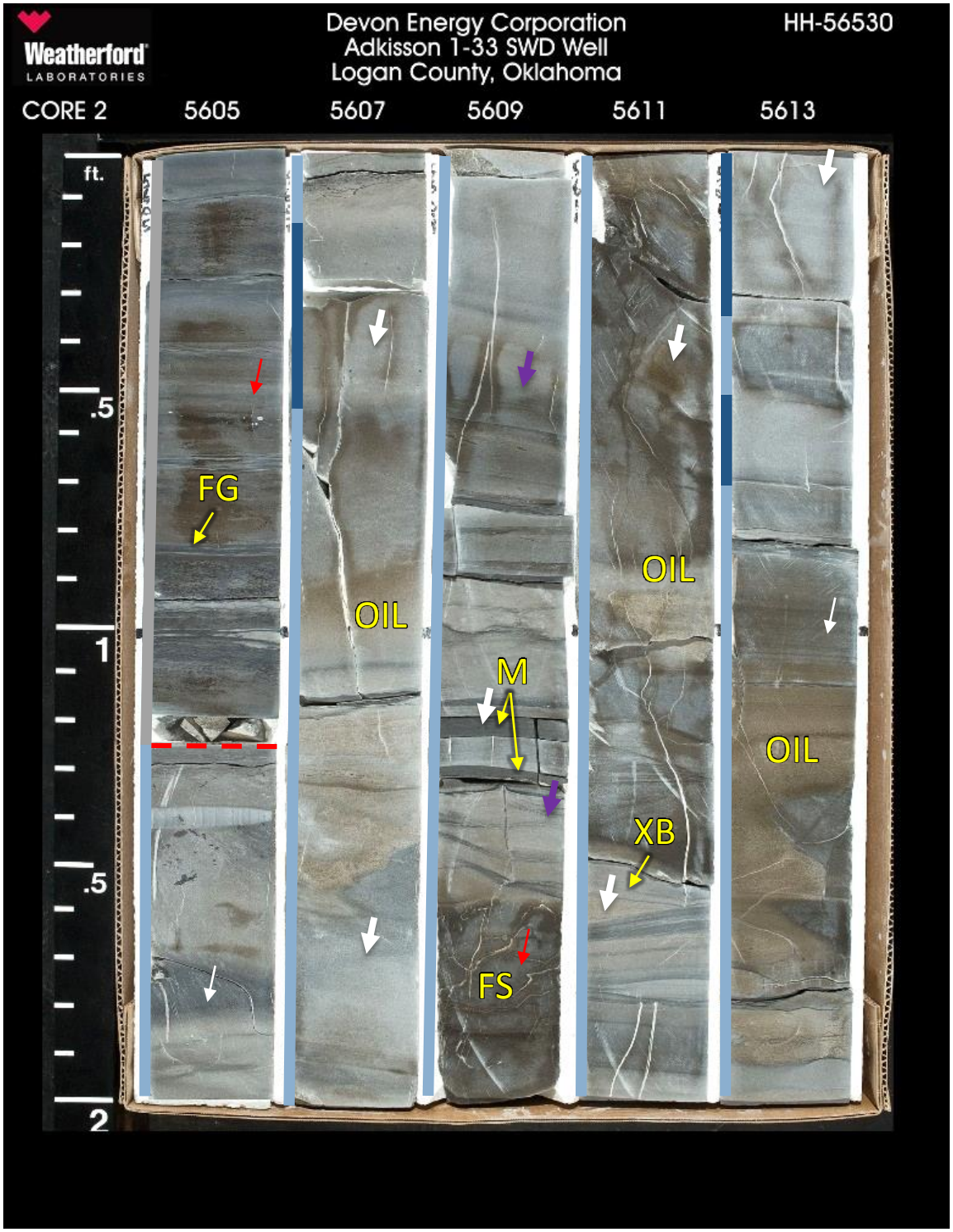
Weatherford
LABORATORIES
Devon Energy Corporation
Adkisson 1-33 SWD Well
Logan County, Oklahoma
HH-56530
CORE 2
5605
5607
5609
5611
5613
ft.
.5
1
.5
2
FG
OIL
OIL
M
OIL
XB
FS

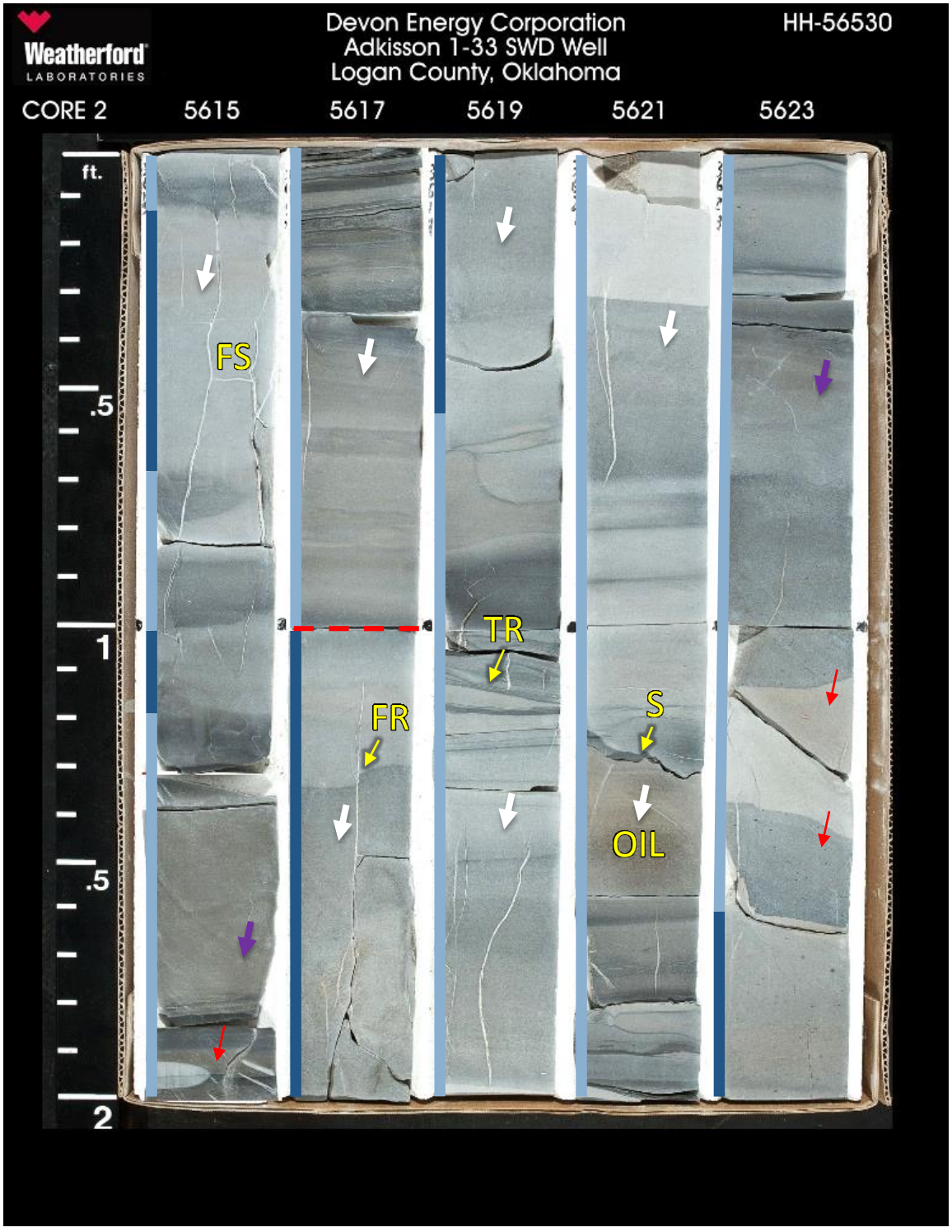
Weatherford
LABORATORIES
Devon Energy Corporation
Adkisson 1-33 SWD Well
Logan County, Oklahoma
HH-56530
CORE 2
5615
5617
5619
5621
5623
ft.
.5
1
.5
2
FS
FR
TR
S
OIL

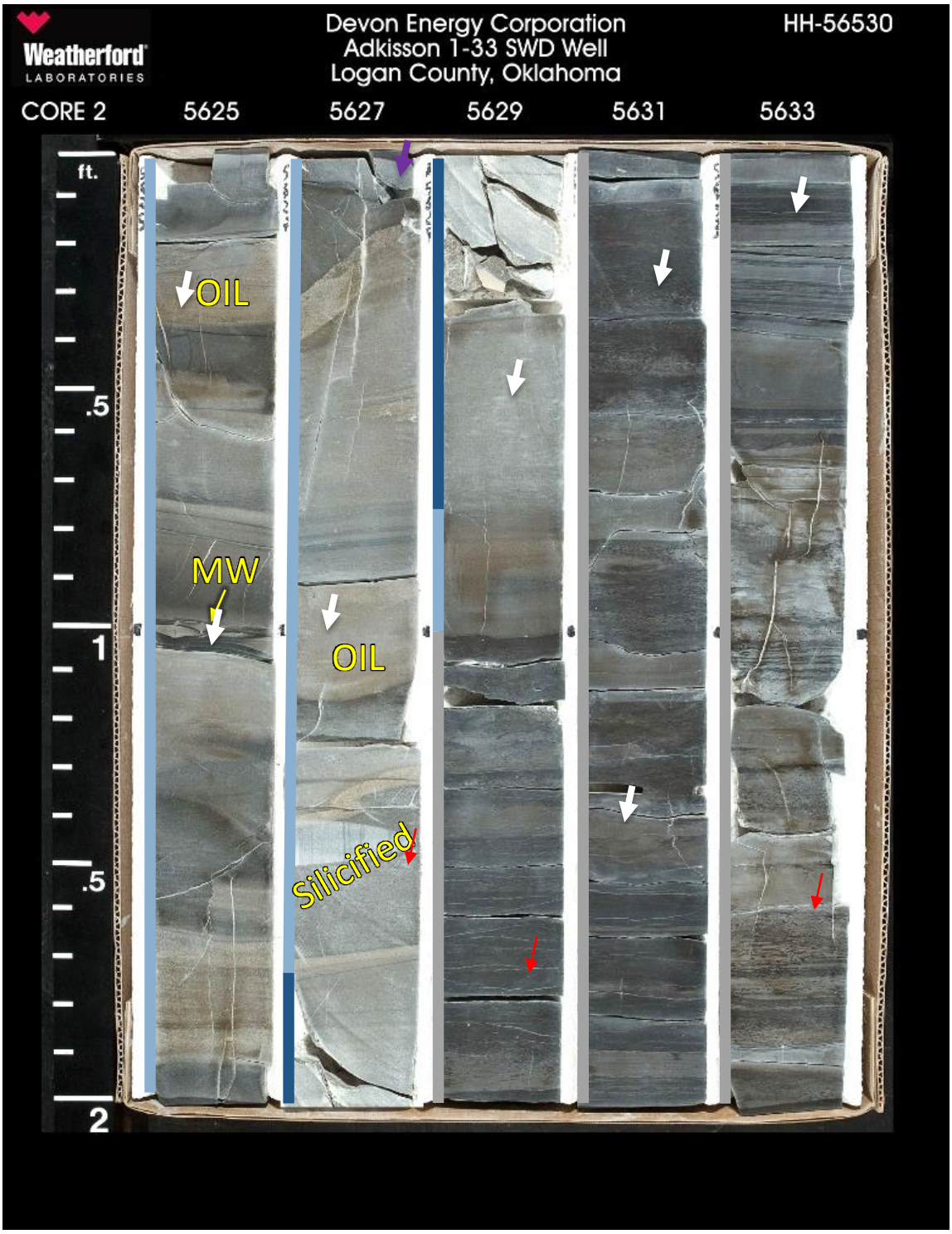
Weatherford
LABORATORIES
Devon Energy Corporation
Adkisson 1-33 SWD Well
Logan County, Oklahoma
HH-56530
CORE 2
5625
5627
5629
5631
5633
ft.
.5
1
.5
2
OIL
MW
OIL
Silicified

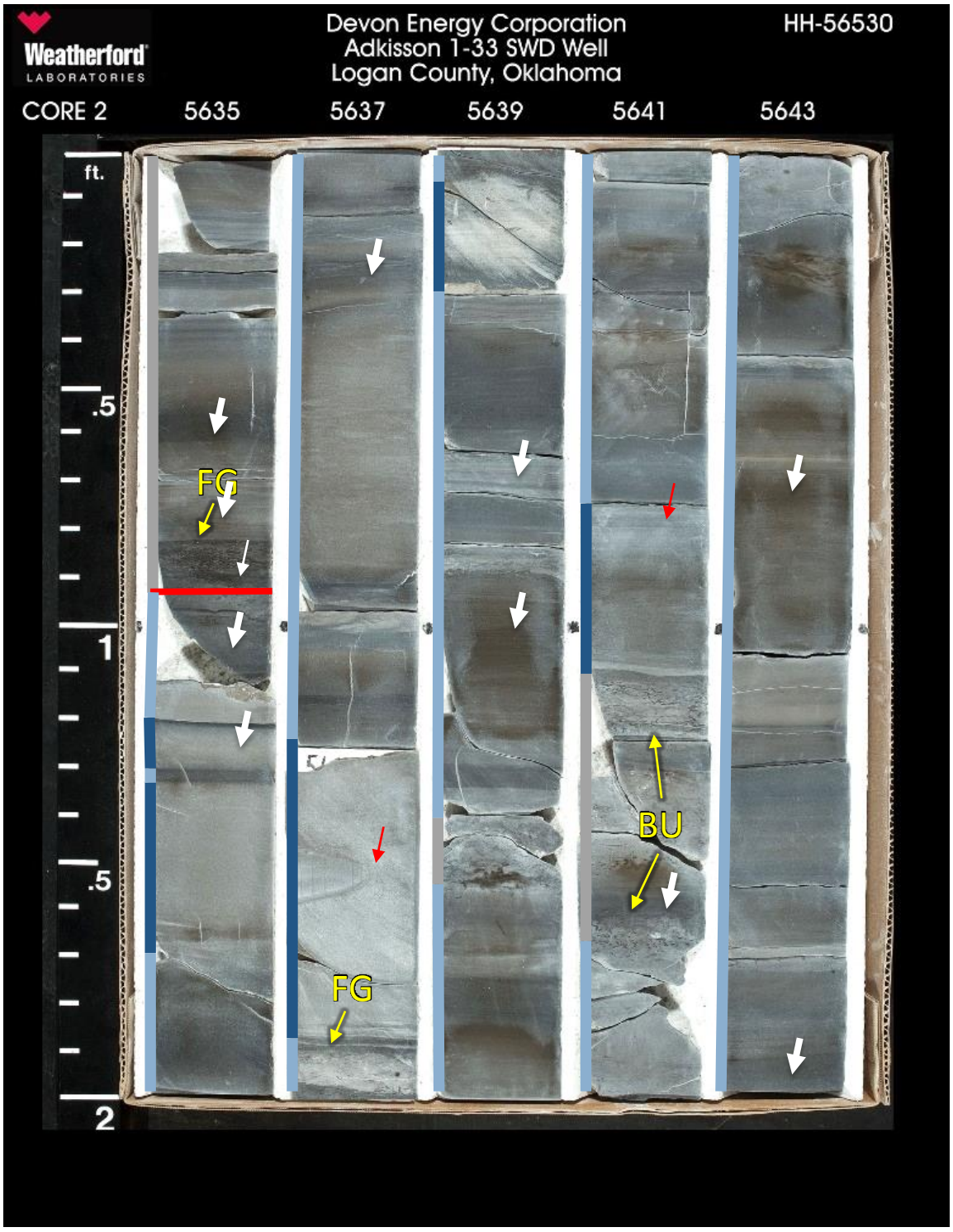
Weatherford
LABORATORIES
Devon Energy Corporation
Adkisson 1-33 SWD Well
Logan County, Oklahoma
HH-56530
CORE 2
5635
5637
5639
5641
5643
ft.
.5
1
.5
2
FG
BU
FG

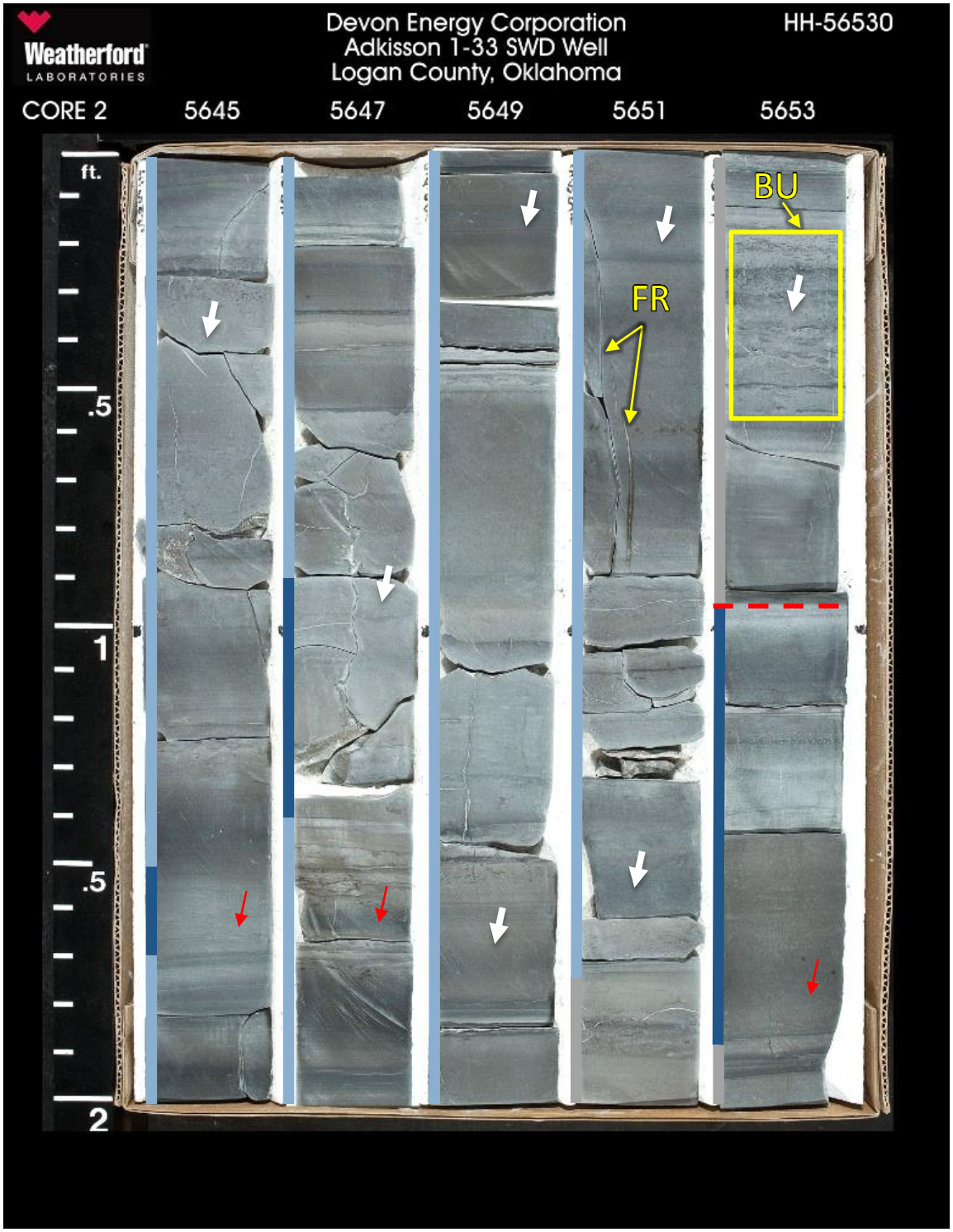
Weatherford
LABORATORIES
Devon Energy Corporation
Adkisson 1-33 SWD Well
Logan County, Oklahoma
HH-56530
CORE 2
5645
5647
5649
5651
5653
ft.
.5
1
.5
2
BU
FR

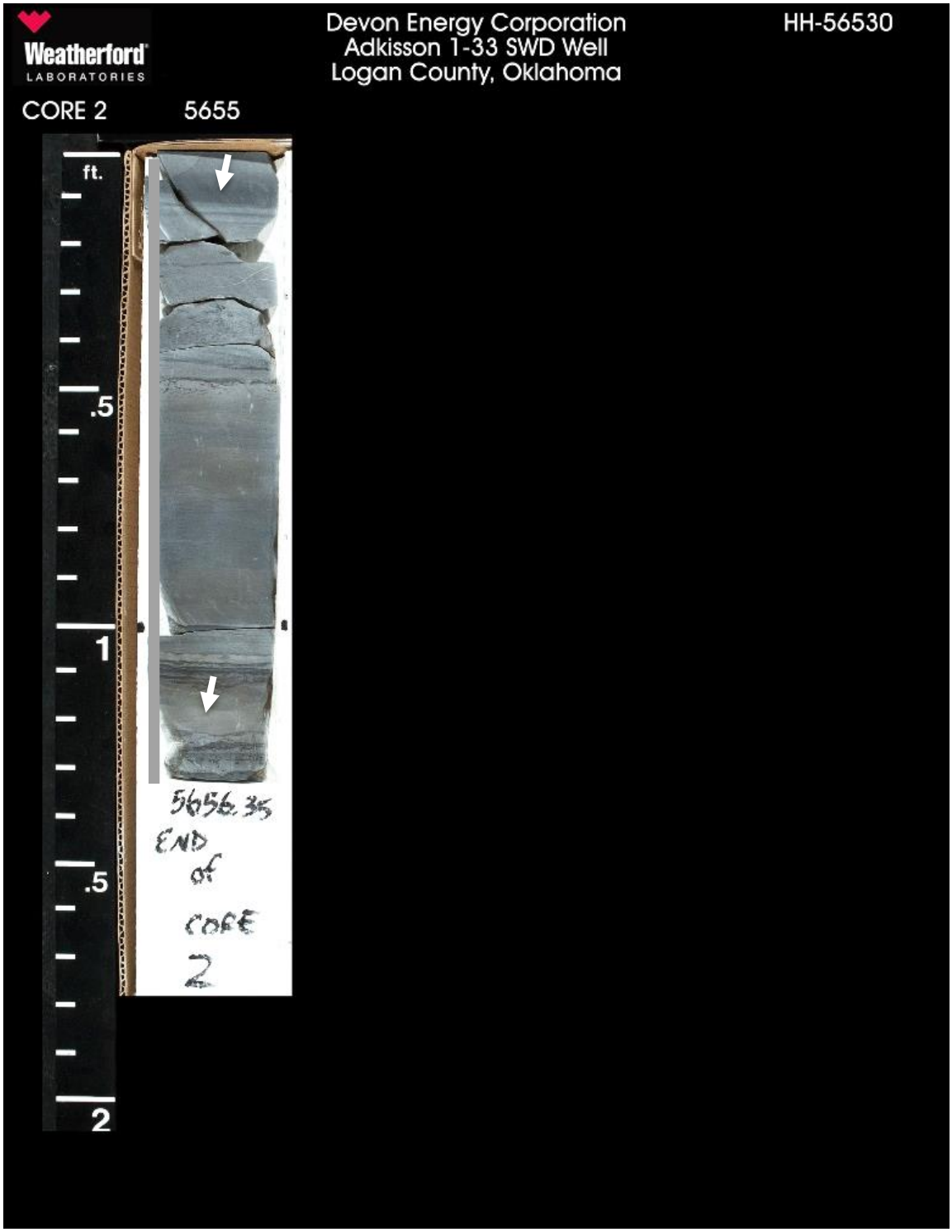
Weatherford
LABORATORIES
Devon Energy Corporation
Adkisson 1-33 SWD Well
Logan County, Oklahoma
HH-56530
CORE 2
5655
ft.
.5
1
.5
2
5656.35
END
of
CORE
2

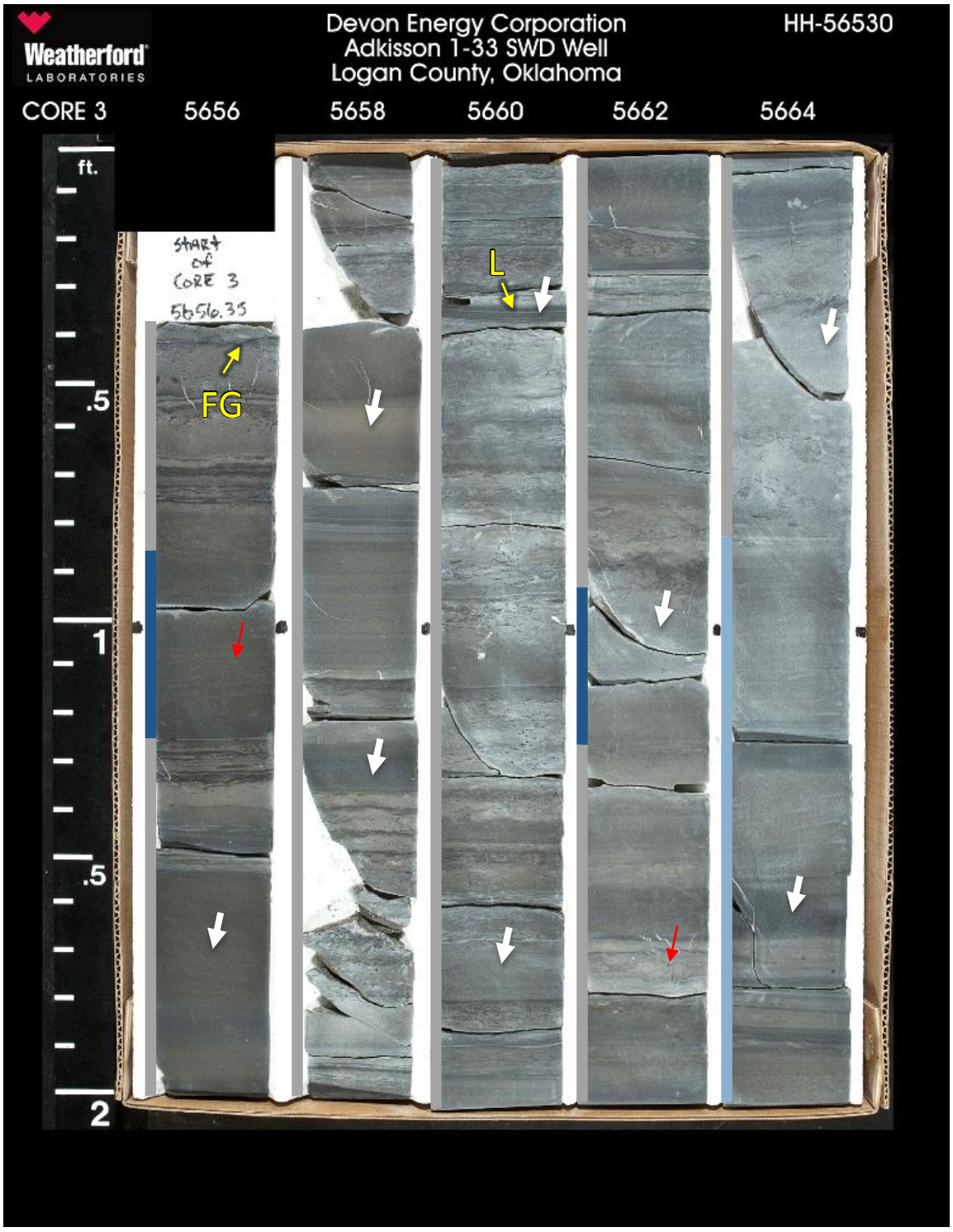
Weatherford
LABORATORIES
Devon Energy Corporation
Adkisson 1-33 SWD Well
Logan County, Oklahoma
HH-56530
CORE 3
5656
5658
5660
5662
5664
ft.
.5
1
.5
2
start of CORE 3
5656.35
FG
L

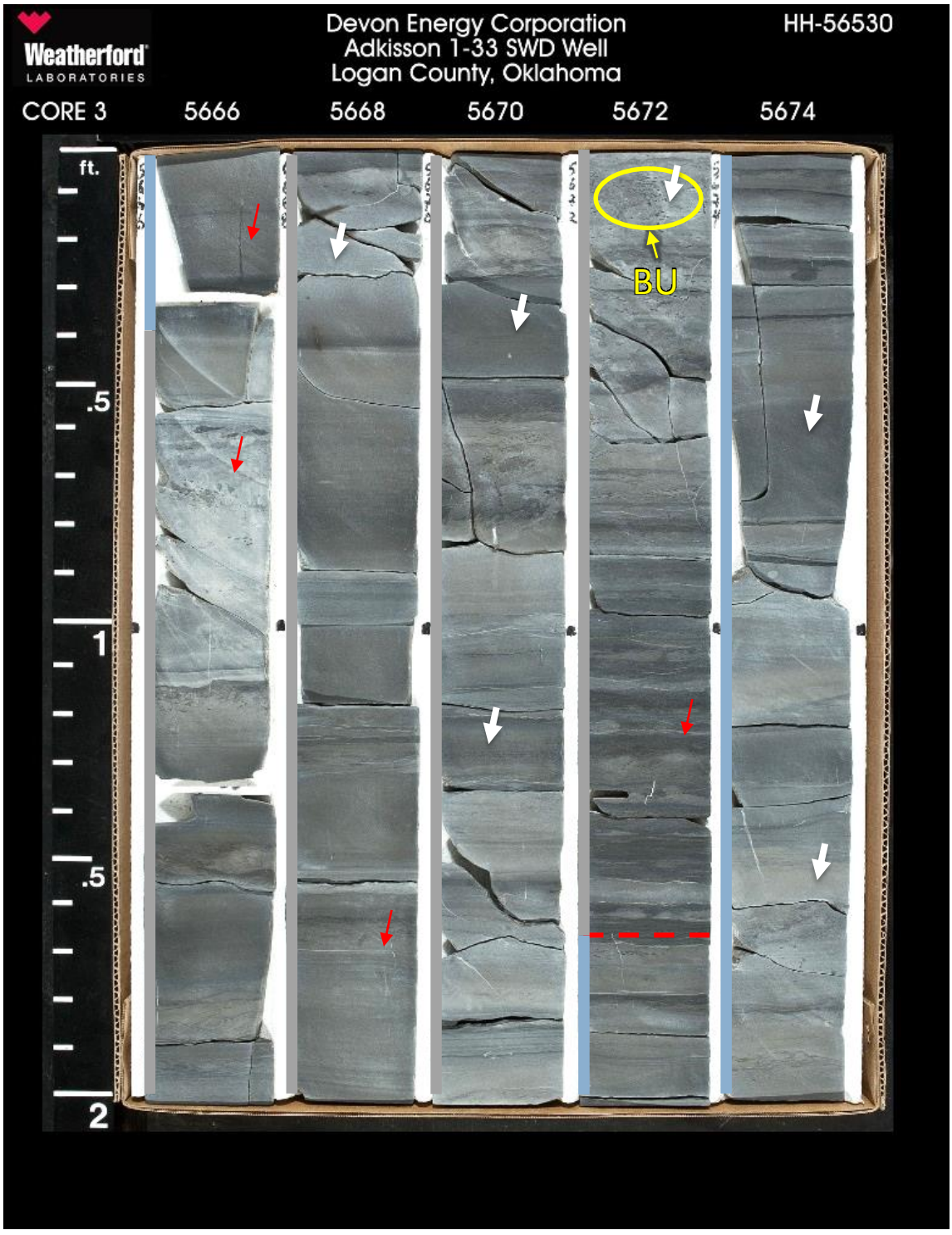
Weatherford
LABORATORIES
Devon Energy Corporation
Adkisson 1-33 SWD Well
Logan County, Oklahoma
HH-56530
CORE 3
5666
5668
5670
5672
5674
ft.
.5
1
.5
2
BU

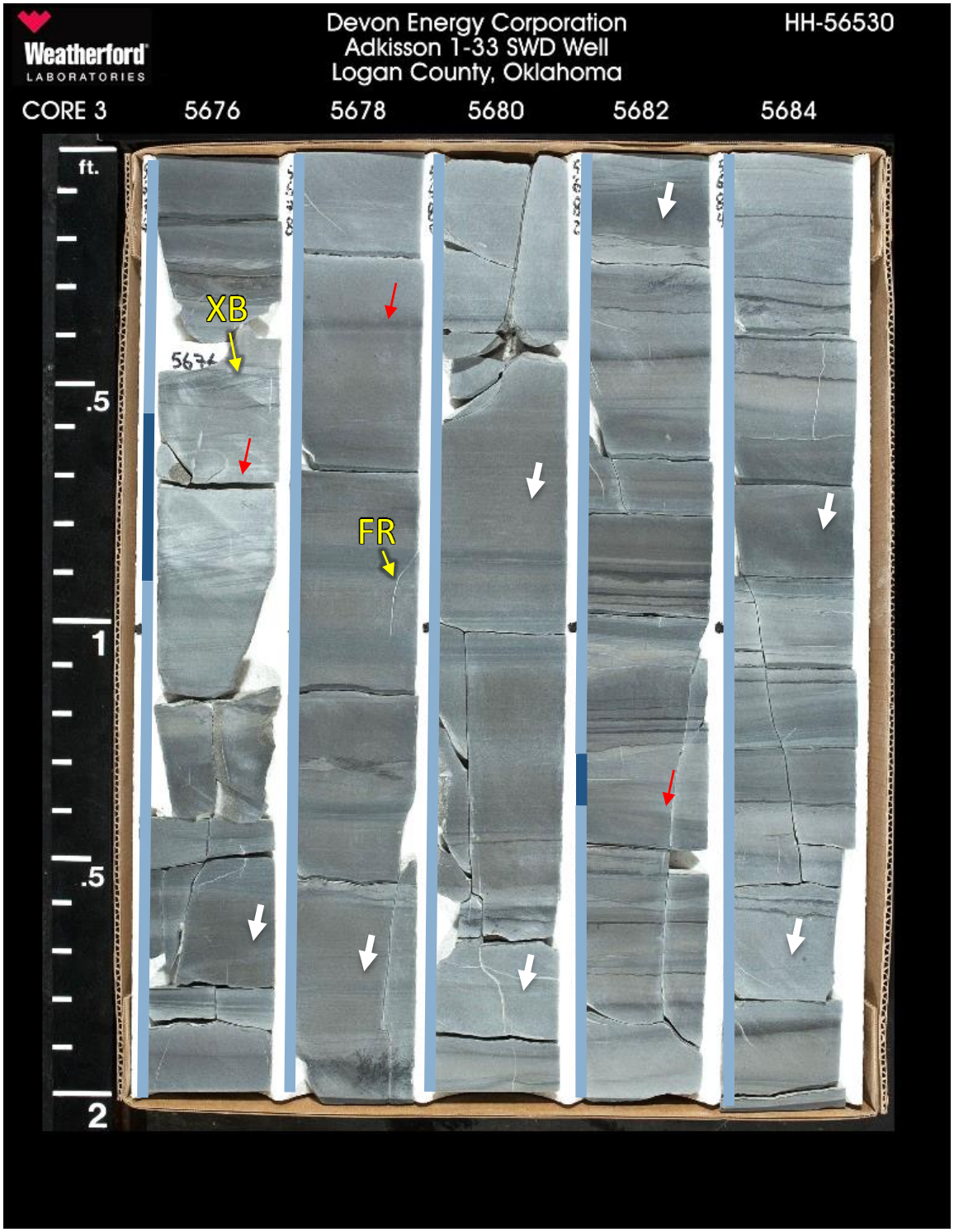
Weatherford
LABORATORIES
Devon Energy Corporation
Adkisson 1-33 SWD Well
Logan County, Oklahoma
HH-56530
CORE 3
5676
5678
5680
5682
5684
ft.
.5
1
.5
2
XB
5674
FR

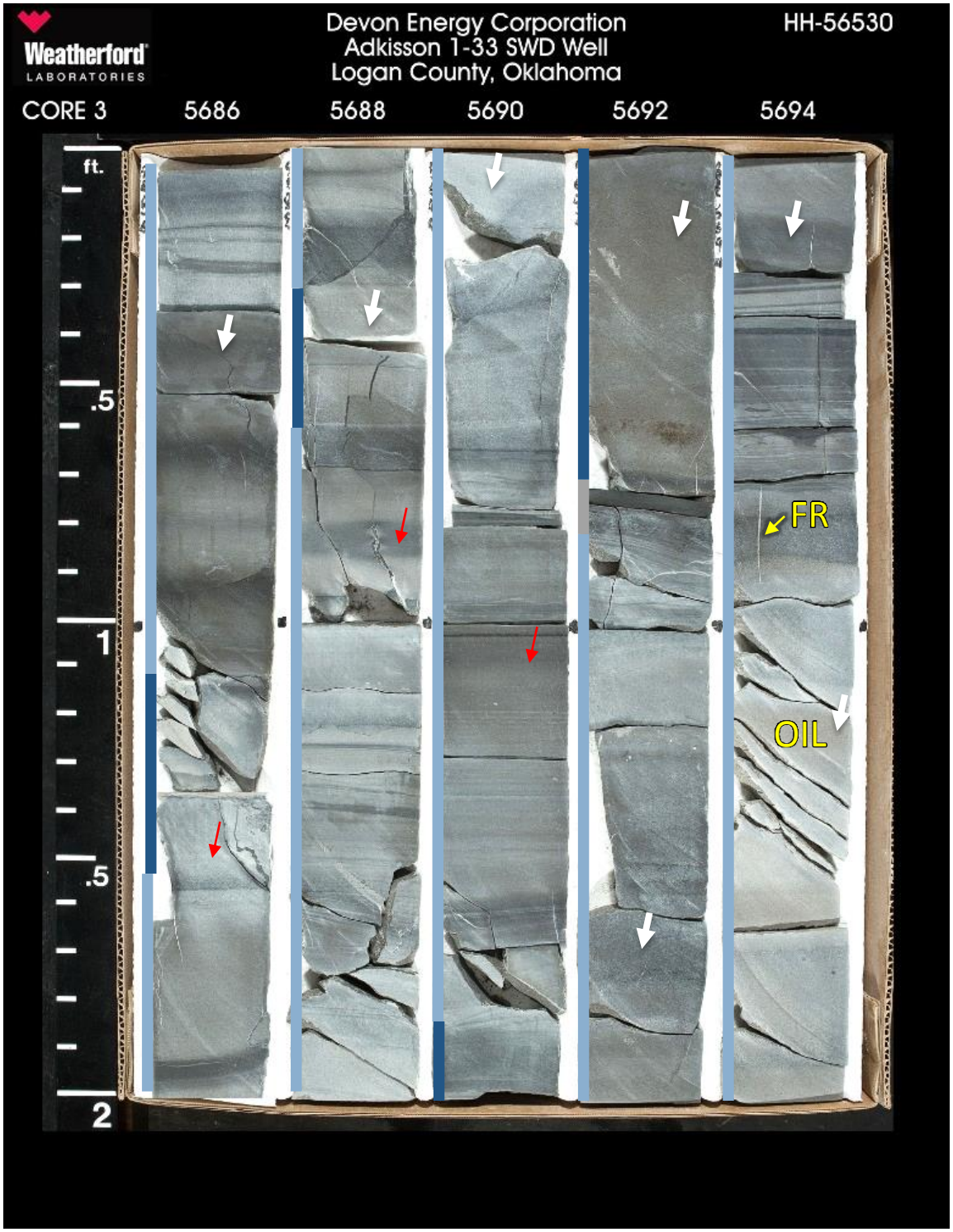
Weatherford
LABORATORIES
Devon Energy Corporation
Adkisson 1-33 SWD Well
Logan County, Oklahoma
HH-56530
CORE 3
5686
5688
5690
5692
5694
ft.
.5
1
.5
2
FR
OIL

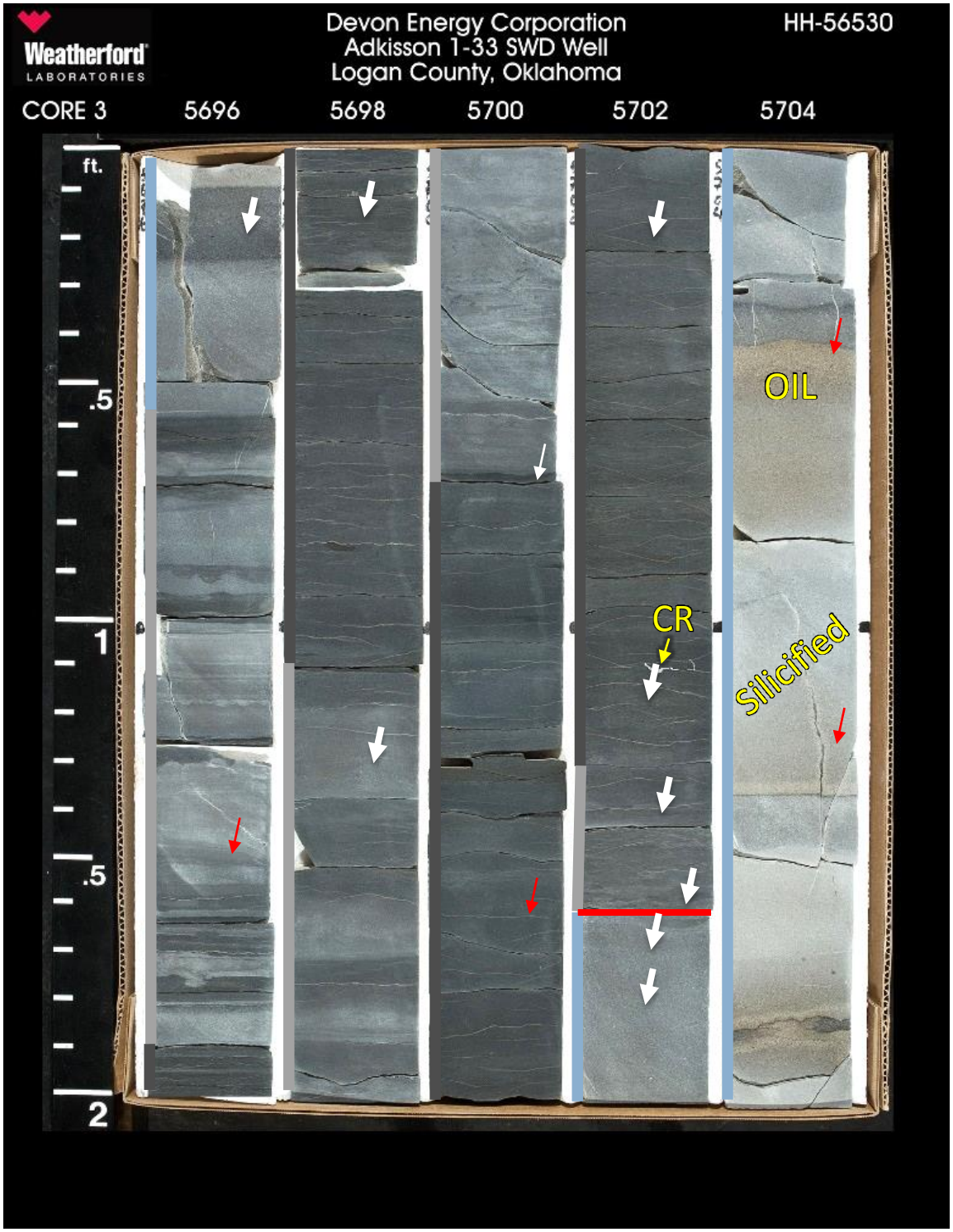
Weatherford
LABORATORIES
Devon Energy Corporation
Adkisson 1-33 SWD Well
Logan County, Oklahoma
HH-56530
CORE 3
5696
5698
5700
5702
5704
ft.
.5
1
.5
2
OIL
CR
Silicified

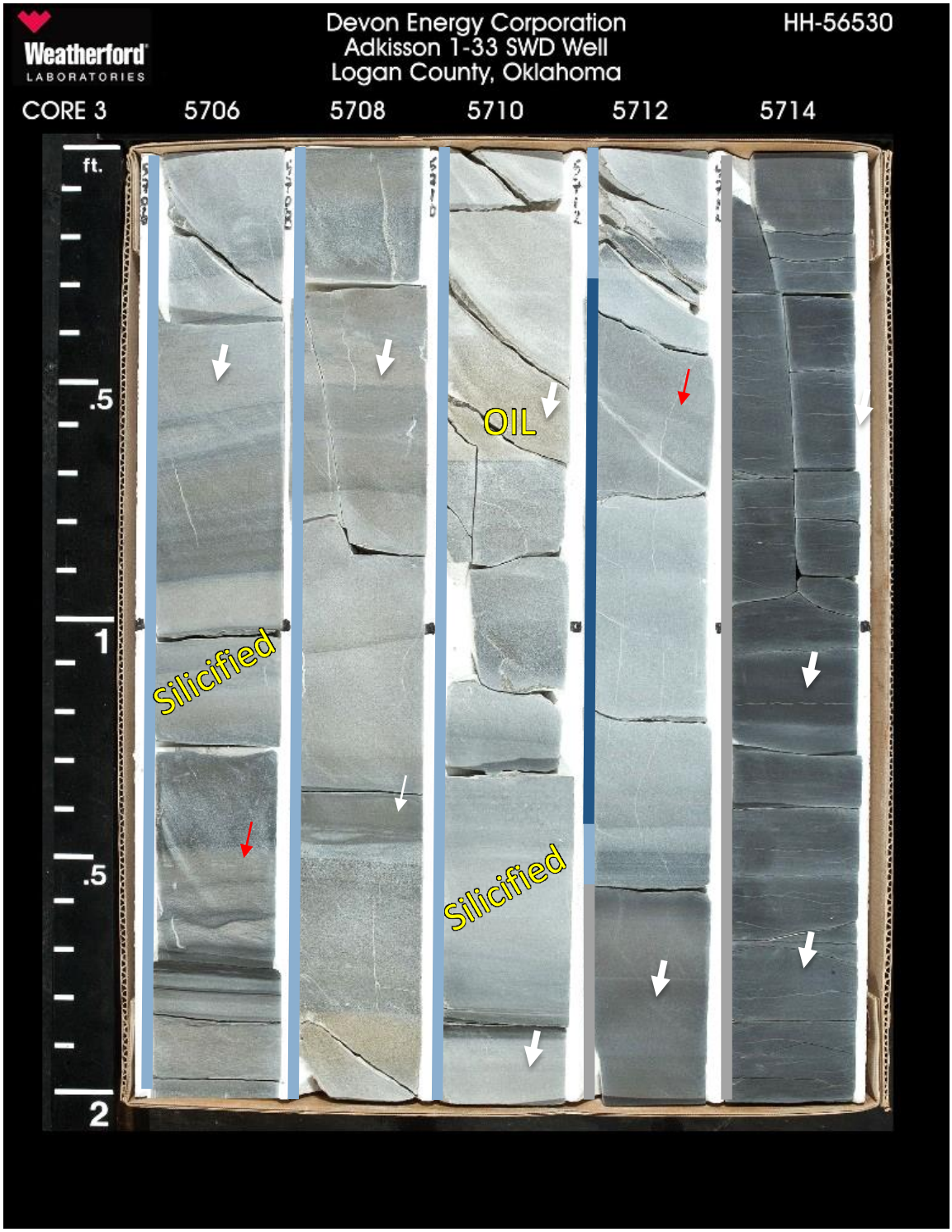
Weatherford
LABORATORIES
Devon Energy Corporation
Adkisson 1-33 SWD Well
Logan County, Oklahoma
HH-56530
CORE 3
5706
5708
5710
5712
5714
ft.
.5
1
.5
2
OIL
Silicified
Silicified

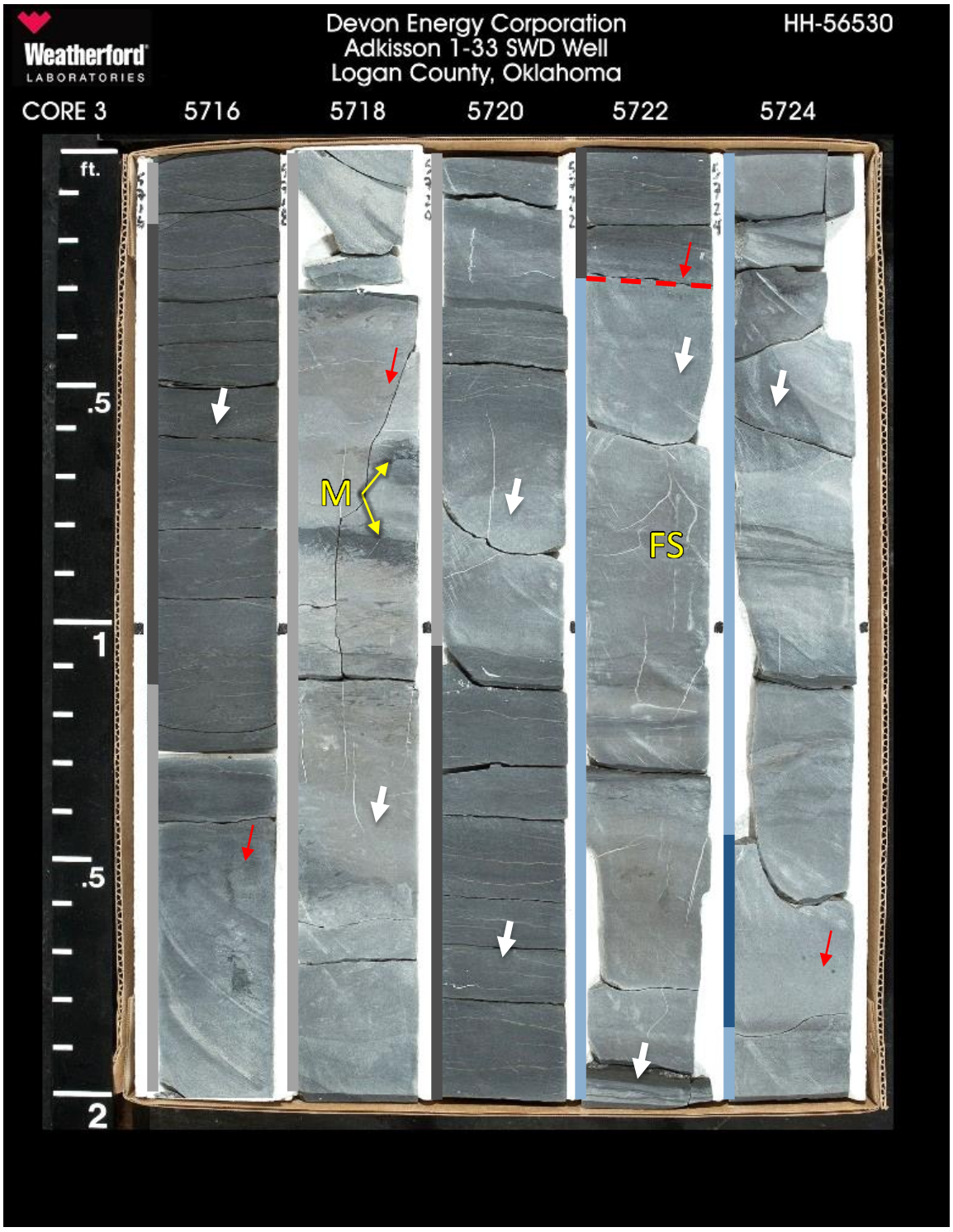
Weatherford
LABORATORIES
Devon Energy Corporation
Adkisson 1-33 SWD Well
Logan County, Oklahoma
HH-56530
CORE 3
5716
5718
5720
5722
5724
ft.
.5
1
.5
2
M
FS

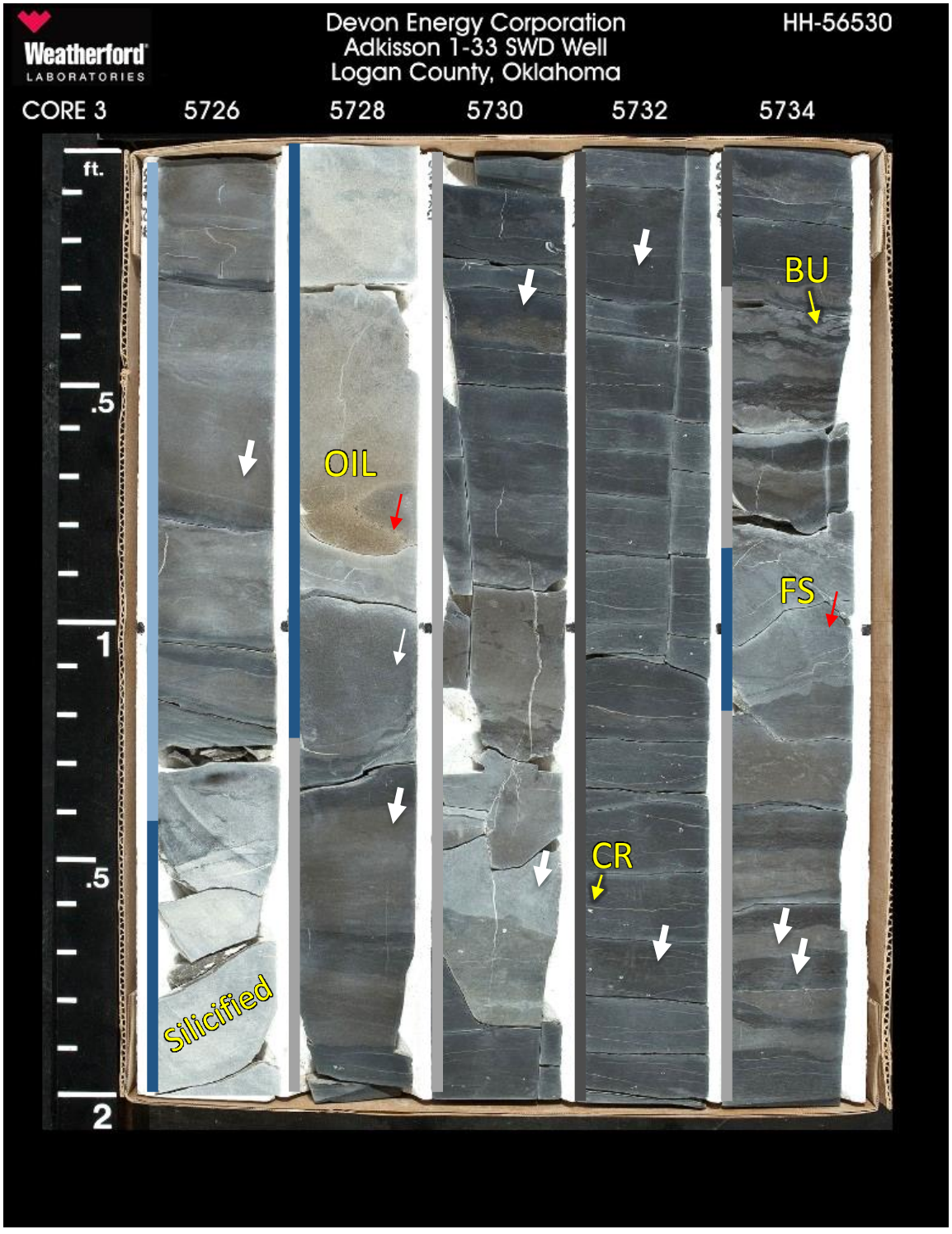
Weatherford
LABORATORIES
Devon Energy Corporation
Adkisson 1-33 SWD Well
Logan County, Oklahoma
HH-56530
CORE 3
5726
5728
5730
5732
5734
ft.
.5
1
.5
2
OIL
BU
FS
CR
Silicified

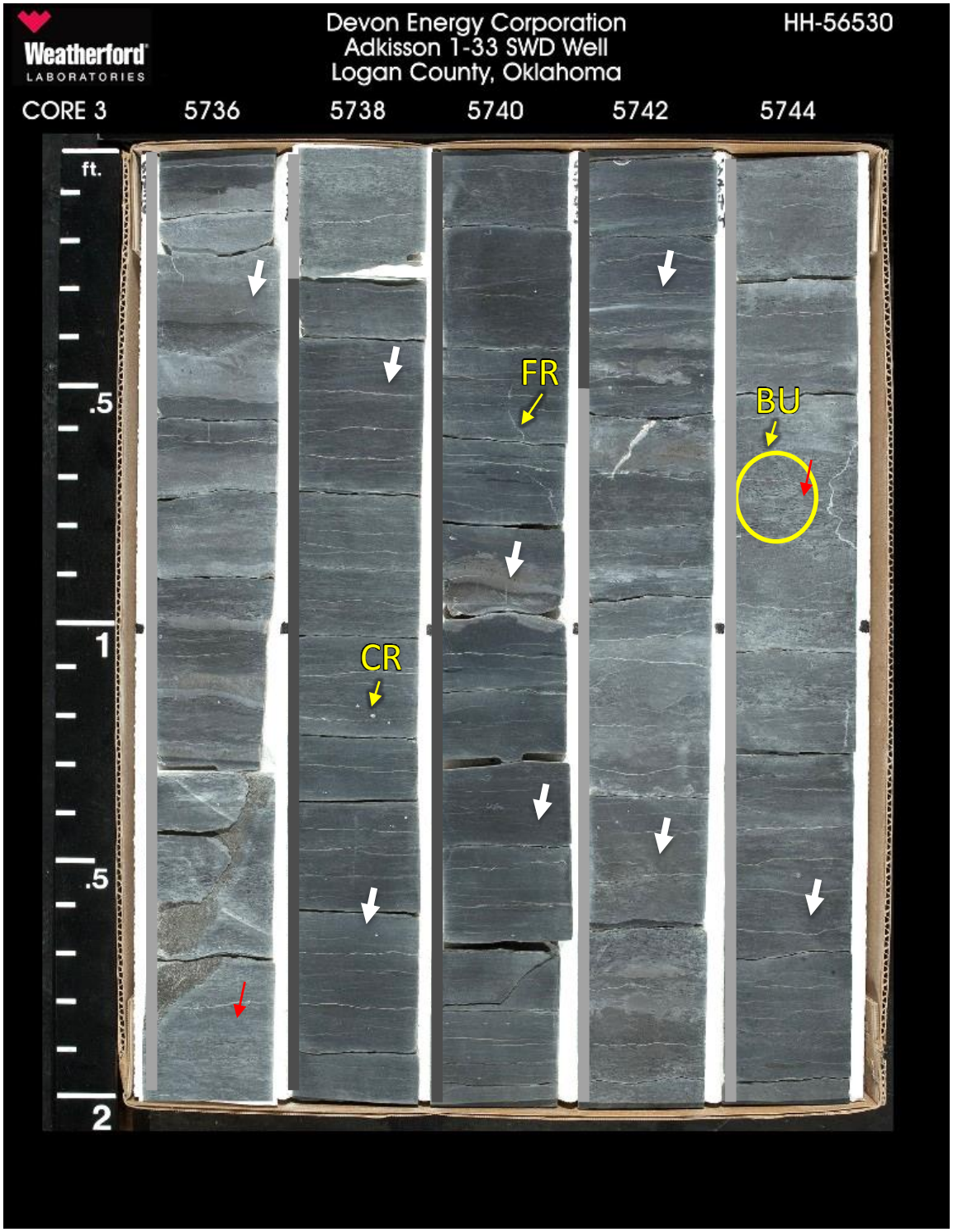
Weatherford
LABORATORIES
Devon Energy Corporation
Adkisson 1-33 SWD Well
Logan County, Oklahoma
HH-56530
CORE 3
5736
5738
5740
5742
5744
ft.
.5
1
.5
2
FR
BU
CR

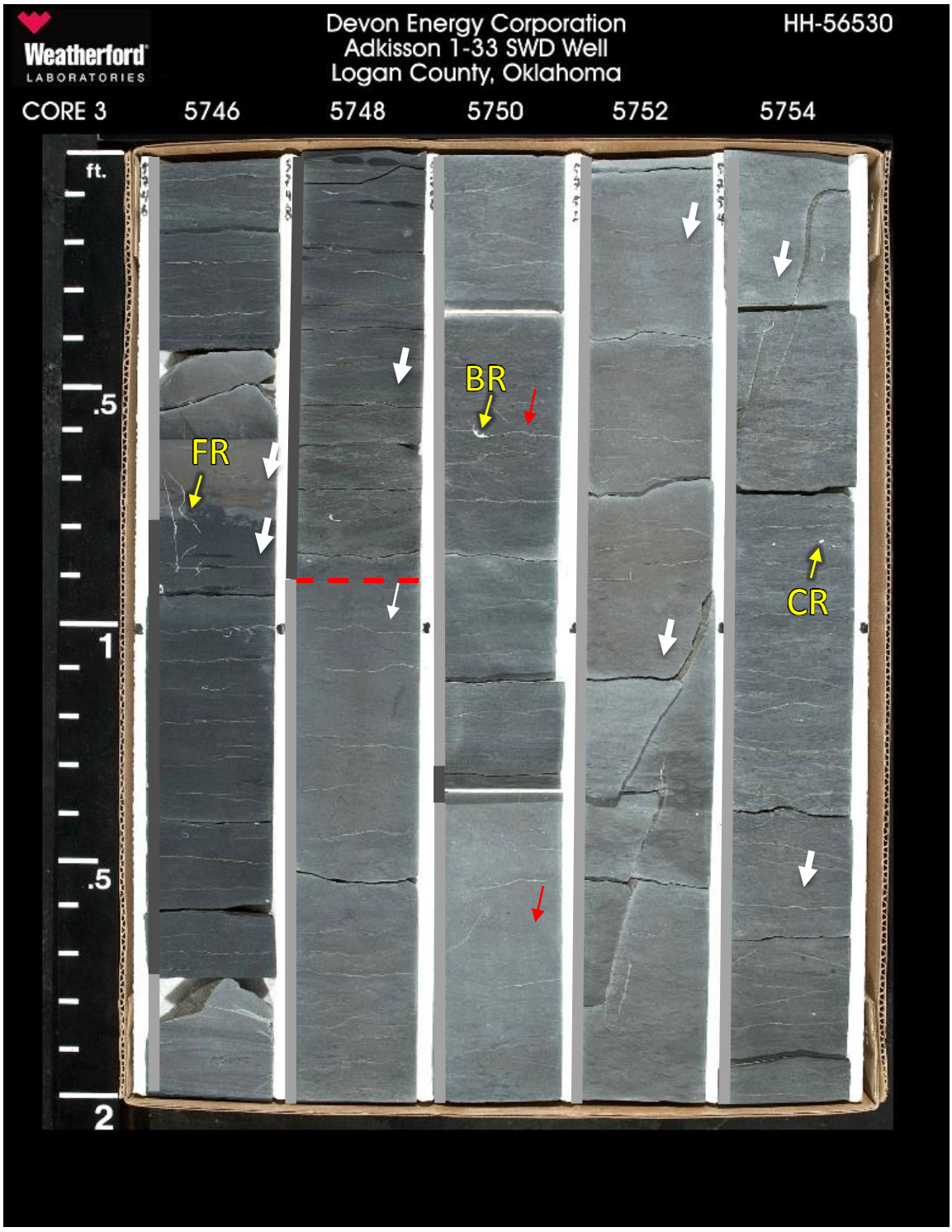
Weatherford
LABORATORIES
Devon Energy Corporation
Adkisson 1-33 SWD Well
Logan County, Oklahoma
HH-56530
CORE 3
5746
5748
5750
5752
5754
ft.
.5
1
.5
2
FR
BR
CR

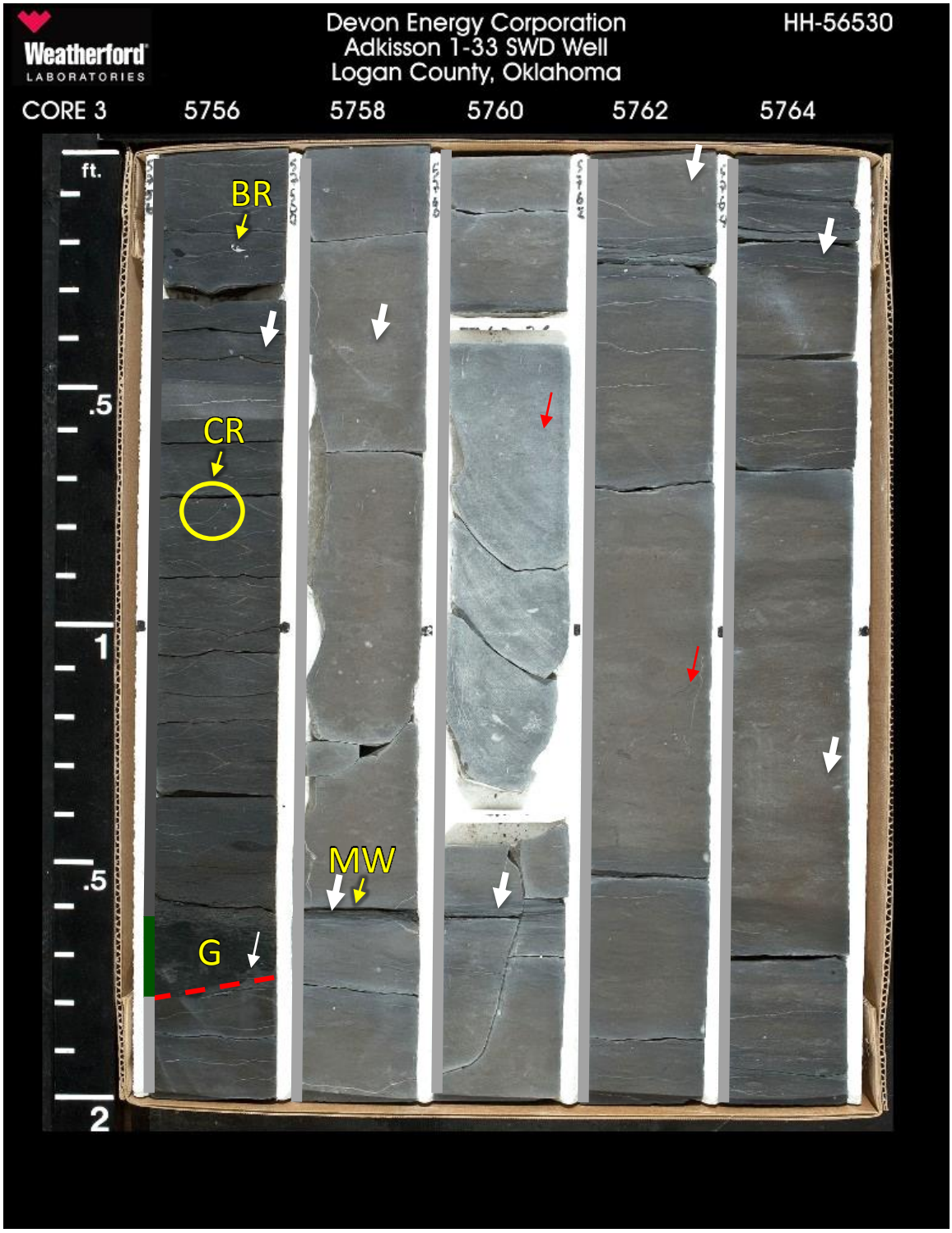
Weatherford
LABORATORIES
Devon Energy Corporation
Adkisson 1-33 SWD Well
Logan County, Oklahoma
HH-56530
CORE 3
5756
5758
5760
5762
5764
ft.
.5
1
.5
2
BR
CR
MW
G

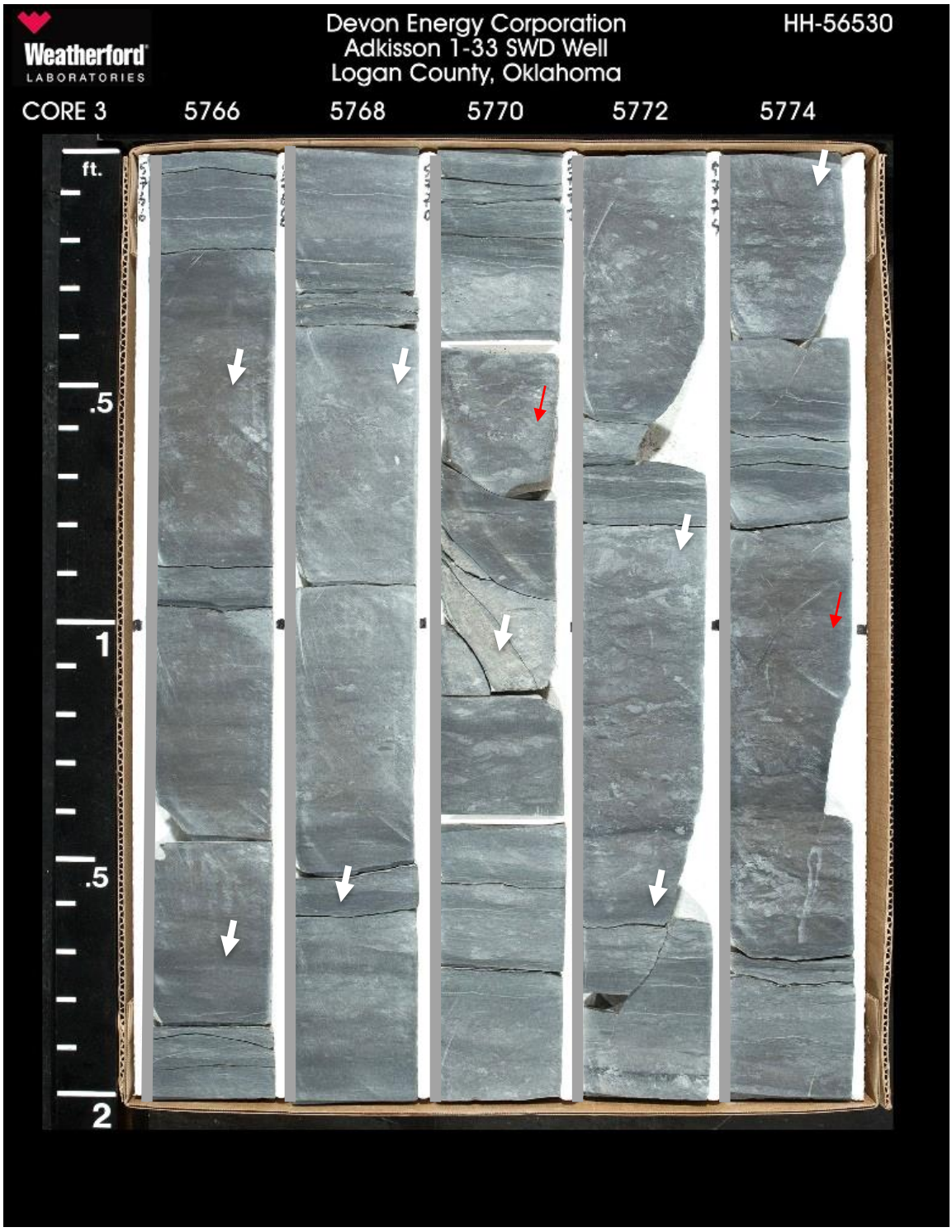
Weatherford
LABORATORIES
Devon Energy Corporation
Adkisson 1-33 SWD Well
Logan County, Oklahoma
HH-56530
CORE 3
5766
5768
5770
5772
5774
ft.
.5
1
.5
2

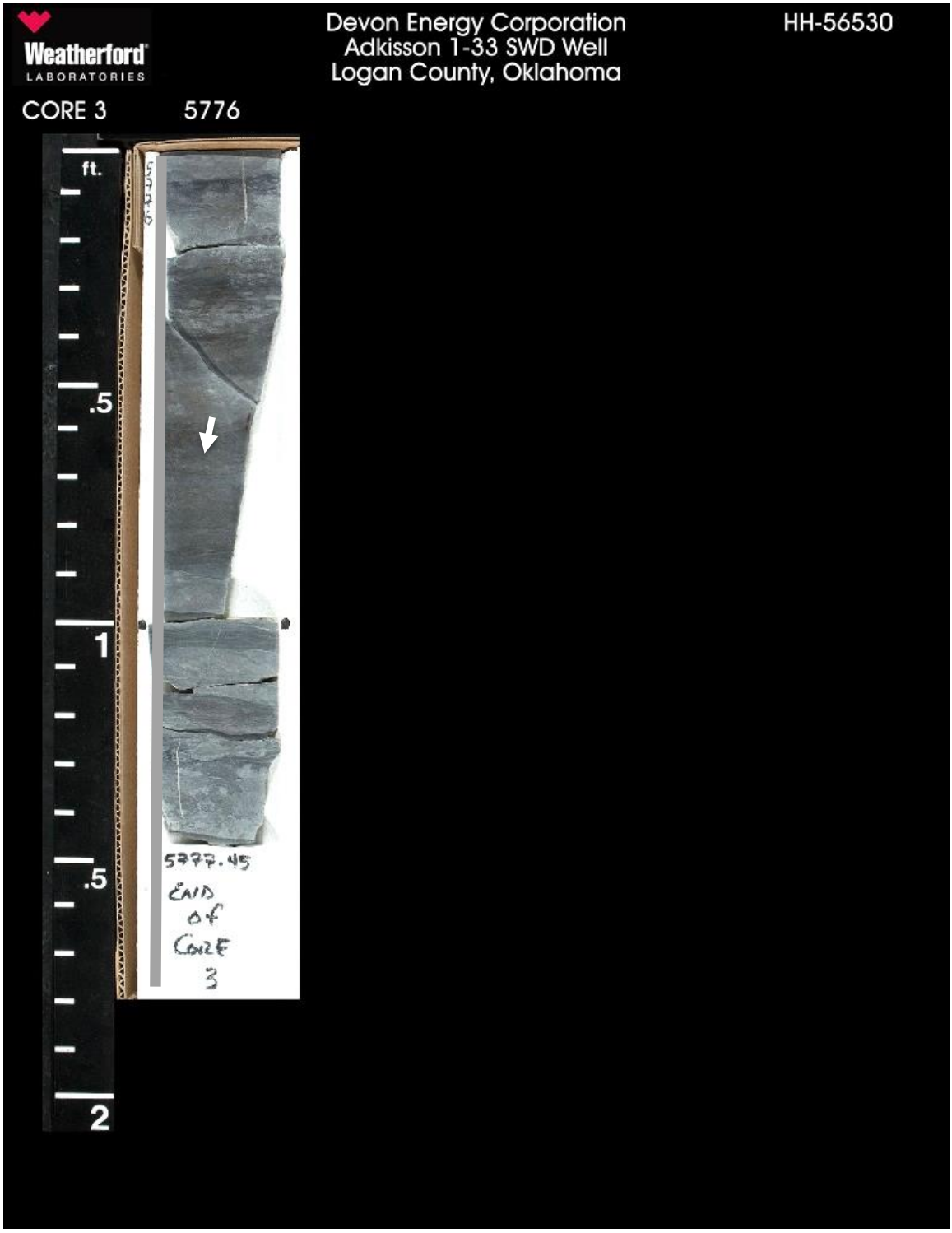
Weatherford
LABORATORIES
Devon Energy Corporation
Adkisson 1-33 SWD Well
Logan County, Oklahoma
HH-56530
CORE 3
5776
ft.
.5
1
.5
2
5777.45
END
OF
CORE
3


Weatherford
LABORATORIES
Devon Energy Corporation
Adkisson 1-33 SWD Well
Logan County, Oklahoma
HH-56530
CORE 4
5777
5779
5781
5783
5785
ft.
.5
1
.5
2
start of CORE 4
4777.45
BU

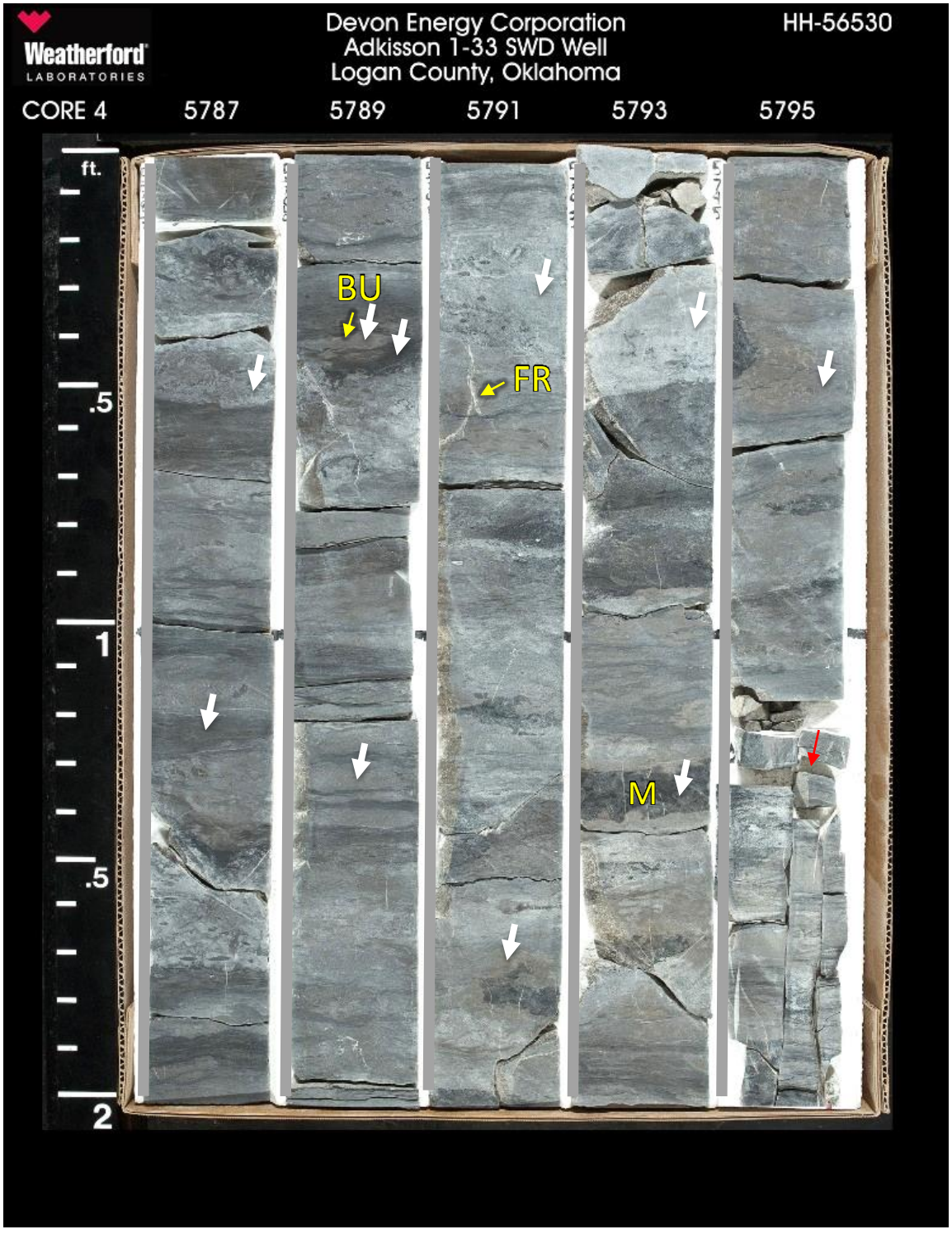
Weatherford
LABORATORIES
Devon Energy Corporation
Adkisson 1-33 SWD Well
Logan County, Oklahoma
HH-56530
CORE 4
5787
5789
5791
5793
5795
ft.
.5
1
.5
2
BU
FR
M

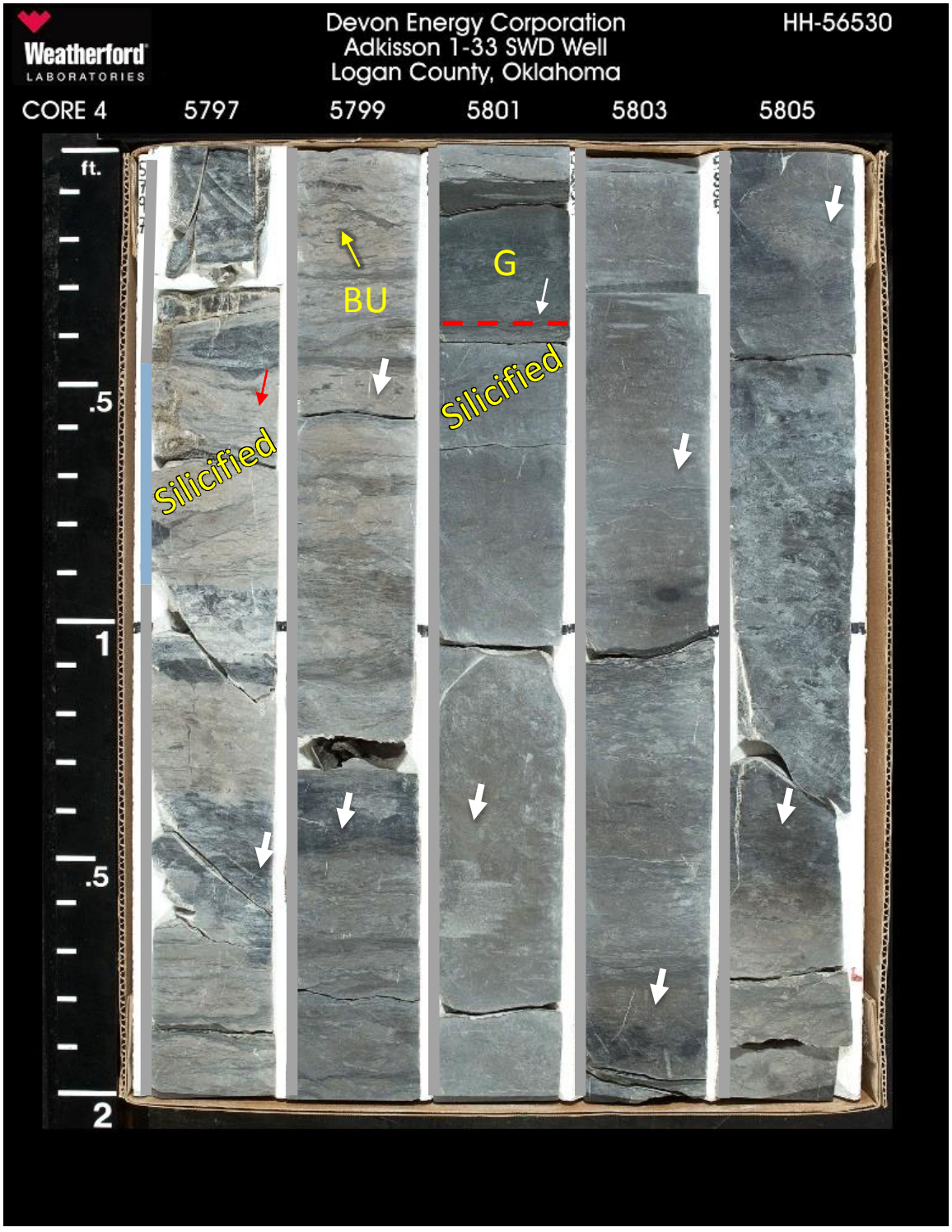
Weatherford
LABORATORIES
Devon Energy Corporation
Adkisson 1-33 SWD Well
Logan County, Oklahoma
HH-56530
CORE 4
5797
5799
5801
5803
5805
ft.
.5
1
.5
2
BU
G
Silicified
Silicified

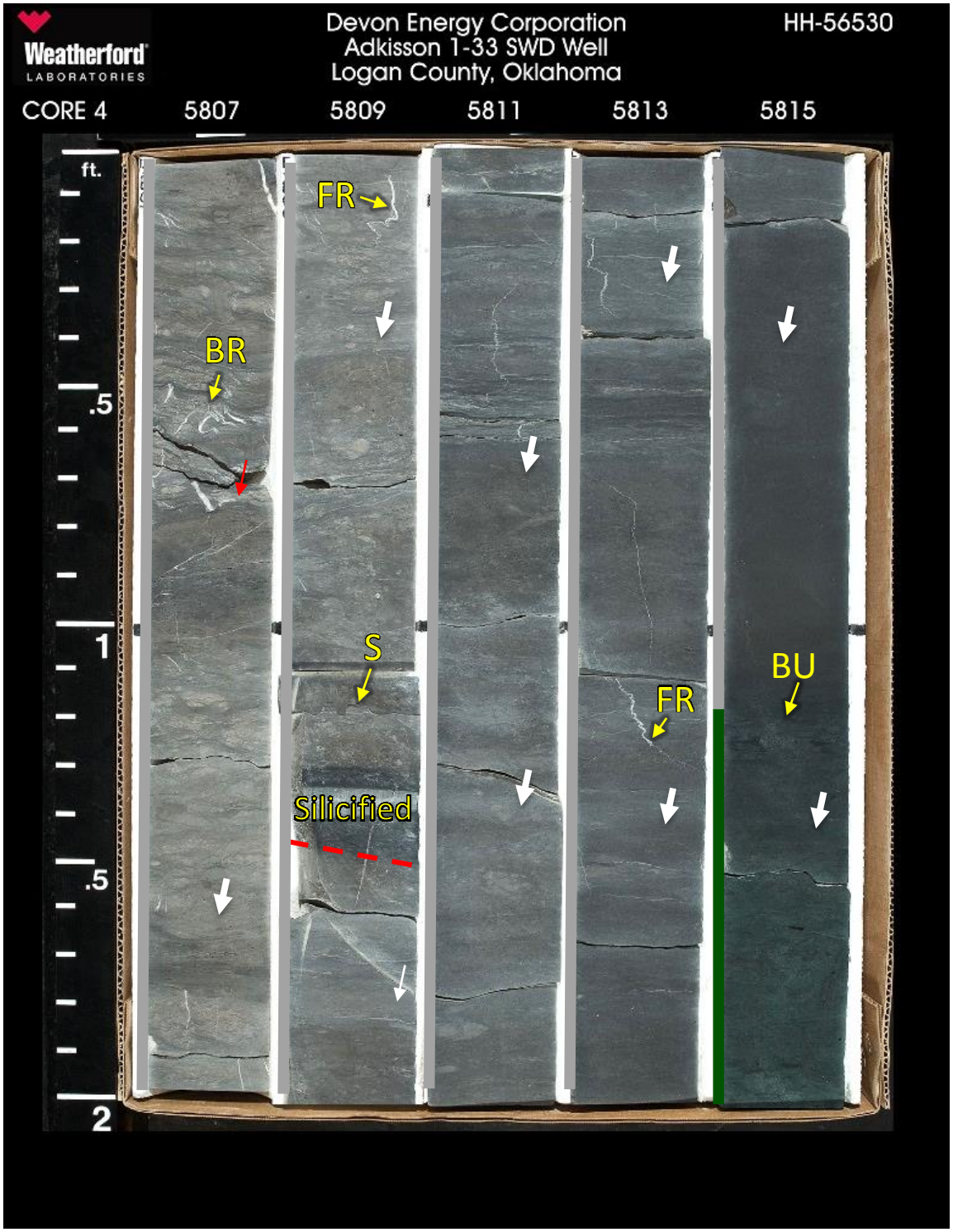
Weatherford
LABORATORIES
Devon Energy Corporation
Adkisson 1-33 SWD Well
Logan County, Oklahoma
HH-56530
CORE 4
5807
5809
5811
5813
5815
ft.
.5
1
.5
2
FR
BR
S
Silicified
FR
BU

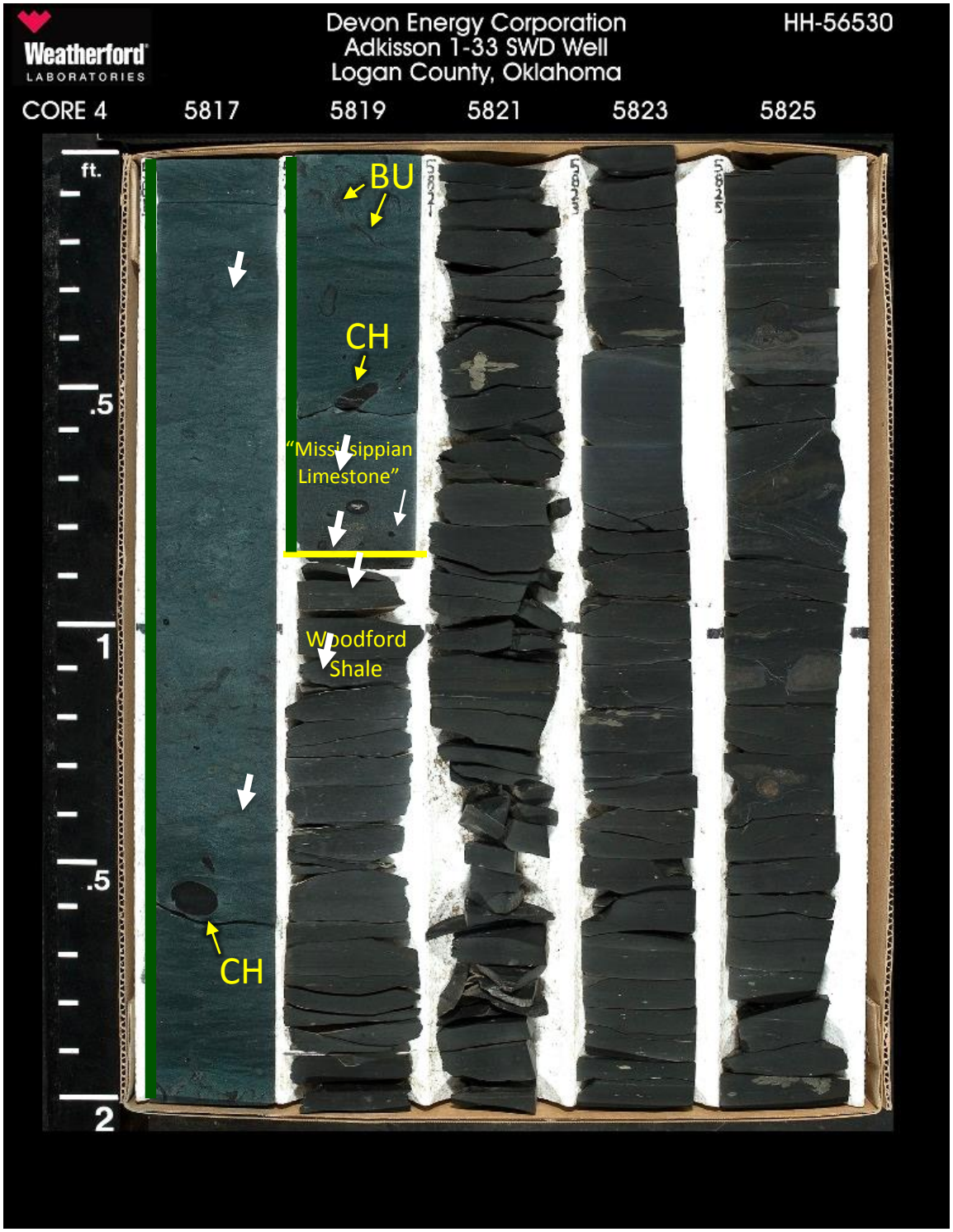
Weatherford
LABORATORIES
Devon Energy Corporation
Adkisson 1-33 SWD Well
Logan County, Oklahoma
HH-56530
CORE 4
5817
5819
5821
5823
5825
ft.
.5
1
.5
2
BU
CH
"Mississippian
Limestone"
Woodford
Shale
CH

Core #2

Winney #1-8 SWD

Interval of Interest: 5257.85-5313.25

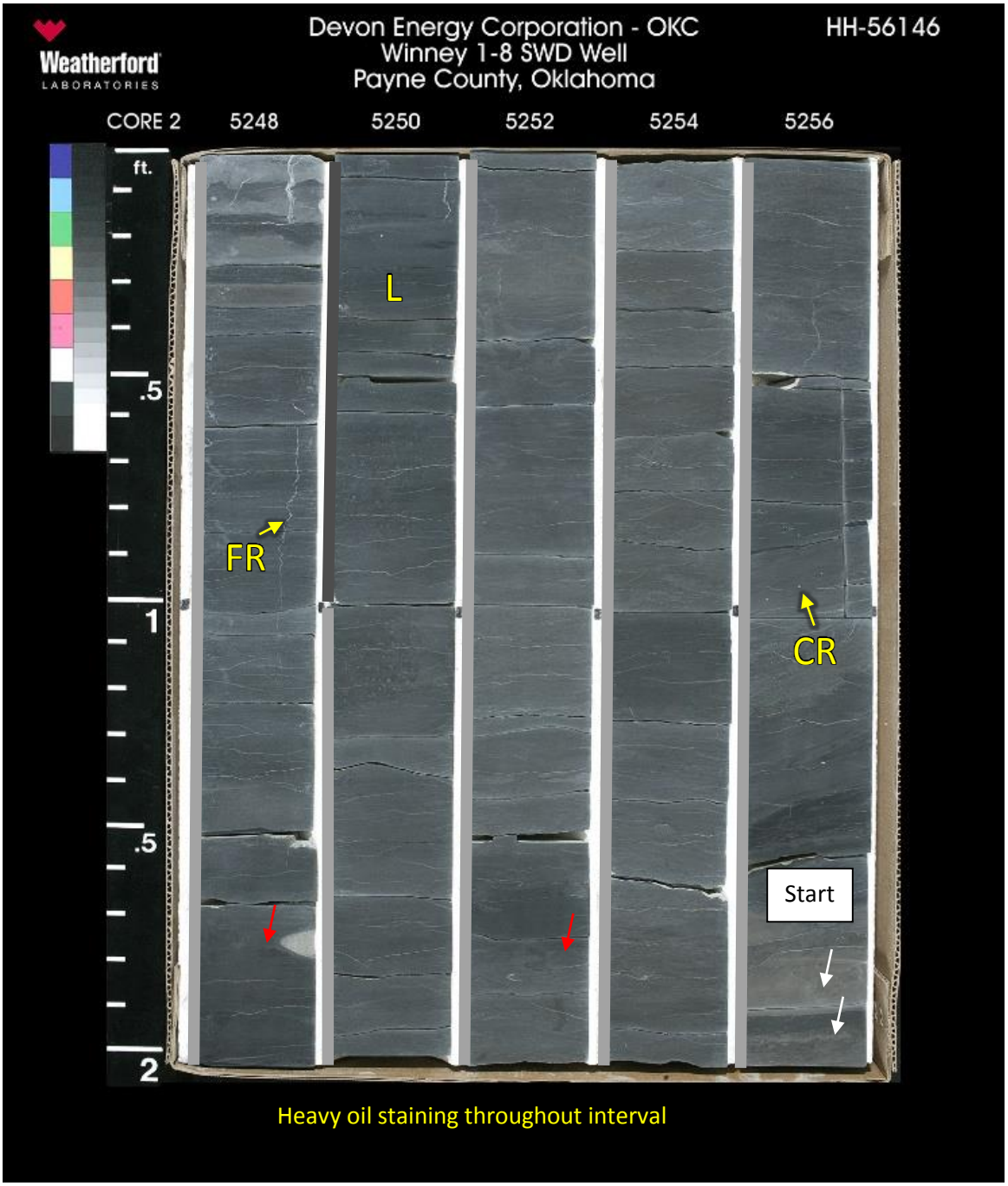

Heavy oil staining throughout interval

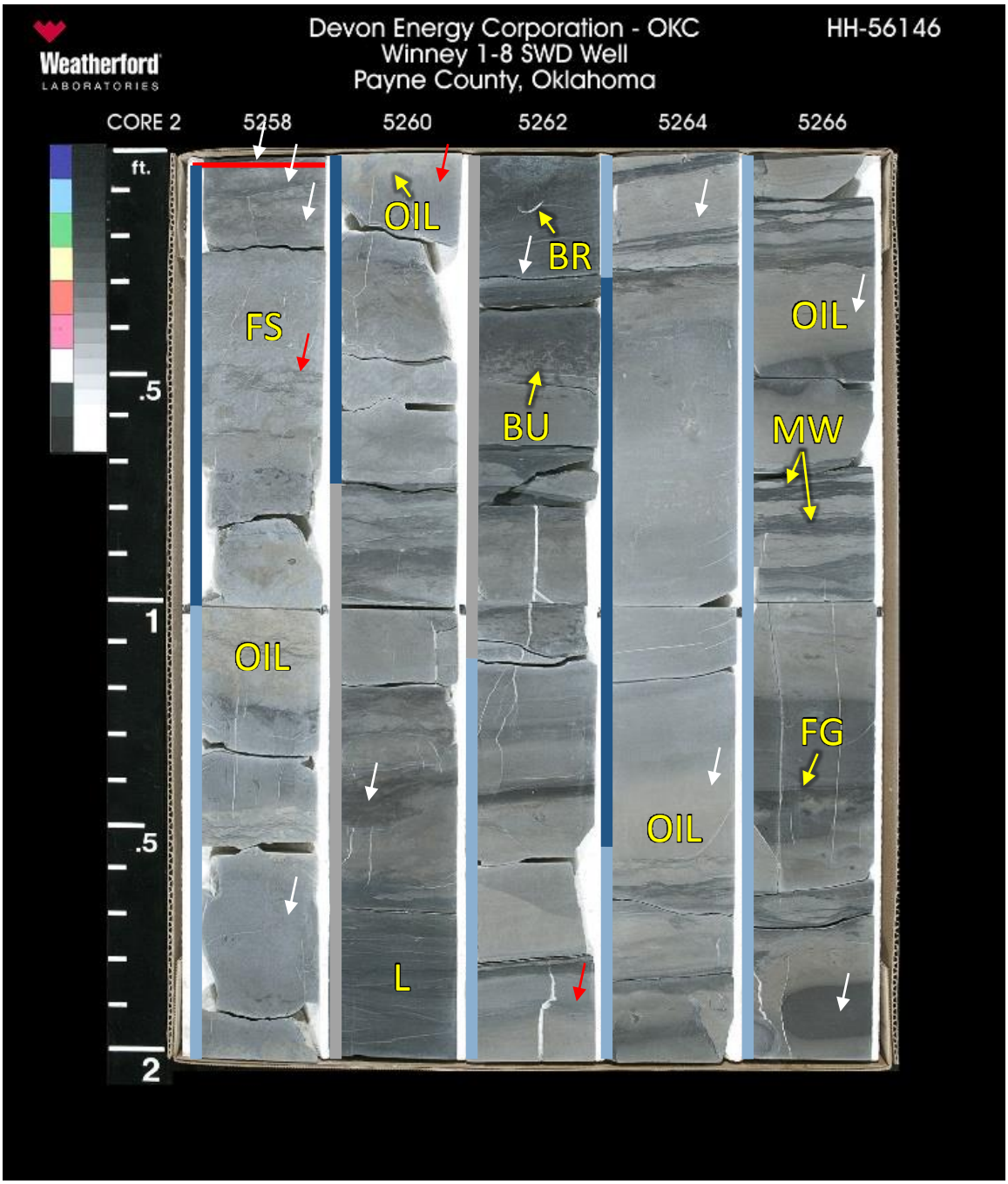
Weatherford
LABORATORIES
Devon Energy Corporation - OKC
Winney 1-8 SWD Well
Payne County, Oklahoma
HH-56146
CORE 2
5258
5260
5262
5264
5266
ft.
.5
1
.5
2
OIL
BR
FS
OIL
BU
MW
OIL
FG
OIL
L

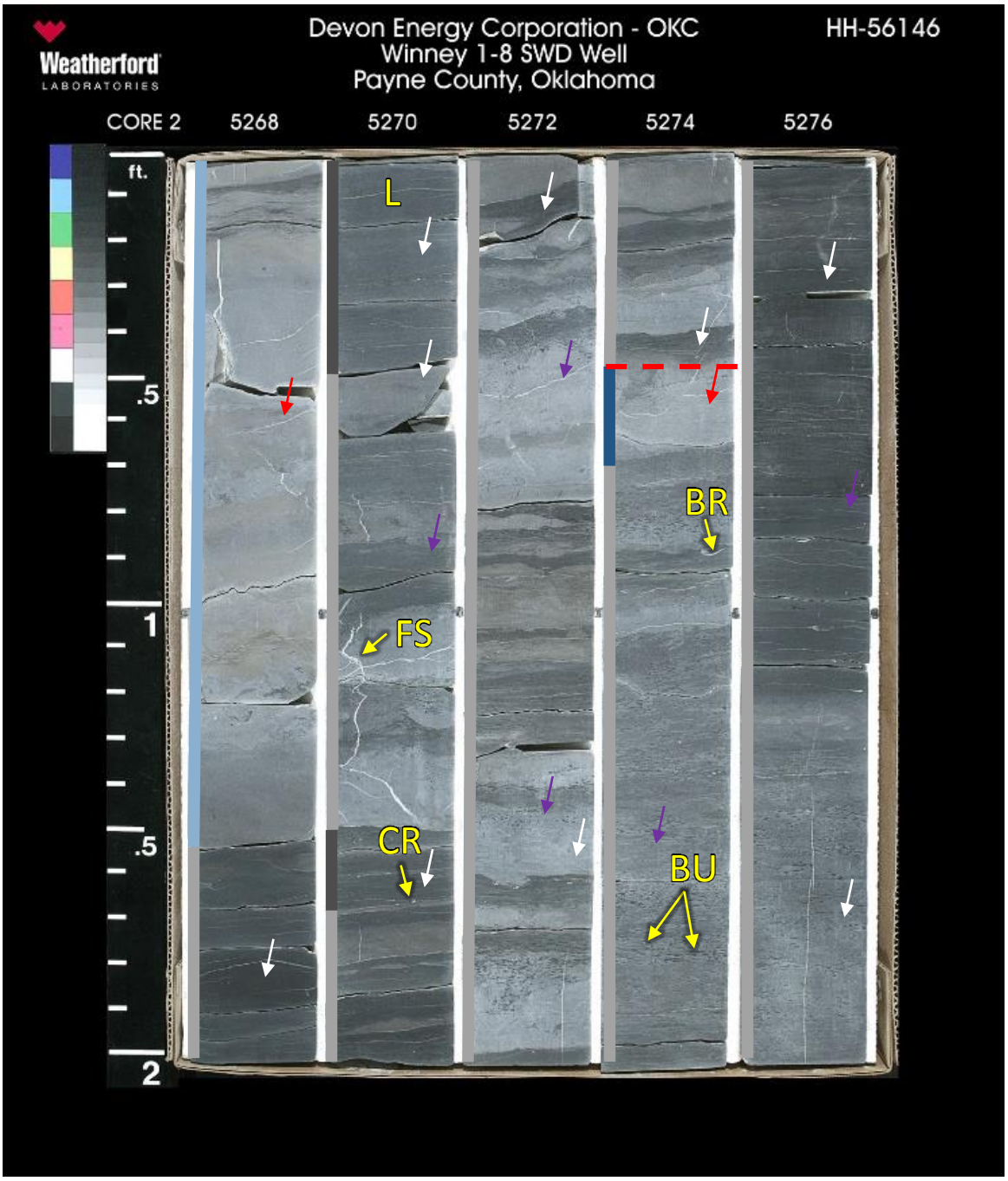
Weatherford
LABORATORIES
Devon Energy Corporation - OKC
Winney 1-8 SWD Well
Payne County, Oklahoma
HH-56146
CORE 2
5268
5270
5272
5274
5276
ft.
.5
1
.5
2
L
BR
FS
CR
BU

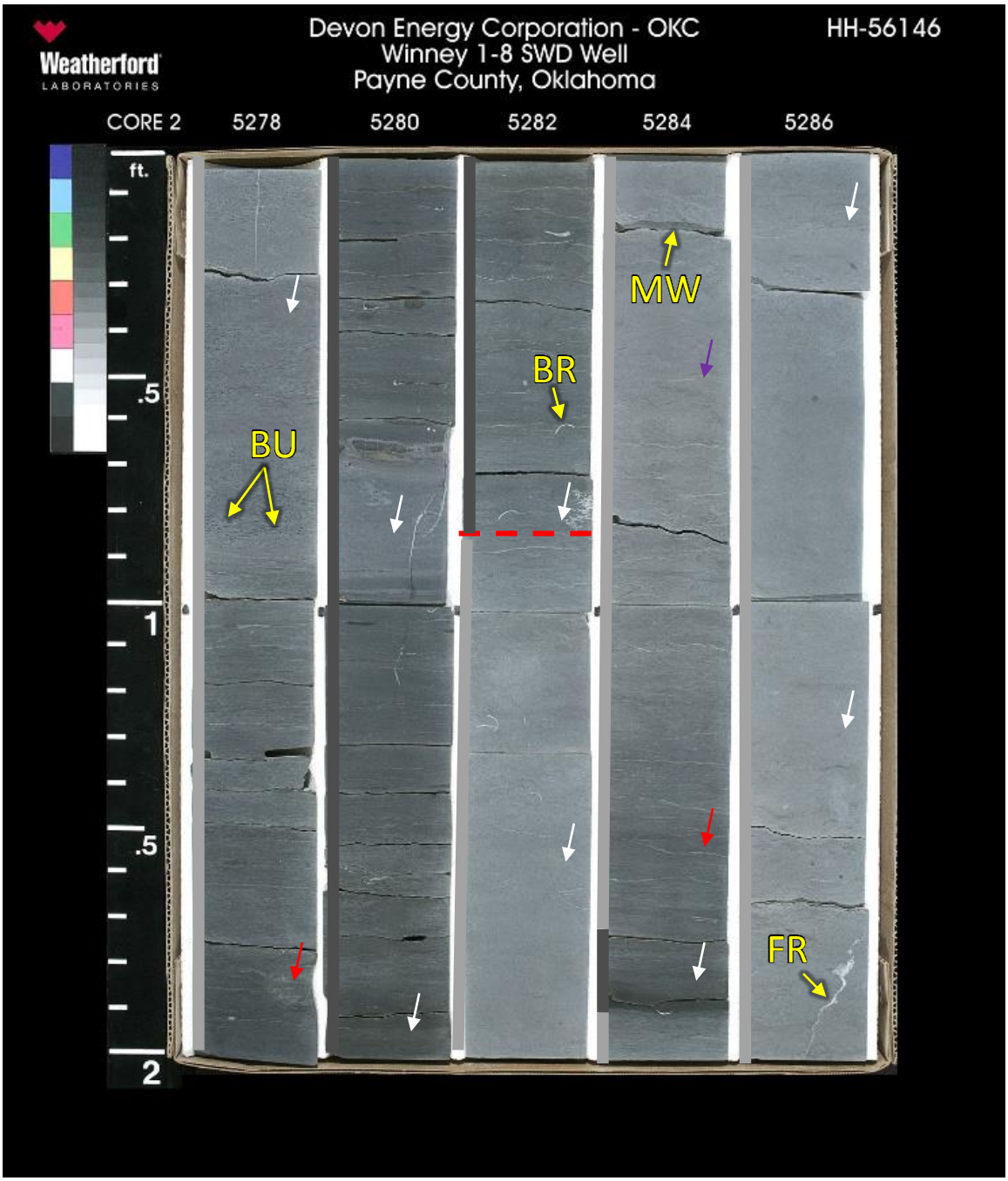
Weatherford
LABORATORIES
Devon Energy Corporation - OKC
Winney 1-8 SWD Well
Payne County, Oklahoma
HH-56146
CORE 2
5278
5280
5282
5284
5286
ft.
.5
1
.5
2
MW
BR
BU
FR

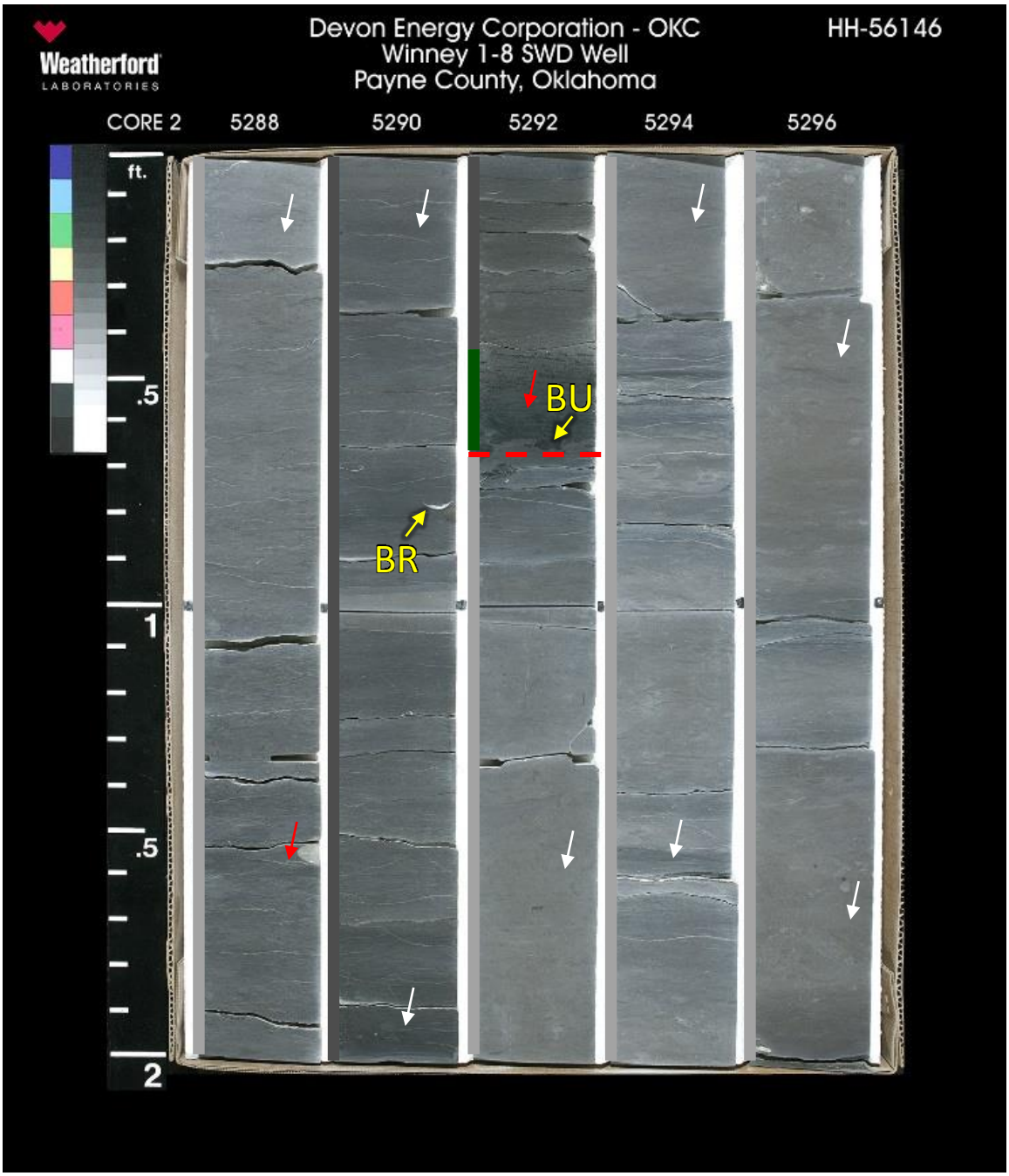
Weatherford
LABORATORIES
Devon Energy Corporation - OKC
Winney 1-8 SWD Well
Payne County, Oklahoma
HH-56146
CORE 2
5288
5290
5292
5294
5296
ft.
.5
1
.5
2
BU
BR

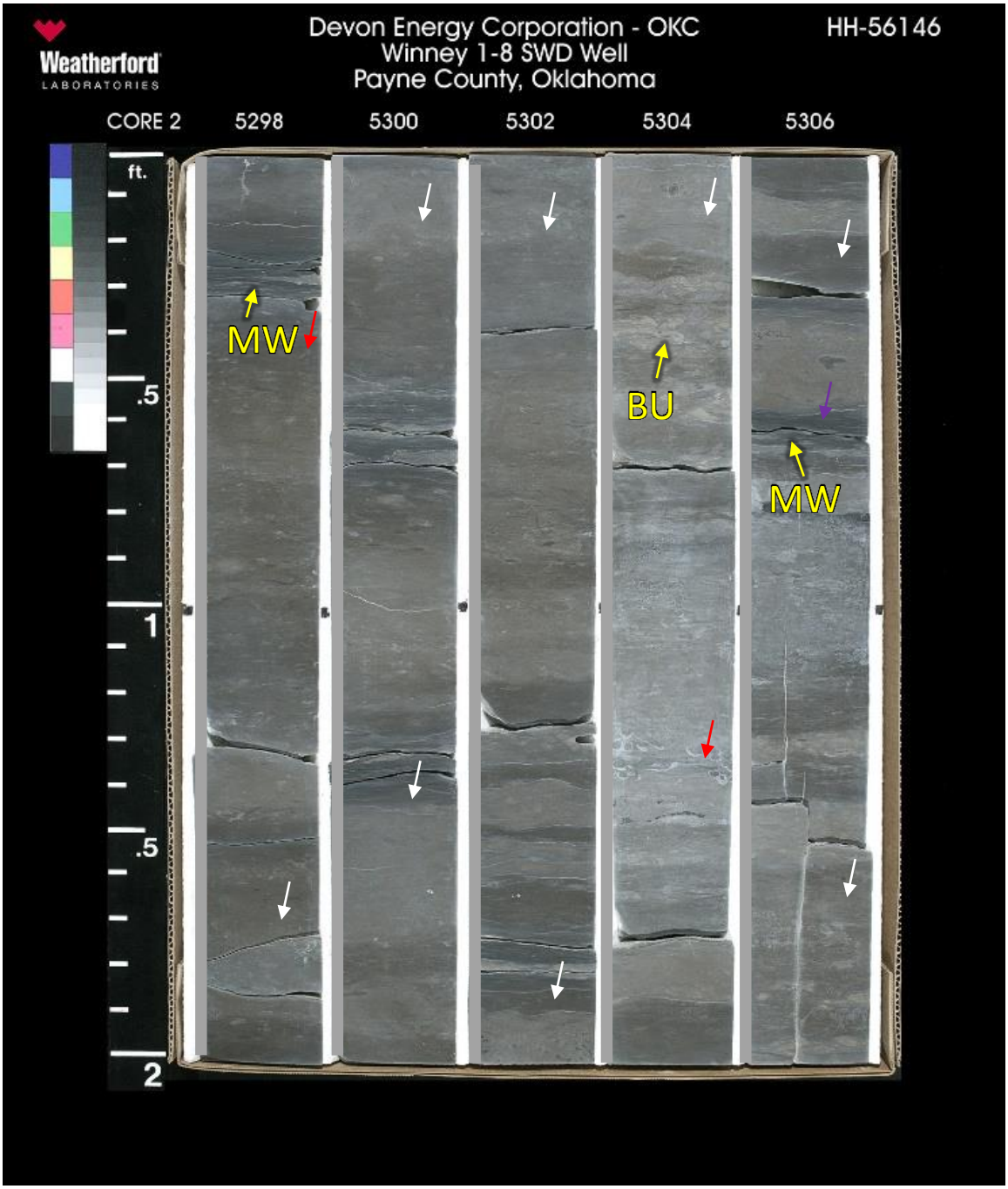
Weatherford
LABORATORIES
Devon Energy Corporation - OKC
Winney 1-8 SWD Well
Payne County, Oklahoma
HH-56146
CORE 2
5298
5300
5302
5304
5306
ft.
.5
1
.5
2
MW
BU
MW

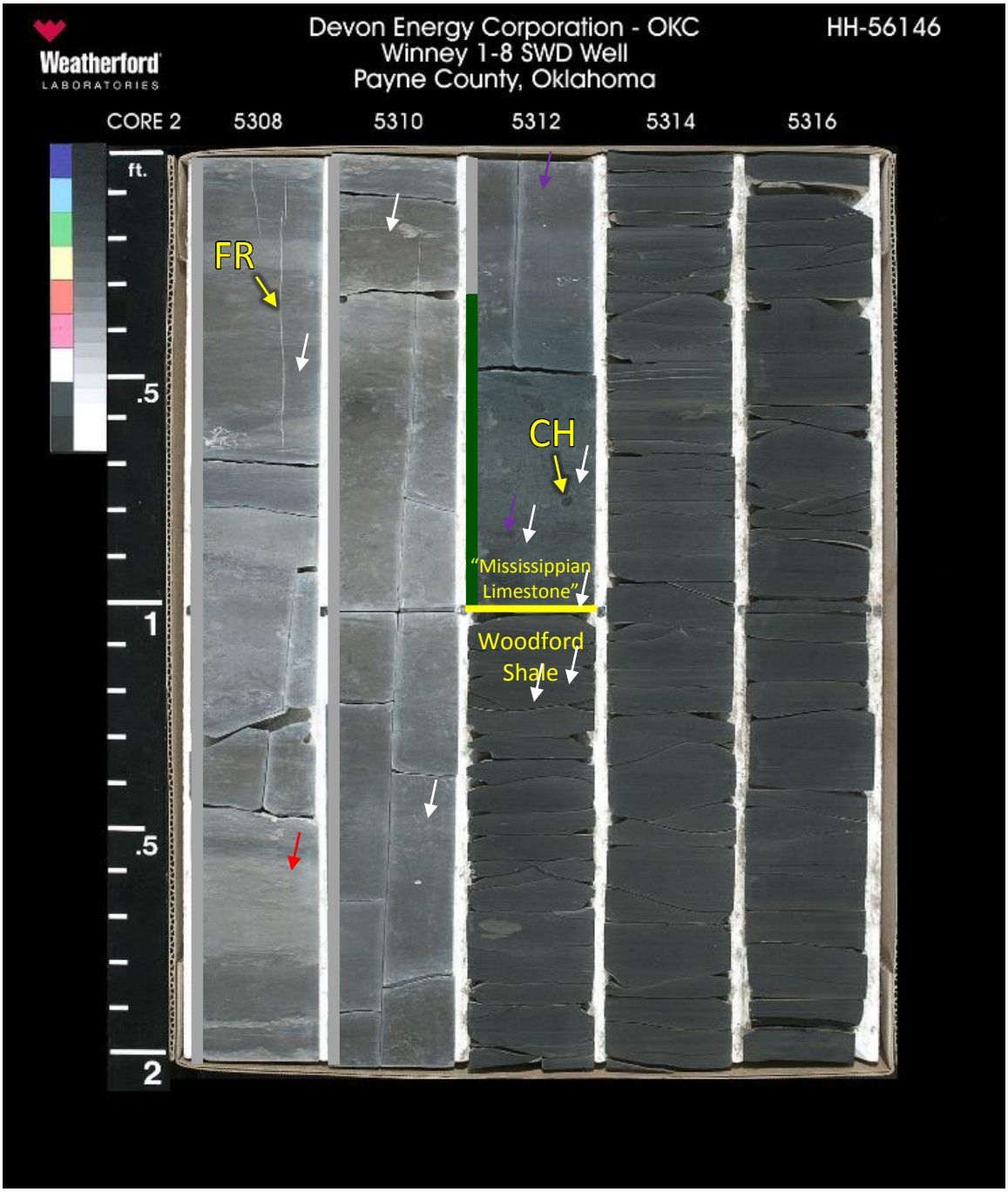
Weatherford
LABORATORIES
Devon Energy Corporation - OKC
Winney 1-8 SWD Well
Payne County, Oklahoma
HH-56146
CORE 2
5308
5310
5312
5314
5316
ft.
.5
1
.5
2
FR
CH
"Mississippian
Limestone"
Woodford
Shale

Core #3

Elinore #1-18 SWD

Interval of Interest: 4453.8-4481.9

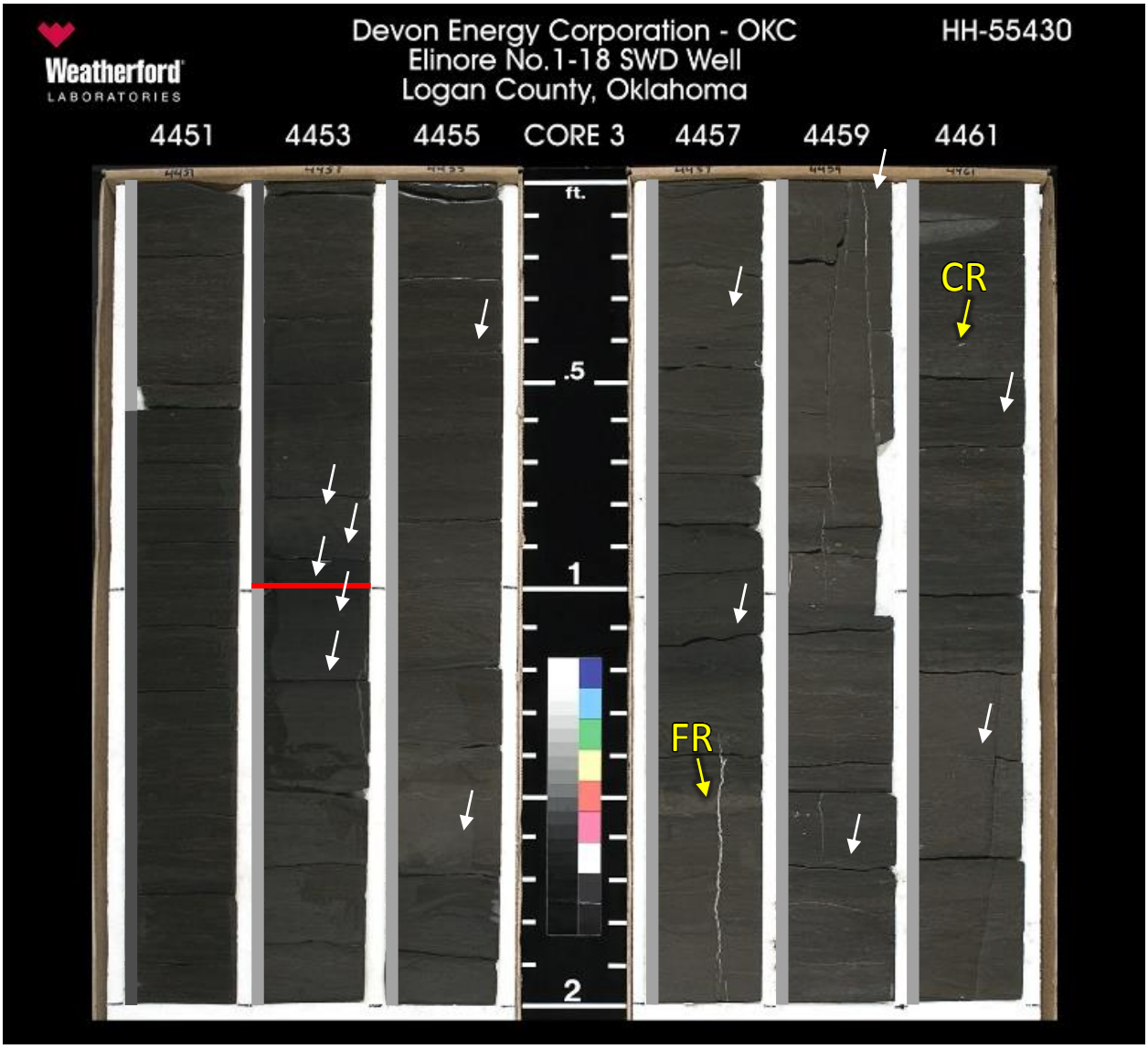
Weatherford
LABORATORIES
Devon Energy Corporation - OKC
Elinore No.1-18 SWD Well
Logan County, Oklahoma
HH-55430
4451
4453
4455
CORE 3
4457
4459
4461
ft.
.5
1
2
CR
FR

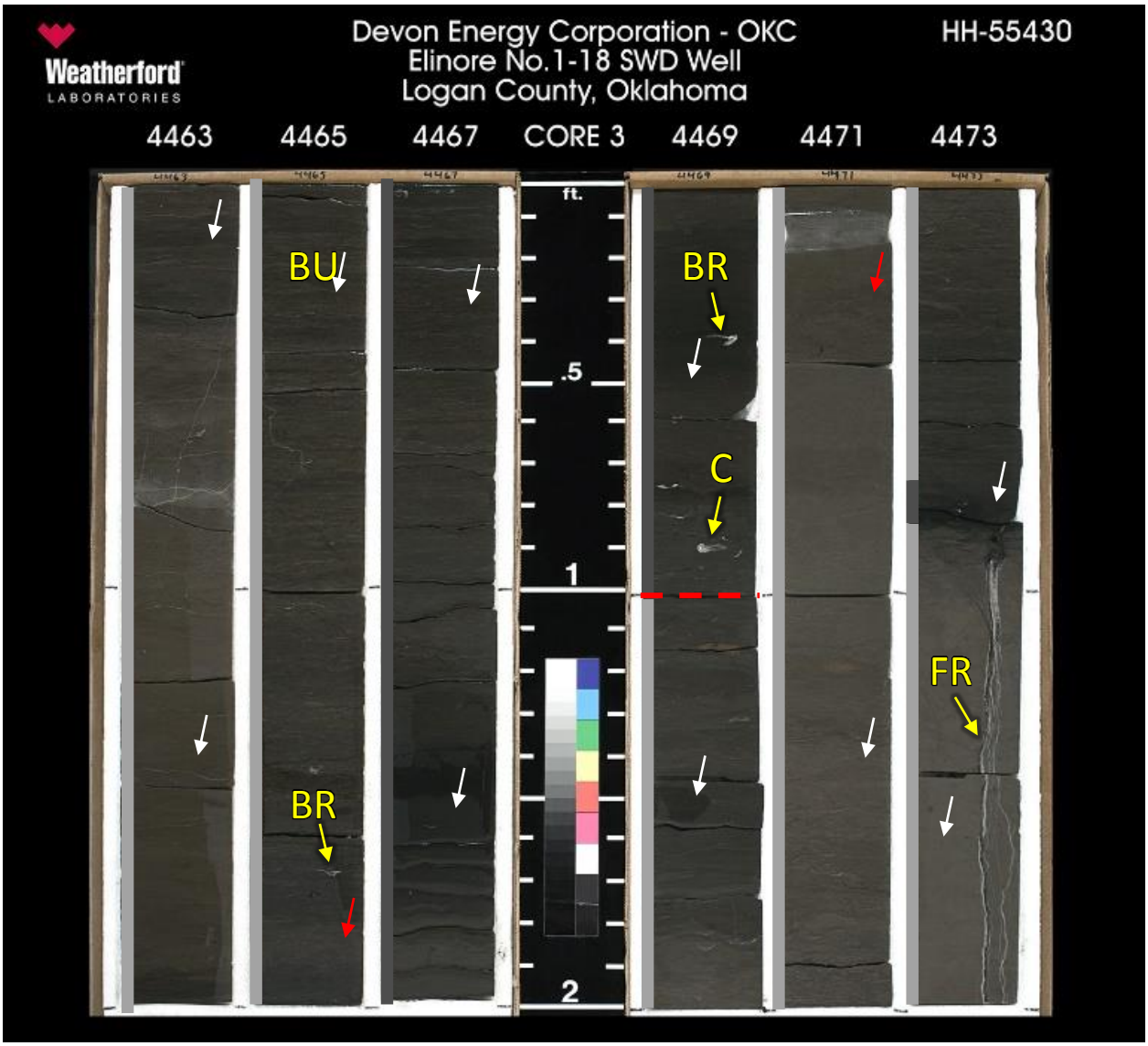
Weatherford
LABORATORIES
Devon Energy Corporation - OKC
Elinore No.1-18 SWD Well
Logan County, Oklahoma
HH-55430
4463
4465
4467
CORE 3
4469
4471
4473
ft.
.5
1
2
BU
BR
C
BR
FR

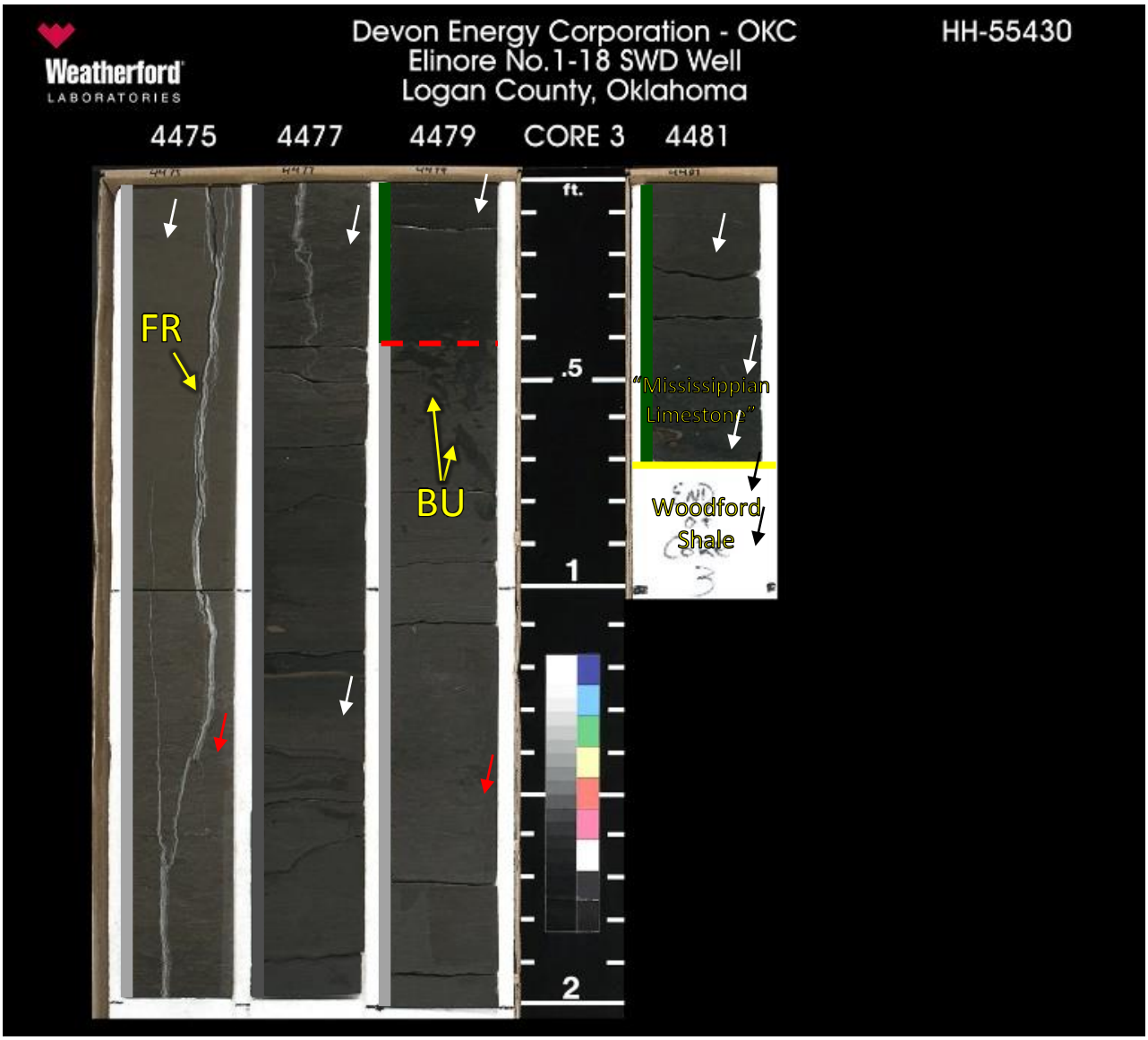
Weatherford
LABORATORIES
Devon Energy Corporation - OKC
Elinore No.1-18 SWD Well
Logan County, Oklahoma
HH-55430
4475
4477
4479
CORE 3
4481
FR
BU
ft.
.5
1
2
"Mississippian Limestone"
Woodford Shale

APPENDIX B

CARBON AND OXYGEN STABLE ISOTOPE RAW DATA

Core #1

Adkisson #1-33 SWD

Depth (ft)	C	O
5495.9	-0.82	-3.43
5496.1	-1.17	-4.43
5496.2	-1.65	-8.28
5496.35	0.97	-3.03
5496.7	0.75	-3.31
5497.25	1.16	-2.70
5498.45	0.81	-3.49
5499.65	0.98	-4.95
5500.15	1.10	-3.07
5501.65	1.20	-2.83
5502.3	1.66	-3.30
5503.3	1.08	-3.83
5504.25	1.28	-3.79
5506.1	1.08	-3.58
5506.8	1.24	-4.13
5507.9	1.35	-2.89
5508.7	1.49	-3.91
5509.1	1.41	-3.91
5510.2	1.63	-3.48
5512	2.00	-2.29
5512.5	1.73	-2.67
5513.2	1.67	-2.93
5514.5	1.55	-3.60
5515.2	1.71	-3.03
5516.1	1.78	-3.66
5517.3	1.78	-4.23
5517.75	1.72	-2.98
5518.4	1.61	-4.21
5519.5	1.58	-3.54
5520.1	1.60	-4.06
5521.2	1.66	-4.18
5522.2	1.63	-3.25
5523.2	1.60	-4.62
5524.65	1.88	-3.76
5525.1	1.95	-3.01

5526.05	1.22	-5.65
5527.8	1.59	-5.03
5528.6	1.85	-3.92
5529.35	1.89	-4.10
5530.85	2.06	-3.60
5531.75	1.84	-4.57
5532.1	2.02	-3.53
5533.2	2.08	-3.72
5534.2	1.87	-4.05
5535.15	2.02	-4.01
5536.6	1.83	-4.81
5537.3	2.12	-2.46
5538.3	1.85	-3.57
5539.4	2.07	-3.13
5540.95	1.75	-4.26
5541.35	1.88	-3.51
5542.1	2.04	-3.40
5543.1	1.94	-3.77
5544.65	2.04	-2.24
5546.1	1.94	-5.12
5546.55	1.85	-4.35
5547.4	2.03	-3.29
5548.75	1.92	-4.29
5549.6	2.15	-2.62
5550.8	1.85	-5.00
5551.7	1.70	-2.38
5552.5	1.88	-3.40
5553.95	1.78	-3.71
5554.95	1.60	-2.37
5555.45	1.71	-4.27
5556.05	2.03	-3.27
5557.25	1.95	-2.90
5558.2	1.72	-3.61
5559.5	1.72	-3.60
5560.15	1.99	-3.46
5561.5	1.64	-3.91
5562.4	1.68	-3.59
5563.3	1.29	-2.70
5565.4	1.44	-4.12
5566.4	1.65	-3.16
5567.4	1.43	-4.53

5568.5	1.66	-3.18
5569.65	1.67	-3.42
5569.9	1.58	-3.14
5571.3	1.39	-3.46
5572.7	1.27	-3.51
5573.3	1.43	-3.02
5574.35	1.25	-3.64
5575.4	1.23	-3.68
5576.25	2.57	-2.84
5577.3	1.51	-2.82
5578.6	1.69	-3.61
5579.6	0.67	-6.14
5580.4	1.83	-1.90
5581.15	1.29	-3.35
5582.1	1.17	-4.99
5583.2	1.82	-3.31
5584.8	0.86	-2.66
5585.15	0.75	-2.35
5585.25	0.27	-3.48
5585.3	0.44	-3.30
5585.4	0.56	-3.63
5585.5	0.41	-3.01
5586.9	1.03	-3.63
5587.3	1.06	-3.55
5588.7	2.01	-2.93
5589.9	2.01	-2.82
5590.8	1.42	-3.99
5591.2	2.05	-2.09
5592.7	1.54	-3.19
5593.3	1.58	-3.32
5594.65	1.42	-3.80
5595.6	1.93	-3.26
5596.8	2.05	-2.36
5597.2	1.85	-4.37
5598.6	1.75	-4.41
5599.4	1.95	-4.74
5600.1	2.14	-2.07
5601.45	1.93	-4.59
5602.5	2.01	-4.53
5603.7	1.72	-3.53
5604.7	2.01	-5.18

5605.5	2.19	-4.52
5606.8	1.82	-2.56
5607.4	2.09	-4.42
5608.7	1.99	-3.89
5610.2	2.69	-1.81
5610.75	1.91	-3.24
5611.4	2.04	-5.19
5612.6	1.96	-4.09
5613.1	2.00	-3.58
5614	2.27	-2.82
5615.3	2.17	-3.59
5616.95	2.06	-4.47
5617.5	2.28	-4.02
5618.4	2.27	-3.18
5619.2	2.31	-3.79
5620.4	2.24	-5.19
5621.5	2.26	-2.47
5622.4	2.19	-5.69
5624.2	2.09	-4.37
5624.5	2.19	-2.61
5625.3	2.36	-4.25
5626.05	2.43	-3.82
5628	2.29	-4.79
5628.5	2.00	-3.16
5629.5	2.16	-6.08
5630.75	2.46	-2.97
5631.3	2.31	-4.13
5632.4	2.33	-4.19
5633.15	2.45	-3.08
5634.65	2.64	-3.07
5635.6	2.34	-3.66
5635.75	2.30	-4.63
5635.9	2.61	-1.96
5636.1	2.35	-3.92
5636.25	2.29	-4.03
5637.3	2.65	-2.96
5638.5	2.22	-2.50
5639.7	2.20	-5.48
5640	2.17	-4.66
5641.8	2.21	-5.12
5642.6	2.38	-2.08

5643.7	2.41	-3.82
5644.95	2.32	-2.32
5645.4	2.38	-2.98
5646.65	2.29	-4.61
5647.95	2.75	-2.20
5648.65	2.32	-3.79
5649.15	2.35	-4.53
5650.7	2.36	-4.32
5651.2	2.32	-5.54
5652.5	2.38	-2.88
5653.3	2.55	-3.74
5654.8	2.53	-5.02
5655.1	2.74	-4.11
5656.2	2.75	-2.57
5657.1	2.61	-4.60
5657.7	2.69	-4.46
5658.6	2.63	-3.82
5659.3	2.72	-4.02
5660.35	3.04	-2.47
5661.7	2.47	-6.81
5663	2.86	-3.26
5663.75	2.89	-4.90
5664.4	2.89	-2.72
5665.6	2.53	-4.09
5666.2	2.37	-6.19
5666.7	2.73	-3.51
5668.25	2.67	-2.19
5669.7	2.69	-3.49
5670.4	2.63	-4.50
5671.25	2.49	-4.02
5672.15	2.79	-2.90
5673.25	2.45	-3.34
5674.6	2.33	-3.85
5675.5	2.79	-3.49
5676.7	2.96	-2.86
5677.7	2.37	-5.14
5678.35	2.65	-3.32
5679.7	2.54	-4.88
5680.7	2.45	-4.43
5681.8	2.72	-2.93
5682.15	2.24	-3.79

5683.4	2.61	-4.53
5684.8	2.40	-3.72
5685.7	2.71	-3.03
5686.45	2.42	-4.18
5687.5	2.84	-2.98
5688.4	2.11	-4.78
5688.85	2.98	-2.91
5690.1	2.22	-4.31
5691.1	2.83	-2.57
5692.2	2.78	-5.18
5693.7	2.51	-4.76
5694.2	2.43	-3.98
5695.25	2.70	-4.72
5696.2	2.74	-3.60
5697.5	2.61	-4.59
5698.2	2.44	-3.09
5699.3	2.19	-4.69
5700.7	2.79	-3.68
5701.65	2.48	-3.00
5702.2	2.24	-2.22
5703.2	3.34	-1.97
5703.4	3.53	-0.41
5703.65	2.77	-3.20
5703.7	1.93	-5.20
5703.8	2.02	-4.72
5704.45	2.58	-3.63
5705.3	2.79	-5.21
5706.5	2.82	-4.36
5707.5	3.13	-3.56
5708.5	2.78	-3.10
5709.4	2.48	-3.07
5710.6	2.23	-4.87
5711.95	2.54	-3.83
5712.55	2.51	-2.73
5713.8	2.16	-3.86
5715.15	2.85	-1.17
5715.7	2.71	-1.66
5716.6	2.65	-1.76
5717.5	2.52	-2.08
5718.55	1.91	-3.78
5719.4	1.81	-4.68

5720.7	1.59	-3.64
5721.7	2.27	-2.45
5722.25	2.25	-3.23
5722.5	1.84	-3.51
5723.95	2.83	-0.43
5724.6	2.07	-3.04
5725.75	2.08	-2.28
5726.7	2.13	-3.70
5728.8	1.91	-4.37
5729.1	2.72	-4.22
5729.4	1.88	-4.33
5730.3	2.50	-3.12
5731.55	2.40	-3.77
5732.3	2.50	-2.81
5733.7	2.39	-3.44
5735	2.18	-3.02
5735.65	1.94	-4.55
5735.7	2.27	-3.20
5736.3	2.23	-3.02
5737.85	2.43	-4.23
5738.5	2.70	-2.94
5739.6	2.73	-2.48
5740.9	2.43	-4.67
5741.4	2.72	-2.57
5742.3	2.43	-3.61
5743.5	2.30	-3.81
5744.75	2.10	-4.22
5745.6	2.52	-3.44
5746.7	2.24	-4.66
5746.85	2.55	-3.60
5748.5	2.56	-3.24
5749	2.40	-3.60
5750.6	2.58	-3.51
5751.65	2.32	-4.17
5752.2	2.25	-4.13
5753.1	2.35	-4.03
5754.3	2.50	-3.52
5755.5	2.67	-3.51
5756.4	2.70	-2.36
5757.85	2.63	-2.86
5758.4	2.29	-3.58

5759.6	2.53	-2.32
5760.6	2.16	-3.94
5761.6	2.35	-2.67
5762.1	2.29	-3.73
5763.15	2.41	-2.60
5764.25	2.43	-2.72
5765.3	2.21	-3.88
5766.5	2.33	-3.35
5767.7	2.33	-3.57
5768.5	2.34	-4.54
5769.6	2.46	-2.34
5770.6	2.50	-3.94
5771.1	2.55	-4.16
5772.85	2.49	-4.24
5773.6	2.59	-2.68
5774.1	2.55	-3.89
5775	2.43	-3.59
5776.65	2.47	-3.05
5777.65	2.52	-3.48
5778.35	2.53	-1.84
5779.25	2.34	-4.46
5780.45	2.32	-2.90
5781.8	2.26	-2.55
5782.7	2.13	-4.90
5783.6	2.25	-4.51
5784.5	2.24	-2.18
5785.65	2.00	-3.74
5785.7	2.16	-3.31
5786.5	2.07	-2.26
5787.5	2.35	-4.22
5788.2	1.99	-2.30
5789.4	2.23	-5.38
5789.45	2.17	-4.44
5790.3	1.55	-5.58
5791.3	2.24	-2.08
5792.7	0.42	-4.56
5793.4	1.29	-3.43
5794.35	-0.24	-5.34
5795.5	0.01	-4.79
5796.35	0.89	-2.33
5797.55	0.61	-4.76

5798.5	1.06	-2.97
5799.5	0.32	-4.48
5800.4	1.43	-4.99
5801.4	0.79	-0.68
5802.4	0.58	-3.97
5803.7	0.55	-3.52
5804.8	0.42	-2.78
5805.2	0.15	-3.95
5806.4	0.09	-2.80
5807.75	-0.83	-4.36
5808.6	0.10	-3.45
5809.4	-0.40	-4.66
5810.8	-0.25	-5.16
5811.7	-0.22	-3.30
5812.35	-0.52	-4.62
5813.3	-0.05	-3.55
5814.4	-0.82	-3.60
5815.4	-0.61	-4.08
5816.4	-2.49	-4.96
5817.3	-4.54	-7.57
5818.4	-3.85	-6.85
5819.7	-4.08	-7.27
5819.8	-4.37	-6.14
5819.85	-3.24	-5.69

Core #2

Winney #1-8 SWD

Depth (ft)	C	O
5257.85	1.04	-5.03
5257.95	1.43	-2.27
5258	1.26	-3.75
5258.1	1.24	-3.82
5258.2	1.29	-3.74
5258.5	0.82	-3.89
5259.7	1.11	-2.94
5260.1	0.94	-2.86
5261.45	0.20	-2.57
5262.3	1.75	-3.06
5263.9	0.98	-3.40
5264.2	1.08	-3.97
5265.4	1.30	-3.57
5266.3	1.15	-3.89
5267.9	1.60	-2.91
5268.6	1.25	-3.24
5269.85	1.82	-2.60
5270.25	1.61	-3.23
5270.5	1.04	-4.29
5271.65	1.36	-3.29
5272.15	1.27	-3.75
5273.6	1.73	-2.84
5274.45	1.06	-3.08
5274.6	0.98	-2.89
5276.3	1.47	-2.75
5277.7	1.58	-3.47
5278.35	1.35	-3.39
5279.85	1.35	-3.40
5280.85	0.77	-3.27
5281.95	1.33	-3.07
5282.85	1.35	-3.74
5283.6	1.23	-3.08
5285.55	1.44	-3.50
5285.85	1.80	-3.39
5286.2	1.35	-4.57

5287.3	0.80	-3.46
5288.2	1.30	-4.05
5289.55	1.41	-3.70
5290.2	1.34	-3.82
5291.95	2.01	-3.60
5292.5	0.60	-2.74
5293.6	2.09	-2.60
5294.2	1.42	-3.74
5295.55	1.61	-3.20
5296.5	0.75	-4.09
5297.7	0.53	-3.17
5298.45	1.38	-3.51
5299.7	1.22	-3.82
5300.15	1.10	-4.27
5301.4	1.47	-2.63
5302.2	1.15	-3.82
5303.85	1.35	-2.42
5304.2	0.87	-4.57
5305.35	-0.06	-2.81
5306.3	1.06	-3.03
5307.7	0.74	-3.73
5308.5	0.87	-2.65
5309.9	-0.29	-4.40
5310.2	0.33	-3.22
5311.5	-0.46	-3.91

Core #3

Elinore #1-18 SWD

Depth (ft)	C	O
4453.8	-0.05	-4.38
4453.9	-0.09	-4.23
4454	1.06	-2.91
4454.1	0.63	-3.23
4454.2	0.32	-3.49
4455.4	-0.02	-3.37
4456.6	-0.84	-3.83
4457.3	0.35	-2.75
4458.1	0.45	-2.60
4459	-0.35	-3.02
4460.65	0.42	-2.78
4461.6	0.18	-2.97
4462.4	-0.24	-2.72
4463.15	-0.49	-3.76
4464.4	-1.23	-3.39
4465.3	-1.06	-3.63
4466.85	-1.04	-4.30
4467.3	-0.68	-3.90
4468.5	0.16	-2.93
4469.5	-0.12	-3.00
4470.5	-0.44	-3.82
4471.3	-0.56	-3.23
4472.4	-0.96	-3.49
4473.8	0.61	-3.10
4474.6	0.15	-2.13
4475.2	-0.66	-2.56
4476.4	-1.73	-3.95
4477.2	-1.22	-3.81
4478.3	-0.83	-3.21
4479.1	-0.46	-3.49
4480.5	-1.01	-3.62
4481.2	-2.72	-4.38
4481.5	-2.54	-4.47

4481.7	-5.68	-3.42
4481.8	-2.04	-2.22
4481.9	-2.50	-2.92

VITA

Ashley Marie Dupont

Candidate for the Degree of

Master of Science

Thesis: HIGH-RESOLUTION CHEMOSTRATIGRAPHY IN THE MISSISSIPPIAN LIMESTONE OF NORTH-CENTRAL OKLAHOMA

Major Field: Geology

Biographical:

Education:
Completed the requirements for the Master of Science in Geology at Oklahoma State University, Stillwater, Oklahoma in July, 2016.

Completed the requirements for the Bachelor of Science in Geology at the University of Georgia, Athens, Georgia in 2013.

Completed the requirements for the Bachelor of Science in Biology at the University of Georgia, Athens, Georgia in 2013.

Experience:
Geoscience Intern at EOG Resources in Tyler, Texas, Summer 2015
Full-time Geologist at EOG Resources in San Antonio, Texas, August 2016

Professional Memberships:
American Association of Petroleum Geologists
Geological Society of America
Oklahoma City Geological Society
Tulsa Geological Society